

January 2014

Nanoparticle Neuromodulation

Agatha Julia Gornisiewicz
Worcester Polytechnic Institute

Alex Michael Margiott
Worcester Polytechnic Institute

Christopher James Savoia
Worcester Polytechnic Institute

Gabrielle E. Demac
Worcester Polytechnic Institute

Follow this and additional works at: <https://digitalcommons.wpi.edu/mqp-all>

Repository Citation

Gornisiewicz, A. J., Margiott, A. M., Savoia, C. J., & Demac, G. E. (2014). *Nanoparticle Neuromodulation*. Retrieved from <https://digitalcommons.wpi.edu/mqp-all/1977>

This Unrestricted is brought to you for free and open access by the Major Qualifying Projects at Digital WPI. It has been accepted for inclusion in Major Qualifying Projects (All Years) by an authorized administrator of Digital WPI. For more information, please contact digitalwpi@wpi.edu.

Nanoparticle Neuromodulation

A Perfusion Delivery System for the Study of the Interaction between
Quantum Dots and Hippocampal Neurons

A Major Qualifying Project

Submitted to the Faculty of



WPI

**In partial fulfillment of the requirements for the
Degree of Bachelors of Science in Biomedical Engineering**

By:

Gabrielle Demac

Agatha Gornisiewicz

Alex Margiott

Christopher Savoia

January 15, 2014

Advisor: _____
Professor M. Rolle, Ph.D.

Authorship

All members of the team both contributed to and edited all sections of this report. Therefore, we accept joint responsibility for the project and decline the option of individual authorships.

Acknowledgements

We would like to first thank our sponsors at The Centre for Biomedical Sciences and Engineering at the University of Nova Gorica in Vipava, Slovenia. To Dr. Giulietta Pinato, thank you from the bottom of our hearts for your dedication in teaching us both practical and theoretical concepts in neuroscience, nanotechnology, and microscopy. To Professor Elsa Fabbretti, for her feedback during our project and efforts to make this collaboration possible. To Tanja Belě, for her assistance with laboratory techniques and helpful advice, as well as a constant smile no matter the circumstance.

We would also like to thank Professor Torre's Laboratory at the International School for Advanced Studies in Trieste, Italy, particularly Federico Iseppon, for providing the team with rat hippocampal cell cultures. Additionally, we would like to thank Carlo Fonda at the Science Dissemination Unit and 3D Printing Laboratory of the International Centre for Theoretical Physics in Trieste, Italy, for his generous assistance with the manufacture of our device.

Finally, we would like to thank our advisors at Worcester Polytechnic Institute in Worcester, MA, USA, for making this dream a reality. Professors Tanja Dominko and Marsha Rolle provided WPI seniors with the first opportunity to complete a Biomedical Engineering Major Qualifying Project overseas in collaboration with a foreign research institute. This was an amazing experience that we hope continues for a long time.

Abstract

The current standards for whole-brain *in vivo* imaging cannot provide the cellular resolution and neuron stimulation needed to study neuronal plasticity, important in memory formation. Current *in vivo* studies of neuronal dynamics are limited to animal models, due to deleterious effects resulting from the application of fluorophores. Nanoparticle (<100nm) quantum dots (QDs) are a promising alternative to traditional fluorophores because they are bright, photostable, and have highly tunable spectra, making them appropriate for a variety of applications. Furthermore, previous studies have shown that QDs have properties that can elicit electrical activity in neurons. Scientists at the University of Nova Gorica in Slovenia are studying this interaction. To help advance this research, we designed a perfusion system to deliver drugs and QDs to cultures of rat hippocampal neurons. This perfusion system successfully delivered Gabazine, Tetrodotoxin, and QDs to the culture, blocked ambient light during imaging, limited mounting time, was easy to manufacture, and was cost effective. Using this device in conjunction with calcium imaging techniques, we demonstrated that the mechanism of interaction between carboxyl-coated QDs and hippocampal neurons is localized to the synapse, producing synchronous electrical activity.

Table of Contents

Authorship	a
Acknowledgements.....	b
Abstract.....	c
Key Terms and Abbreviations	k
Key Terms.....	k
Abbreviations	m
1 Introduction	1
2 Background	4
2.1 Clinical & Research Significance of Neuroscience.....	4
2.2 Neurobiology.....	5
2.2.1 The Hippocampus	6
2.2.2 Neurons and Neuronal Cells	7
2.2.3 Action Potentials and Calcium Ions.....	11
2.3 Quantum Dots.....	13
2.3.1 Optical Properties	15
2.3.2 Electrical Properties	17
2.4 Quantum Dot-Neuron Interaction with Calcium Imaging.....	18
2.4.1 Calcium Imaging Data	18
2.4.2 Current Microscope Setup at UNG	20
3 Project Strategy.....	26
3.1 Client Statement	26
3.1.1 Current Methodology	26
3.1.2 Revised Client Statement.....	29
3.2 Objectives, Constraints and Functions.....	30
3.2.1 Objectives.....	30
3.2.2 Constraints	32
3.2.3 Functions.....	33
3.3 Project Approach	34
4 Design Alternatives and Evaluations.....	35
4.1 Design Specifications	36
4.2 Design Alternatives	38

4.2.1	Design 1: Open System with Selectable Perfusion	38
4.2.2	Design 2: Closed System with Selectable Perfusion	39
4.2.3	Design 3: Closed Loop Perfusion System	40
4.2.4	Design 4: Static Beaker System	42
4.3	Design Evaluation Matrix	43
4.3.1	Open Perfusion System	44
4.3.2	Closed Perfusion System	44
4.3.3	Closed Loop Perfusion System	45
4.3.4	Static Beaker System	45
4.3.5	Finalized Matrix	46
4.4	Prototypes	47
4.4.1	Prototype One: Results & Modifications	47
4.4.2	Prototype Two: Results & Modifications	49
4.4.3	Prototype Three	52
4.4.4	The Low Fluid Alarm	53
4.4.5	Beta Design	57
4.4.6	Modifications to Beta Design	59
5	Design Verification	61
5.1	Verification Experiments	61
5.1.1	Mechanical Interference	61
5.1.2	Low Fluid Alarm	61
5.1.3	Perfusion Effectiveness	62
5.1.4	Consistent Inflow and Outflow Positions	62
5.1.5	Thermal Control Compatibility	63
5.1.6	Constant Volume	63
5.1.7	Light Blocking Capability	64
5.1.8	Individual Specification Verification	64
6	Discussion and Results	69
6.1	Device Implementation	69
6.2	Quantum Dot Experimentation	72
6.3	Design Considerations	77
6.3.1	Economic Impact	77
6.3.2	Environmental Impact	77

6.3.3	Societal Influence	77
6.3.4	Political Ramifications	77
6.3.5	Ethical Concerns.....	78
6.3.6	Health and Safety Concerns.....	78
6.3.7	Manufacturability	78
6.3.8	Sustainability	78
7	Final Design and Validation.....	79
7.1	Design Workflow	79
7.2	Design Assembly	80
7.3	Financial Considerations	81
7.4	Device Verification Testing	84
7.5	Experimental Validation Testing	85
8	Conclusions and Recommendations	86
8.1	Engineering Design Conclusions	86
8.2	Experimental Conclusions.....	87
8.3	Engineering Device Recommendations	88
8.4	Experimental Recommendations.....	89
	Works Cited.....	91
	Appendices.....	I
	Appendix A: Original Statement of Client Needs.....	I
	Appendix B: Work Breakdown Structure.....	II
	Appendix C: Gantt Chart	IV
	Appendix D: Standard Operating Procedure for Staining Cells Prior to Imaging.....	V
	Appendix E: Verification Protocol Testing for Mechanical Interference, Cell Shearing, and Issues of Manual Dexterity	VI
	Appendix F: Verification Protocol Testing Used to Test the Low Fluid Alarm	X
	Appendix G: Verification Testing Protocol Used to Determine Concentration of a Substance in the Slide Chamber as a Function of Perfusion Time	XI
	Determination of the Relationship Between Concentration and Time	XII
	Appendix H: Verification Protocol Testing the Consistency of Positions of the Inflow and Outflow	XV
	Appendix I: Verification Protocol Testing for Compatibility with the Thermal Control Setup	XVI
	Appendix J: Verification Protocol Testing the Consistency of Fluid Volume in the Slide Chamber.....	XVII
	Appendix K: Verification Testing the Effectiveness of the Light Shield	XVIII
	Appendix L: Standard Operating Procedure for Insertion of a Slide into the Slide Chamber	XX

Appendix M: Standard Operating Procedure for Breakdown of the Olympus Microscope XXI
Appendix N: MATLAB Script used for Data Analysis and Presentation XXII
Appendix O: Standard Operating Procedure for the Production of Ringer’s Solution XXIV
Appendix P: Standard Operating Procedure for Production of Complete Neuron Medium XXVI
Appendix Q: Standard Operating Procedure for Changing of Cell Medium XXVII

Table of Figures

Figure 1: The hippocampus, a region of the brain known to play a role in memory formation	6
Figure 2: A cartoon schematic of a human astrocyte cell.....	8
Figure 3: Structure of a neuron.....	9
Figure 4: Structure and function of a neuron synapse	10
Figure 5: Visualization of the membrane potential during an action potential	12
Figure 6: Hippocampal neurons stained with intracellular Oregon Green BAPTA (OGB) dye.....	13
Figure 7: The structure of a Qdot® 655 ITK.....	14
Figure 8: Hippocampal neuron with Carboxyl-coated QDs	15
Figure 9: The excitation and emission spectrum of CdSe-ZnS Qdots®	16
Figure 10: The effect of the electric dipole moment of a QD.....	17
Figure 11: Calcium imaging method.	19
Figure 12: Plotted Regions of Interest	20
Figure 13: Olympus microscope calcium imaging setup.....	21
Figure 14: Parts of the base plate of the Olympus Microscope.....	21
Figure 15: Computer model of the thermal control ring.	22
Figure 16: The perfusion chamber, which holds a circular glass slide.....	22
Figure 17: The microscope arm.	23
Figure 18: The perfusion system at UNG	24
Figure 19: The cardboard box light shield.....	25
Figure 20: The path followed by the perfusion system	27
Figure 21: Volume of fluid in the slide chamber.....	29
Figure 22: Computer model of the open perfusion system.....	38
Figure 23: Computer model of the closed perfusion system	39
Figure 24: Computer model of the closed loop system.....	41
Figure 25: Computer model of the static beaker system	42
Figure 26: Components of the first prototype design	47
Figure 27: The interference of prototype one with the metal holder	49
Figure 28: Computer model and real model of the revised prototype	50
Figure 29: The light shield of prototype two	50
Figure 30: Issues with prototype two	51
Figure 31: Prototype three, featuring a 45 degree shift in pipette access point.....	52
Figure 32: A comparison of the prototype two and three light shieldse.....	53
Figure 33: A simplified diagram of the Low Fluid Alarm system.	54
Figure 34: Major components of the Low Fluid Alarmil.	55
Figure 35: Computer model of the beta design.....	57
Figure 36: Interior View of bottom section of the Beta Design.....	58
Figure 37: The printed beta design.....	59
Figure 38: Expanded holes in the side of the printed components.....	60
Figure 39: Plug-ins of the thermal control ring.....	63
Figure 40: Calcium imaging of multiple neurons with TTX and perfusion system.....	70
Figure 41: Calcium imaging of multiple neurons with Gabazine and perfusion system	71
Figure 42: Calcium imaging of multiple neurons with 0.8nm of Streptavidin QD-655.....	73

Figure 43: A 3D reconstruction of carboxyl-coated Quantum Dots. 74
Figure 44: Calcium imaging of multiple neurons with 0.8nm of carboxyl-coated QD-655. 75
Figure 45: The effect of Gabazine on neuron cultures. 75
Figure 46: The effect of TTX on calcium activity of neruons stimulated by carboxyl-coated QD..... 76

Table of Tables

Table 1: Top level project objectives	30
Table 2: Pairwise Comparison Chart	31
Table 3: Morphological Chart of the functions and means of the device	35
Table 4: Specifications of the Design.	36
Table 5: Design Evaluation Matrix of the four design alternatives.....	46
Table 6: An overview of the state of completion of the various specifications	64
Table 7: Costs of all materials needed to manufacture the beta device	82
Table 8: Costs of all materials needed to manufacture any future devices	83

Key Terms and Abbreviations

Key Terms

Absorption Spectrum – The range of frequencies of light which are absorbed by a substance

Action Potential – A movement of voltage along an axon, which carries information from one neuron to another

Axon – A long projection, extending away from a neuron, which carries information to other cells

Bright Field Microscopy – A simple technique of microscopy that uses the full, un-manipulated visible spectrum of light

Calcium Imaging – A technique of observing relative levels of calcium concentration in cells by adding a calcium-sensitive dye to the cellular environment

Carboxyl-coated Quantum Dots – A quantum dot coated with COOH- functional groups that can adhere to parts of neurons

Cell Shearing – Removal of adhered cells from a glass slide, caused by fast-moving liquid in their environment

Dendrite – The protrusions from a neuron body, which receive signals from other neurons

Dipole Moment – A measure of the positions of electrical charges on a molecule or nanoparticle that causes a change in voltage in the local environment

Emission Spectrum – The frequencies of light released from a substance as it moves from a state of high energy to low energy

Fluorescence – A property of some materials that absorb light in one spectrum of frequencies and re-emit it in another spectrum

Fluorescence Microscopy – A technique of microscopy that uses fluorescent dyes to observe specific cellular events

Gabazine – A drug that prevents any inhibition of neural activity by blocking GABA-receptors in the synapse

Glial Cells – Cells other than neurons in the brain that serve a variety of supporting functions and use calcium as a secondary signaling mechanism

Hippocampus- A region of the brain responsible for the formation of memories

Ion Channel – A pathway through the cell membrane that allows for the flow of charged particles, which can be opened and closed by environmental factors

Light Shield – A component of some microscopes which blocks ambient light from entering into the system

Membrane Potential – The difference in electrochemical potential between the inside and outside of the cell membrane

Micropipette – A device used to measure and inject small, precise volumes of solution

Molar Extinction Coefficient – A measure of how well a sample absorbs light of a certain frequency

Neuron – The functional unit of the brain

Neurotransmitter – A chemical which can interact in the synapse to regulate the transmission of action potentials

Numerical Aperture – A quantity related to the maximum resolution of a lens, higher numerical apertures allow for more detailed imaging

Objective Lens – A microscope component that gathers light from the sample

Oregon Green BAPTA – A fluorescent dye which glows more brightly in the presence of high concentrations of calcium

Perfusion – A flow of fluid over the surface of a cell culture

Photobleaching – A loss of brightness over time experienced by many fluorescent dyes that is caused by exposure to ambient light

Plasticity – The ease with which a group of neurons forms new synaptic connections

QD-655 – A filter which allows the microscope camera to absorb only the frequency of light released by certain quantum dots

Quantum Dot – A nanoparticle with fluorescent properties that produces a temporary voltage upon exposure to certain frequencies of light

Quantum Yield – A ratio of the number of photons a fluorescence sample emits to the number of photons it absorbs

Quenching – A process which reduces the brightness of a fluorescent sample

Ringer's Solution – A solution that mirrors the concentrations of ions and nutrients found in the brain

Semiconductor – A material that can have either conductive or insulative properties

Soma – The large, central part of the neuron containing the nucleus

Spectrophotometer – A device which measures the opacity of a solution to a particular frequency of light

Stokes Shift – The difference between the peak of the spectra of frequencies of light absorbed and emitted by a particle

Streptavidin – A molecule used to help bind functional coatings to the surface of nanoparticles

Synapse – The junction between a dendrite and an axon of two neighboring neurons

Two-photon Microscopy – a technique used in fluorescence microscopy which reduces background interference due to ambient light

Ultraviolet Light – A high-energy region of the light spectrum that is invisible to humans

Voltage – A tendency for electrically charged particles to move

Abbreviations

ABS – Acrylonitrile Butadiene Styrene, a polymer used in 3D printing

DIC – Differential Interference Contrast microscopy, a technique which can be used to amplify contrast in otherwise transparent samples

EPSP – Excitatory Postsynaptic Potential, a voltage across the synapse that makes an action potential more likely to occur

fMRI – Functional Magnetic Resonance Imaging, a noninvasive method for detecting brain activity

FRET – Fluorescence Resonance Energy Transfer, a technique used in fluorescence microscopy to study the chemical or physical interactions between two particles

GABA – gamma-Aminobutyric acid, a neurotransmitter responsible for inhibiting the propagation of action potentials in a synapse

IPSP – Inhibitory Postsynaptic Potential, a voltage across the synapse that makes an action potential less likely to occur

ICTP – The International Centre for Theoretical Physics

OGB – Oregon Green BAPTA, a fluorescent dye

PEG – Polyethylene Glycol, an inert polymer added to the surface of quantum dots to prevent interaction with biological processes

PET – Positron Emission Tomography, an invasive method for gaining information on the functioning of a biological sample using a radioactive dye

QD – Quantum Dots, semiconductor nanoparticles less than 100nm in diameter

ROI – Region of Interest, a particular area of an image

TTX – Tetrodotoxin, an inhibitor of action potentials that blocks fast-acting sodium channels

UNG – The University of Nova Gorica

WPI – Worcester Polytechnic Institute

1 Introduction

A neuron sits on a small glass slide, bombarded with intense blue light and shining back with green fluorescent shine. With a sudden change in the concentration of calcium ions inside the cell, there is a flash of green brilliance. The random waves of electrical activity in the isolated neuron trigger a transient release of chemicals. When one neuron grows next to another, however, they physically connect, and engage in patterned and synchronized waves of electrical and chemical activity.

Human beings possess 86 billion synchronously communicating neurons, held together in a single three-pound mass (Azevedo F. A., et al., 2009). The human brain may be the most complex living network of any kind in the known universe. This level of detail and complexity has scientists working across the globe to develop technologies with sufficient resolution and throughput to map the entire brain: from cell, to system, to thought.

The public demand to understand neuroscience is also apparent; in 2004 alone, the total cost of treatment for nervous system disorders across Europe was €447 billion (Andlin-Sobocki, 2005). For instance, when the hippocampus is destroyed on both sides of a mammal's brain, the ability to form new memories is largely lost (Johnston, 2004). Thus, the neurons in this region of the brain have come under scrutiny in order to better understand neural plasticity, the ability to form new memories (Wiocur, Wojtowicz, Sekeres, Snyder, & Wang, 2006). The hippocampus has a simple structure, consisting of a single folded layer of neurons. Additionally, genetic mutations in hippocampal neurons have been linked to epilepsy (Alberts, 2008), a chronic condition in which synchronous firing of neurons in the hippocampus causes dramatic seizures.

There are currently several gold standard methods used to study neuron signaling, which gather information at the level of both the individual neuron and at the level of the overall brain structure. Techniques have been applied to both *in vitro* samples and living subjects. However, there is no technology that exists capable of bridging these levels. *In vitro* cultures are generally studied with patch clamping, the Nobel Prize winning electrophysiological method that directly measures the electrical activity in cells and tissue slices. Patch clamping recordings can be varied in scale from a single pore in a membrane to the overall voltage in the cell culture. The method, though, cannot be used *in vivo*, due to physical limitations of the large electrodes in a small space (Hamill, Marty, E, B, & J, 1981). With increasing complexity in the brain, fluorescent dyes are used to reveal the waves of calcium oscillations among groups of cells. Calcium levels are reliable and indirect indicators of electrical activity in neurons

(Innocenti, Parpura, & Haydon, 2000). Fluorescent *in vivo* imaging has even been pioneered using dyes that require radiation from two photons of light to simultaneously strike a target molecule, limiting the chance background particles shining into the focal plane (Stosiek, Garaschuk, & Holthoff, 2003). Finally, conscious and subconscious mental activity can be studied using fMRI. This technique measures the different magnetic responses of oxygenated and deoxygenated blood in the brain, resulting in an effective map of brain activity (Logothetis, Pauls, Augath, & Trinath, 2001). However, fMRI offers insufficient spatial and temporal resolution, which impacts the ability to record transient signals.

Nanoparticle Quantum Dots (QDs) are a promising alternative that may one day unite the many facets of neuroscience, due to their unique optical and electrical properties. Their bilayer crystalline structure consists of a metallic core and ceramic coating, which combine to impart fluorescent and electrical properties to the particle. Optically, QDs are much brighter than traditional fluorescent dyes. These particles are resistant to photobleaching, or fading over time, and also have a higher optical efficiency than these dyes, reemitting a large percentage of the energy they absorb as light (Murphy, 2013). Additionally, QDs have tunable properties, depending on the size of the core, which dictate the color at which the QDs emit light, allowing for unique experimental approaches (Murphy, 2013).

Electrically, QDs have shown the ability to interact with neurons. Specifically, certain types of QDs dramatically modify the characteristics of action potentials, the electrochemical signals that neurons use to rapidly transmit signals (Zhao, Xu, Zhang, Ren, & Yang, 2009). The frequency and pattern of action potentials determines the information sent from one neuron to the next. Zinc-Oxide QDs embedded in a polymer matrix have been shown to increase both the frequency and duration of action potentials in neurons (Lugo, Miao, Rieke, & Lin, 2012). The efforts to bridge the different levels of neuroscience are global in scale. In addition to efforts by Lugo et al in Seattle, USA, researchers at the University of Nova Gorica (UNG) in Slovenia are studying the effects of Zinc-Sulfide shelled, Cadmium Selenium core QDs on rat hippocampal neurons. Dr. Giulietta Pinato has noted that *in vitro* application of QDs to a culture of hippocampal neurons causes synchronous action potentials in the culture. At UNG, researchers are conducting experiments to learn more about the interaction between QDs and hippocampal neurons.

These experiments were completed at the newly renovated Centre for Biomedical Sciences and Engineering in the town of Vipava, Slovenia. This relatively new laboratory offers many opportunities for improvements to both the available equipment and techniques used. Dr. Pinato's experiments have proven to be time and labor intensive, due in part to a handmade and highly variable perfusion system,

used to supply various concentrations of molecules to neural cultures during calcium imaging. The goal of our project was to design and build a device that rapidly removes unwanted material from the culture, blocks ambient light from the microscope, minimizes the use of expensive test materials, and increases both ease-of-use and consistency. This device was created using mostly available parts and at a total cost of less than €20 (\$30). Simultaneously, the team furthered Dr. Pinato's research into the electrical interactions of various CdSe-ZnS QDs with hippocampal cells. After the seven-week project, the students presented their research findings and new device to UNG sponsors and Worcester Polytechnic Institute advisors.

2 Background

The University of Nova Gorica's (UNG) Centre for Biomedical Sciences and Engineering is a newly opened research campus in Vipava, Slovenia. Researchers at this Centre need accurate and inexpensive ways to advance their current research. This section describes the important requisite information needed to understand the research efforts in neuroscience and nanoparticles at the Centre. This chapter first portrays the societal, clinical, and research significance of neuroscience. Particular emphasis is placed on current methods and techniques used to measure the physiological processes of the brain. Next, a background in neuroscience is provided, detailing physiological signaling events in the hippocampus, then in groups of neurons, and finally, single cells. At this level, electrical activity of hippocampal neurons can be stimulated and synchronized by nanoscale particles called Quantum Dots (QDs). We will outline the state of the art to study QDs and neurons simultaneously, with particular emphasis on fluorescence microscopy. With fluorescence microscopy, QDs can be visualized simultaneously with calcium ions in the cell, by use of dyes that change with ion concentration. Fluorescence microscopy is often performed with a perfusion system on the microscope that delivers test solutions to the culture, used in this case to characterize neural activity.

2.1 Clinical & Research Significance of Neuroscience

Diseases affecting the brain are common causes of medical problems across the world, with the cost of treatment for brain-related illnesses in 2004 in Europe amounting to €447 billion (Andlin-Sobocki, 2005). The cost is due in part to the incredible complexity of the brain. With 86 billion neurons, each with approximately 1000 connections, the human brain is a higher-order labyrinth that, to this day confounds the biggest super-computers and most intelligent scientists (Azevedo F. , et al., 2009).

However, significant progress has been made to map the activities of the brain from cell, to system, to thought, in order to better understand and treat brain disorders. The history and success of neuroscience is a result of many specific techniques, ranging from single-cell electrodes, to ion measurements across many cells, and on to whole brain scans of anatomy and mental activity. Uniting these aspects of neuroscience will be crucial to develop treatments for neurological problems.

It is possible to directly measure the electrical activity of a single neuron. In 1981, Robert Keher published a novel technique, called patch clamping, which revolutionized the understanding of the brain. This technique allowed, for the first time, direct measurements of the electrical properties of a single pore in the plasma membrane, further elucidating the mechanisms by which neurons are able to

transfer electrical information. Ten years later, Keher was awarded a Nobel Prize for his work. For many years, this technique provided significant insight into neuronal function. However, because the technique requires the precise placement of relatively large pipettes and electrodes in a small culture, there is a limit to the number of simultaneous recordings (Hamill, Marty, E, B, & J, 1981).

At the next level, fluorescent imaging is used to infer information about the electrical activity of neurons. Commonly, the dye Oregon Green BAPTA (OGB) is used, which fluoresces brighter when bound to calcium ions (Bootman, Reitdorf, Walker, & Sanderson, 2013). As a neuron generates an electrical signal, the change in intensity of light from the dye can be detected under a microscope and measured.

Currently, calcium imaging using dyes has been expanded to *in vivo* environments, using a two-photon system. In this approach, the fluorescent dye responsible for the calcium signaling needs the simultaneous energy of two photons of light striking it at once in order to reemit one photon of longer-wavelength light (Stosiek, Garaschuk, & Holthoff, 2003). Studies have shown that *in vivo* Fluorescent Resonance Energy Transfer (FRET) imaging has been used effectively with QDs (Ingram & Zhang, 2013).

At the highest levels of brain function, functional Magnetic Resonance Interference (fMRI) imaging and Positron Emission Tomography (PET) scans are used to map the activity of the overall brain. fMRI uses the ratio of the magnetic resonances, a unique molecular property, of oxygenated and deoxygenated hemoglobin in the brain to better understand the metabolic activity of the brain. fMRI does not require the injection of dyes or stains into the body, but the procedure does lack spatial and temporal resolution (Logothetis, Pauls, Augath, & Trinath, 2001). PET, by contrast, uses an injected positron-emitting radionuclide tracing material to track particles in the brain. Oftentimes, PET radionuclides are conjugated to a glucose analog that allows scientists and doctors to track metabolic activity (Cheng, et al., 2006).

2.2 Neurobiology

UNG researchers tasked the team to investigate the relationship between quantum dots and hippocampal neurons, a type of brain cell. In order to investigate the electrophysiological interaction, it was first necessary to understand the biological functioning of the hippocampus itself and related cellular processes.

2.2.1 The Hippocampus

The hippocampus is part of the limbic system and is a target for stress hormones. This region of the brain resides in the medial temporal lobe of the brain, underneath the cerebral cortex, as seen in Figure 1 (McEwen, 1999). The hippocampus is composed of two sheets of neurons folded onto each other, taking the shape of a seahorse (Bear, Connors, & Paradiso, 2007). This relatively simple physical organization, as compared to other sections of the brain, makes the hippocampal region ideal for studying synaptic transmission (Bear, Connors, & Paradiso, 2007).



Figure 1: The hippocampus, a region of the brain known to play a role in memory formation

The neurons in this region of the brain have come under scrutiny in order to better understand neural plasticity (Wiocur, Wojtowicz, Sekeres, Snyder, & Wang, 2006). Plasticity is the ability of neurons to change and form new connections with other neurons. It is related to the rate at which neurons fire action potentials, which varies depending on the magnitude and duration of stimulation. Plasticity causes changes in the expression of genes, which encode for receptors on the cell membrane of neurons. Moreover, neurons can atrophy from over-stimulation due to hormones and loose physical connections with their neighbors (McEwen, 1999). This ability for neurons to adapt their physical synaptic connection is thought to play an important role in the formation of memory.

2.2.2 Neurons and Neuronal Cells

Hippocampal plasticity results from two neurons interacting and changing the frequency or duration of their electrical activity. Neurons require a highly controlled extracellular environment to effectively transmit signals. By themselves, neurons are not capable of regulating the entire brain. The other cells of the brain are collectively called glial cells. In mammals, glial cells are distinct from typical neurons in that they are able to continuously divide and reproduce over the lifetime of an organism (Eriksson, 1998). From the Greek word 'glue', glial cells serve as supporting cells for neurons, fulfilling four main functions; (1) providing structural support for neurons, (2) supplying neurons with nutrients and oxygen, (3) insulating the axons and dendrites of neurons for more efficient signaling, and (4) phagocytizing, or ingesting and destroying, pathogens and dead neurons.

There are several glial cell types, which vary in function and morphology. The most notable types of glia are astrocytes, oligodendrocytes, and microglia (Haydon, 2001). Astrocytes, seen in Figure 2, are the primary supporting cells in the brain, possessing numerous branches that extend away from the neuron cell body. Dendrites regulate the extracellular chemical environment of neurons. Astrocytes recycle neurotransmitters from the synapse to minimize the delay between action potentials, as well as remove excess ions, notably potassium, from the extracellular environment (Haydon, 2001). Astrocytes have been shown to exhibit calcium signaling when a messenger molecule, IP₃, is released into gap junctions between neighboring cells. IP₃s release stimulates a calcium wave that propagates from cell to cell, although this wave is distinct from action potentials (Innocenti, Parpura, & Haydon, 2000). Oligodendrocytes are cells that insulate the axons of neurons to increase the efficiency of electrical signaling in action potentials (Haydon, 2001). Microglia are highly specialized macrophages that are capable of phagocytosis in the central nervous system. These are active even in the healthy brain tissue, clearing undesirable dead neurons and pathogens that have intruded into the brain's environment (Ballabh, Braun, & Nedergaard, 2004).

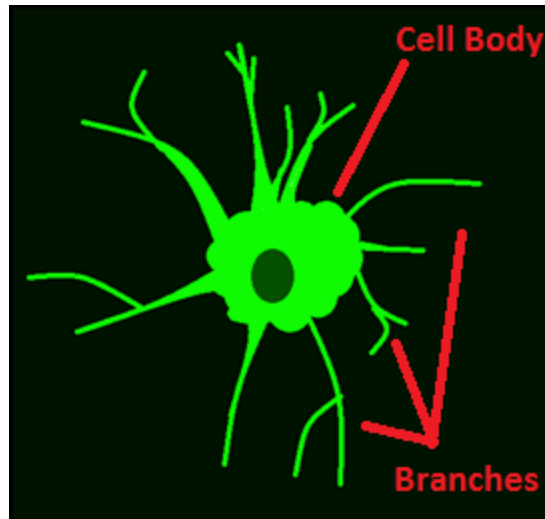


Figure 2: A cartoon schematic of a human astrocyte cell; A supporting cell that regulates neurotransmitters and ion concentrations outside neurons. Note the numerous branches that extend from the neuron cell body. Astrocytes exhibit calcium waves, but do not propagate action potentials.

It is important to identify glial cells of *in vitro* cultures when studying the brain, as they do not have the ability to fire action potentials, but still exhibit waves of calcium signals as a form of secondary messaging. Thus, glial cells have electrophysiological properties of their own and contribute to the calcium ion flux of neural networks. These properties result in many artifacts during calcium imaging that might be identified as neurons without concurrent visualization with conventional bright field imaging. Overall, the magnitude of calcium transients during wave propagation in astrocytes is not as great as calcium transients in action potentials. They produce smaller, but detectable, signals during calcium imaging, which may be confused with the calcium signals of action potentials. (Fields & Stephen-Graham, 2002).

Neurons are the most basic cells of the nervous system, which can be separated into three categories: sensory, motor, and interneurons. Despite their different functions, most neurons are comprised of the same four components: the cell body, the axon, the dendrites, and the synapse, as seen in Figure 3.

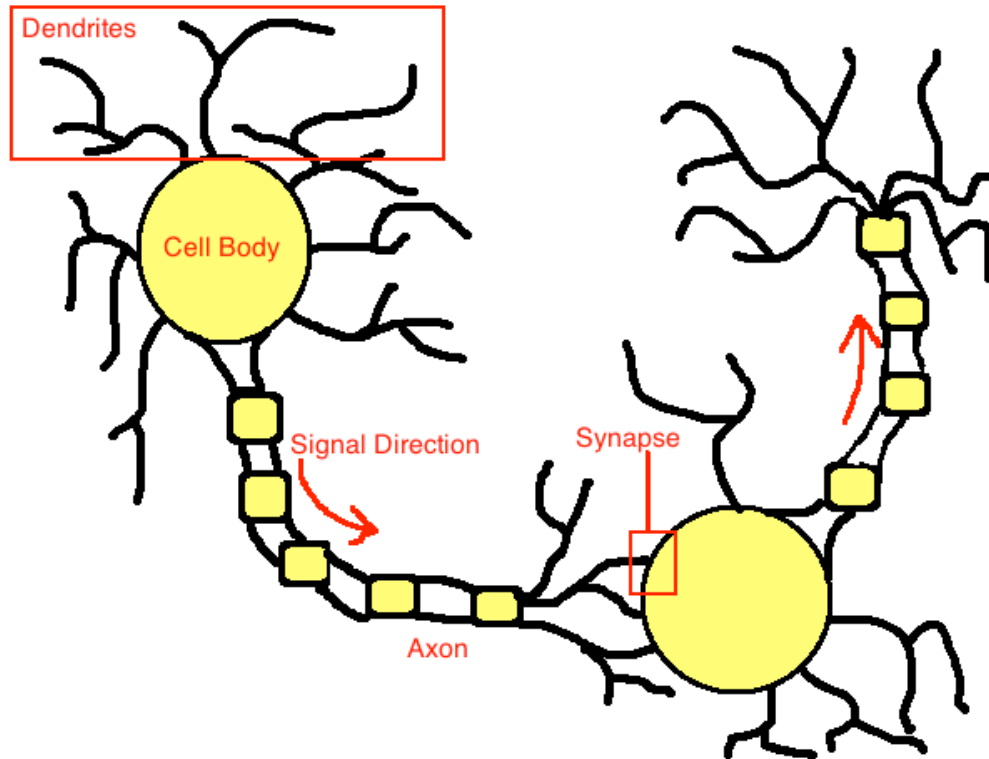


Figure 3: Structure of a neuron; Axons carry information from one cell body to the dendrites of another, allowing cells to communicate. Adapted from (Alberts, 2008)

The soma, or cell body, is the roughly spherical center of the neuron. It is about $20\mu\text{m}$ in diameter and houses the nucleus (Bear, Connors, & Paradiso, 2007). The dendrites are finger-like extensions of the cell body that extend to neighboring neurons. Dendrites essentially function as a neuron's antenna, receiving signals from neighboring cells (Bear, Connors, & Paradiso, 2007). On one side of the cell body, the axon extends to reach other neurons. The axon is uniquely responsible for sending information over long distances. The beginning of the axon, connected to the cell body, is called an axon hillock; this is where an action potential begins. Axons may either branch or remain a single conduction path; regardless, each axon branch ends with a synapse, which connects to nearby dendrites (Bear, 38). The release of neuron-specific signaling molecules, called neurotransmitters, from the synapse causes the proliferation of action potentials in the brain.

A synapse is the junction between two cells across which neurons transmit action potentials. Action potentials are all-or-nothing chain reactions that proceed down the length of the axon. Two types of neurotransmitters play roles in passing along action potentials to post-synaptic cells, as seen in Figure

4. Neurotransmitters cause either excitatory postsynaptic potentials (EPSPs), if neurotransmitters elicit the flow of positive ions, or inhibitory postsynaptic potentials (IPSPs), if neurotransmitters elicit the flow of negative ions. If the sum of the EPSPs minus the sum of the IPSPs is greater than the action potential threshold, then the action potential is transferred across the synapse to the neighboring cell (Johnston, 2004).

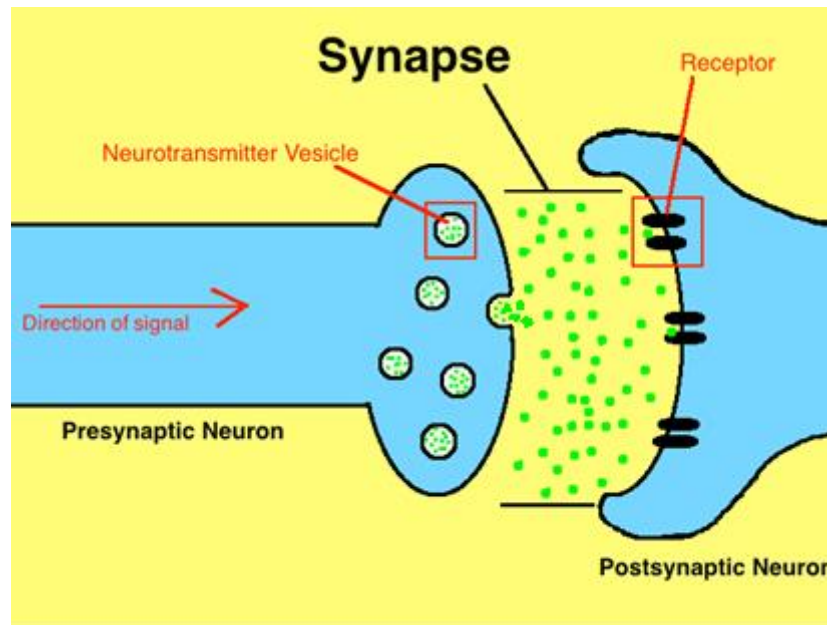


Figure 4: Structure and function of a neuron synapse; Information is carried from one neuron to another in the form of neurotransmitter chemicals. The terms 'presynaptic' and 'postsynaptic' refer to the transmitting and receiving cells, respectively. Adapted from (Alberts, 2008)

The neurotransmitters acetylcholine, glutamate, and serotonin usually evoke the EPSP response by opening the transmitter-gated cation channels in synapses, while the presence of gamma-Aminobutyric acid (GABA) or glycine evokes the IPSP response by opening transmitter-gated anion channels (Alberts, 2008). Cations are positively charged ions, such as sodium, potassium, or calcium, while anions are negatively charged ions, such as chlorine. GABA is the primary IPSP neurotransmitter in the mammalian central nervous system, causing a reduction in the frequency and duration of action potentials.

Gabazine is a frequently used drug in scientific research that blocks the activation of GABA-mediated neurotransmitter receptors in the synapse. Gabazine is an anti-IPSP drug that prevents the

opening of anion channels that normally inhibit action potentials in the post-synaptic cell. Thus, Gabazine cancels out all inhibition in synapses, causing frequent and synchronous action potentials (Lüscher & Keller, 2004).

2.2.3 Action Potentials and Calcium Ions

Most organisms possess the ability to rapidly respond to external optical, physical and chemical stimuli in their environment. Sensory neurons receive and translate these signals into electrical information, called action potentials, which are quickly conveyed throughout the organism. Action potentials are localized, temporary changes in the concentrations of cations and anions around neurons. When there is no net movement of ions across the membrane, the membrane is said to be in equilibrium. The electrical potential of a neuron is -70mV , commonly referred to as the resting potential. The negative sign comes from the convention to subtract the external potential, which is usually positive, from the internal potential, which is usually negative (Cooper & Hausman, 2013). This electrochemical potential is the tendency for ions to move across a cell membrane when an ion channel opens. A single neuron might typically contain 10 or more different types of ion channels, located in different regions of its plasma membrane (Alberts, 2008).

The electrical activity at any one spot on the axon during an action potential can be visualized on a graph similar to Figure 5, with the x-axis representing time in milliseconds (msec) and the y-axis representing membrane potential in millivolts (mV).

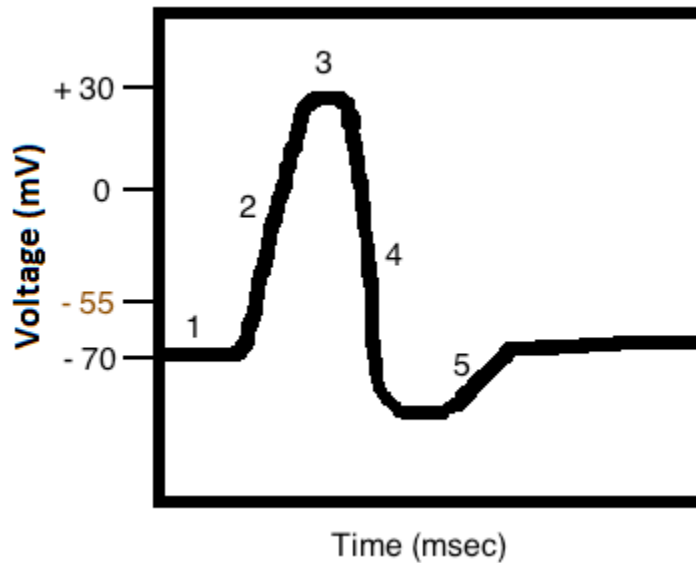


Figure 5: Visualization of the membrane potential during an action potential; (1) resting membrane potential, (2) the rising stage, or depolarization, when sodium flows into the cell, (3) hyperpolarization, when cytosol is more positive than extracellular environment, (4) falling phase, or repolarization, when potassium slowly resets, (5) refractory, or rest, period

The first part of the action potential is called the rising phase, or depolarization; it correlates with the rapid influx of positive sodium ions into the cell and corresponds with (2) in Figure 5. This positive feedback loop continues until the local plasma membrane potential has shifted from a resting value of -70mV to +50mV, almost the sodium equilibrium potential (Alberts, 2008). The peak of the spike at (3) is when the inside of the cell is more positive than the outside, also referred to as hyperpolarization (Bear, 82). The falling phase at (4), or repolarization, follows hyperpolarization and is characterized by the slow movement of potassium ions out of the cell (Alberts, 2008). The action potential lasts roughly 2ms and ends with the neuron returning to resting potential at -65mV. A relative refractory period of approximately 1ms is the time it takes for a neuron to be ready to conduct another action potential.

In equilibrium, the concentration of sodium ions is about 30 times greater outside the cell than inside, with the reverse being true for potassium ions (Alberts, 2008). Sodium ion channels have the benefit of efficiency; up to 100 million ions can pass through a channel per second, allowing for high signaling frequency (Alberts, 2008). However, sodium moves too fast in neurons to be accurately resolved with modern research-grade cameras and microscopes. The use of calcium ions as indicators is much more effective to infer electrical activity for three reasons (Alberts, 2008). First, transient

movement of calcium ions across the membrane is relatively slow (10-100ms) compared to fast-activating sodium ions. Second, calcium ion fluctuations are monotonic, meaning every action potential elicits a corresponding change in calcium concentration inside the cell. Third, there are 1000 times more calcium ions in the extracellular matrix than in the cytosol of the neuron. As a result, calcium ions are often used as indicators for action potentials in cells, as seen in Figure 6, because even a small influx of calcium ions into the can elicit action potentials (Alberts, 2008).

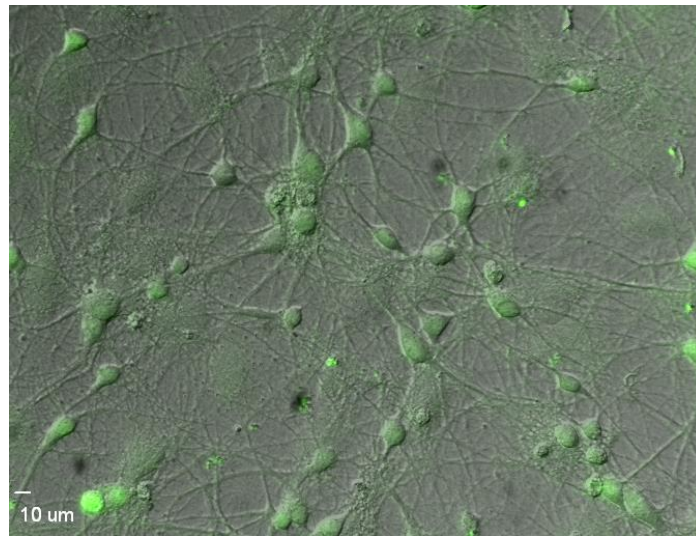


Figure 6: Hippocampal neurons stained with intracellular Oregon Green BAPTA (OGB) dye, which fluoresces brighter when bound to calcium, such as during action potentials.

When neurons are immersed in fluorescent Oregon Green BAPTA (OGB) dye, the dye permeates the plasma membrane and undergoes a conformational change that renders OGB membrane-impermeable. In this way, the dye accumulates on the inside of the cell. When calcium rushes into the cell, it binds to OGB and causes the dye to fluoresce brighter, similarly to an action potential. Thus, calcium-bound OGB can be used to effectively determine action potential signaling.

2.3 Quantum Dots

Modern biology requires scientists to visualize and understand molecular interactions, which are difficult to measure *in vivo*. One of the most promising avenues of sub-cellular imaging is QD-based fluorescence microscopy. When the electrons in a semiconductor are excited, they tend to remain at a

certain fixed distance from positive charges, called the excitation radius. QDs are 10-50nm diameter fluorescent nanoparticles that exhibit semiconductor capabilities. Their semi-conductive properties allow the dots to switch rapidly between states of highly conductive and highly insulative properties (Michalet, et al., 2005).

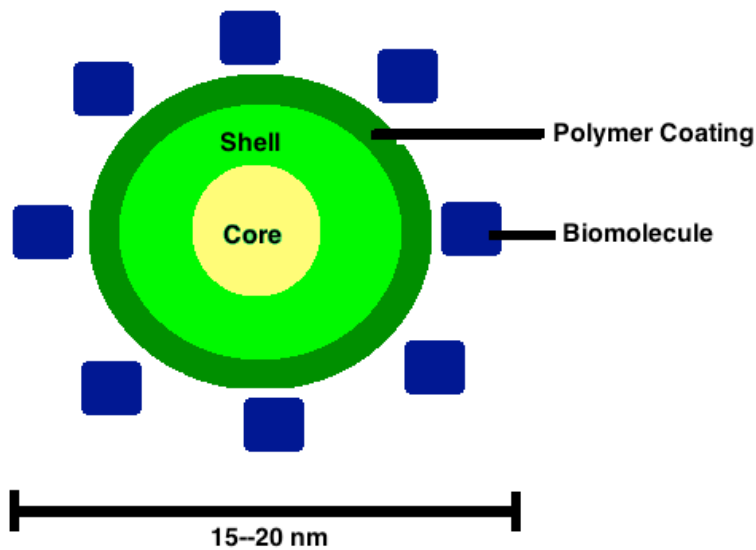


Figure 7: The structure of a Qdot® 655 ITK by Invitrogen, Life Technologies. Adapted from (Qdot Nanocrystals—Section 6.6)

Quantum Dots consist of three layers: the core, shell, and polymer coating. This coating is often conjugated with biomolecules that change the way QDs interact with cells, as seen in Figure 7. At UNG, research is focused on the CdSe-core, ZnS-shelled QDs with polyethylene-glycol (PEG) coatings used to minimize toxic effects by reducing the amount of heavy metals exposed to living tissue (Hardman, 2006). Additional functional groups can be conjugated to the polymer coating, namely carboxyl groups and streptavidin groups. Carboxyl groups are highly reactive, allowing QDs to be conjugated with a variety of materials. These QDs can be seen in Figure 8.

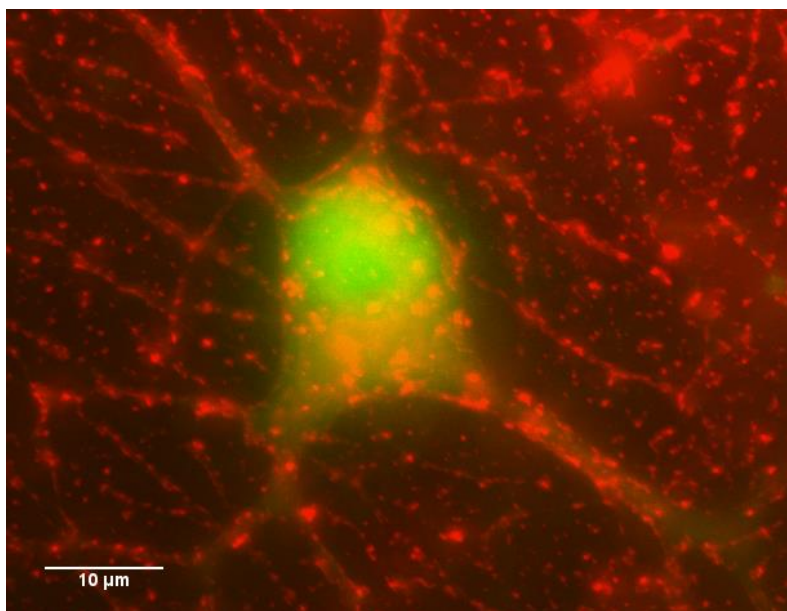


Figure 8: Hippocampal neuron with Carboxyl-coated QDs, shown in red, attached to its surface of the neuron. OGB bound to calcium, green, indicates the location of the neuron

Streptavidin is a biomolecule that has a high specificity for biotin molecules. Biotin molecules easily conjugate with most antibodies, allowing for specific molecule tracking and highly specific cell targeting (Howarth, Takao, Hayashi, & Ting, 2005). For example, QDs have shown the ability to fluoresce through up to 10mm of living tissue when targeted to cancer tumors in mice (Gao, 2004).

2.3.1 Optical Properties

Fluorescence is the emission of photons by atoms or molecules whose electrons have been excited to a higher energy state by radiation. The excited electrons almost immediately fall back to the lower energy states. In the process, electrons release the potential energy as either heat or as another photon of light (Murphy, 2013). Fluorescence microscopy uses this principle to resolve incredibly fine molecules, such as QDs, that would typically not be visible under a microscope, therefore allowing the distribution of a single molecular species to be visualized.

One of the most significant limiting factors in fluorescence microscopy with traditional fluorescent molecules, or fluorophores, is the effect of photobleaching, also known as fading. This phenomenon occurs when a fluorophore loses the ability to fluoresce, due to chemical damage or covalent modification. This causes a degradation in signal intensity over the course of imaging, as more

molecules become damaged (Murphy, 2013). QDs are incredibly resistant to photobleaching and can be tracked for long periods of time with no degradation in signal (Lacoste, et al., 2000).

Fluorescent molecules absorb photons of light at shorter wavelengths and emit photons of light at longer wavelengths (Murphy, 2013). The absorbance and emission peaks are never sharp, but rather are comprised of ranges of wavelengths, known as spectra. A graph of the excitation and emission wavelengths of eight different QD conjugates can be seen in Figure 9.

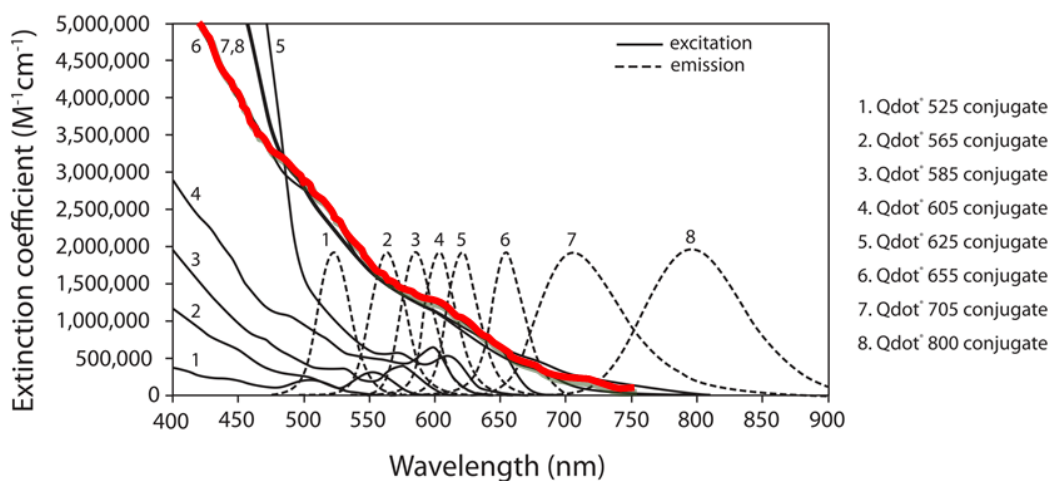


Figure 9: The excitation and emission spectrum of CdSe-ZnS Qdots® by Invitrogen, Life Technologies. Adapted from (Qdot Nanocrystals—Section 6.6)

The difference between the peaks in the absorbance and emission spectra is known as the Stokes shift. QDs have a remarkably wide and adaptable Stokes shift (Murphy, 2013). A large Stokes shift translates to more resolution in fluorophores, because the wavelength of light used to excite molecules is well separated from the wavelength of light used to record the signal. The size of the core of QDs dictates the emission spectral profile, with cores of sizes as small as 2nm emitting in the blue wavelengths of light, and larger cores of sizes 5-7nm emitting in the yellow and red wavelengths of light (Murphy, 2013). In practical terms, this means that smaller particles are harder to excite and produce more bluish light, while larger particles are easier to excite and produce more reddish light (Alivisatos, 1996). The emissions spectrum of QDs is remarkably symmetrical and exhibits large quantum efficiency

values in almost any medium, meaning they reemit a greater proportion of absorbed photons than typical fluorophores.

UNG currently uses a Quantum Dot called Qdot-655 by Invitrogen, a division of Life Sciences. The Qdot-655 has an absorption spectrum ranging from below 400nm up to 750nm, and an emission spectrum ranging from 600nm to 700nm. Sometimes, when a QD is excited by radiation, a temporary, local voltage can form in the area, otherwise known as a dipole moment. This unique property has produced innovative research exploring the use of QDs to stimulate electrical activity in neurons.

2.3.2 Electrical Properties

Quantum dots can be used to stimulate and intentionally trigger action potentials. The dipole moment of QDs is understood and has been quantified (Lugo, Miao, Rieke, & Lin, 2012). Lugo et al, has determined that if a QD is within a distance r from an ion channel, the ion channel can open and induce an action potential, as seen in Figure 10.

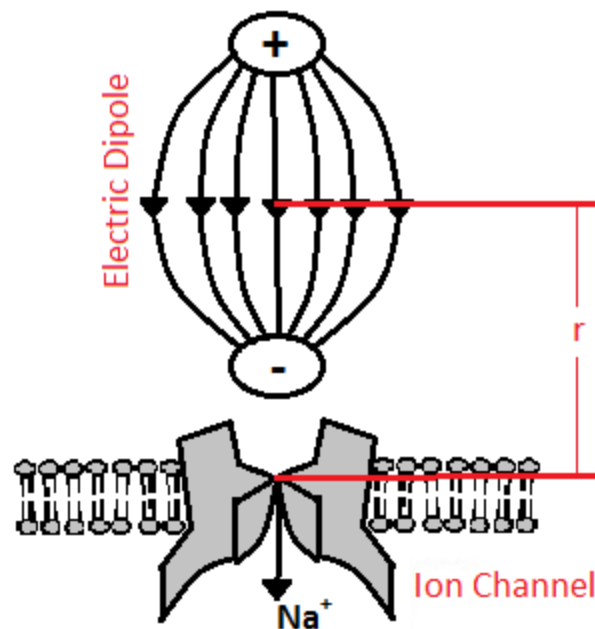


Figure 10: The effect of the electric dipole moment of a QD can interact with an ion channel in order to stimulate an action potential in neurons, when the QD is within distance r of that channel. Adapted from (Lugo, Miao, Rieke, & Lin, 2012)

Moreover, $r=20\text{nm}$ when the medium between ion channel and the surface of the QD shell is pure water. The value of r decreases in biological environments, or when QDs are coated with polymers or proteins (Lugo, Miao, Rieke, & Lin, 2012). Now, scientists are exploring the possibility of using QDs to elicit specific signals in neurons. This can be used to better understand neuronal plasticity and network dynamics (Cossart, Ikegaya, & Yuste, 2005).

Zinc Oxide nanoparticles have been shown to modify the profile and characteristics of action potentials (Jingxia, Lanju, Tao, Guogang, & Zhuo, 2008). At UNG, QDs used in culture cause unexpected effects with action potentials. The temporary voltage changes appear to trigger unexpected patterns of activity in hippocampal neuron cultures. Instead of orderly and sequential action potentials, all of the neurons appear to be depolarizing simultaneously and periodically. This makes experimental use of QDs as passive imaging agents for hippocampal neurons nearly impossible, as the QDs significantly change the functioning of the neural network. However, this effect has the potential to be used by scientists to intentionally stimulate action potentials, if more research is dedicated to understanding the mechanism of interaction of QDs and hippocampal neurons.

2.4 Quantum Dot-Neuron Interaction with Calcium Imaging

As discussed in Section 2.2.3, calcium is a good indicator of action potentials in neurons and the dye Oregon Green BAPTA (OGB) can be used to visualize the change in calcium concentration across the cell membrane. When calcium ions rush into the cell during an action potential, the OGB binds to the calcium and undergoes a conformational change. With a higher concentration of calcium, the dye fluoresces brighter, producing a higher intensity signal. OGB has an emission spectrum centered on the cyan color band at 488nm, with a peak excitation wavelength of 496nm and peak emission wavelength of 524nm (Long-Wavelength Calcium Indicators, 2005).

2.4.1 Calcium Imaging Data

Initially, calcium dyes are membrane-permeable, until they diffuse into cells, where the dye undergoes a conformational change to become membrane-impermeable. The molarity of the dye also changes as it is cleaved, so an excess of dye is able to accumulate inside the cell. After the unabsorbed dye is washed away from the culture, calcium imaging is performed using fluorescence microscopy.

There are, however, some inherent flaws with calcium imaging, as fluorescent intensity is dependent on many factors aside from the concentration of calcium in a cell. The concentration of dye loaded into cells can be highly variable between experiments and even between cells in the same culture. Additionally, intensity is influenced by the effective thickness of the neuron, as thicker neurons with more volume will have a greater concentration of calcium ions and accumulated dye relative to smaller neurons (Alberts, 2008).

The approach to calcium imaging is relatively straightforward, as seen in Figure 11.

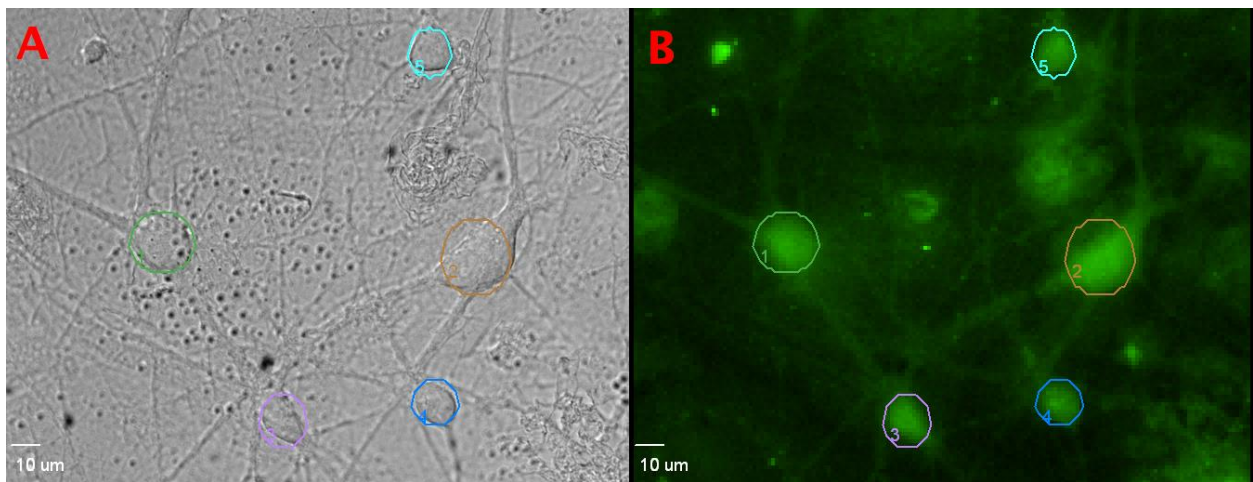


Figure 11: Calcium imaging method; (A) Differential Interference Contrast (DIC) image with Region of Interests (ROIs) over hippocampal neurons, (B) Fluorescent calcium imaging, measuring the intensity of light in the ROIs, with OGB dye seen fluorescing in green.

Regions of Interest (ROIs) are designated by colored circles in Figure 11A and represent the cell bodies of neurons. In a timelapse image, one frame of which is shown in Figure 11B, ROIs measure fluctuations in the intensity of light from OGB over time, generated by a change in calcium concentration. Calcium concentrations are monotonic with action potentials, as discussed in Section 2.2.3. A graph of the intensity of light versus time is shown in Figure 12.

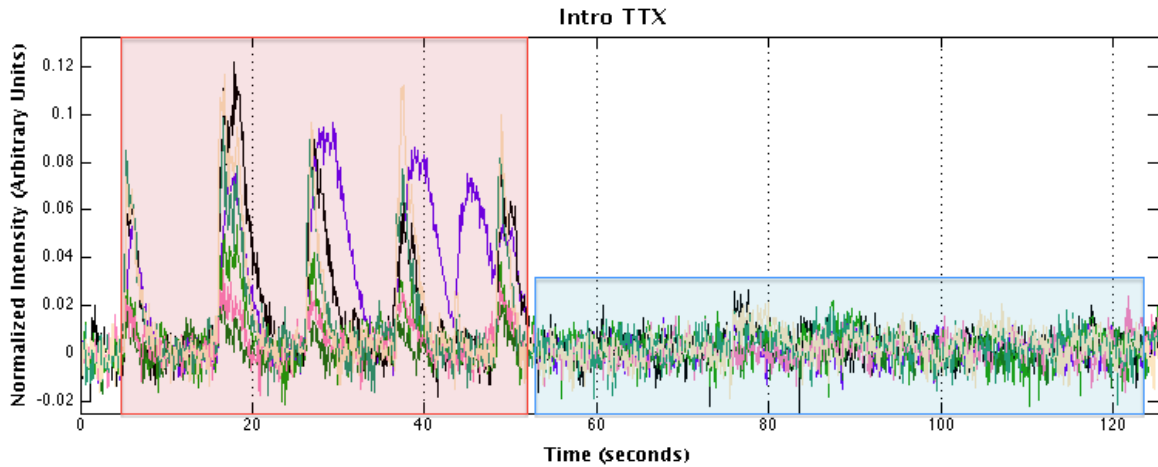


Figure 12: Plotted Regions of Interest; these indicate large fluctuations in calcium concentrations (red region) until the sodium channel blocker, TTX, is introduced and stops calcium flow due to action potentials (blue region)

The red highlighted region of Figure 12 indicates high levels of calcium signaling, a result of the presence of QDs in the culture. When TTX is introduced to the cells, sodium ion channels are blocked, ceasing action potentials and overall calcium activity. The introduction of test solutions containing drugs like TTX or QDs into cultures during live calcium imaging is a robust method to study the effects on networks of neurons.

2.4.2 Current Microscope Setup at UNG

The University of Nova Gorica at Vipava uses an Olympus IX81 Inverted Microscope and a 40x 0.9 Numerical Aperture air-immersion objective lens for calcium imaging of cultures of neurons, such as those seen in Figure 11. Although the microscope contains complex software and optics, the physical setup is comprised of only a few simple subsystems. The subsystems that the device interacts with are in the immediate vicinity of the cell culture and are shown in Figure 13. The microscope components of interest include the base plate, the thermal control ring, the slide chamber, the microscope arm, and the perfusion system.

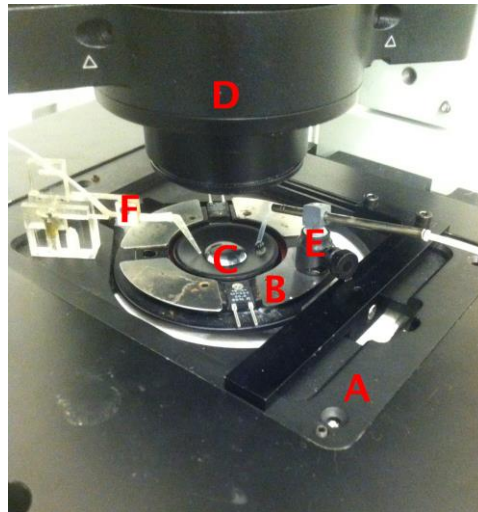


Figure 13: Olympus microscope calcium imaging setup; (A) base plate, (B) thermal control ring, (C) slide chamber, (D) microscope arm, (E) perfusion inflow, (F) perfusion outflow.

The first piece of the calcium imaging setup is the base plate. The base plate is an interchangeable part that can be switched out to allow imaging with alternative base plates. In the case of calcium imaging, the base plate holds the thermal control ring. The plate is made of a nonmagnetic, painted aluminum alloy and may be snapped into and out of the microscope, as seen in Figure 14. While inserted into the microscope, the base plate may be translated in the horizontal plane by computer control.

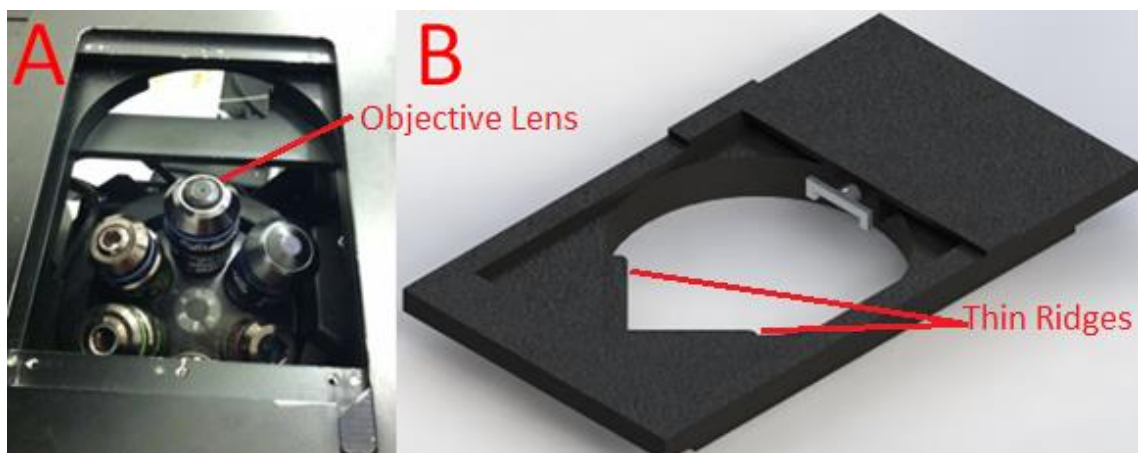


Figure 14: Parts of the base plate of the Olympus Microscope; (A) the void in the microscope that fits the base plate, with the objective lenses just below, (B) a computer model of the base plate, showing the thin ridges that the thermal control ring sits on

The base of the thermal control ring is a circular piece of nonmagnetic, painted aluminum that easily snaps into the base plate. The ring includes two-temperature control plug-ins and four pieces of steel on its surface. To achieve temperature control, cords must be plugged into both temperature control ports. In the current experimental setup, a magnet is attached to one of the steel plates and is used to hold the perfusion inflow in place relative to the slide. The thermal control ring is seen in Figure 15.

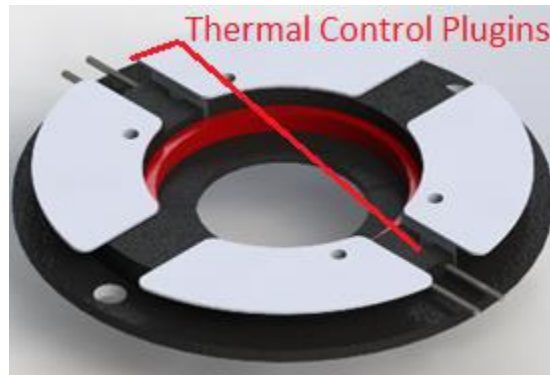


Figure 15: Computer model of the thermal control ring, with temperature control plug-ins on the left and right sides.

The slide chamber consists of two donut-shaped rings that fit together with a friction-press fit. The slide, which has a cell-coated surface during imaging, is held between them. When the slide is inserted into the slide chamber, the composite system forms a dish, capable of holding liquid without leaking, as seen in Figure 16.

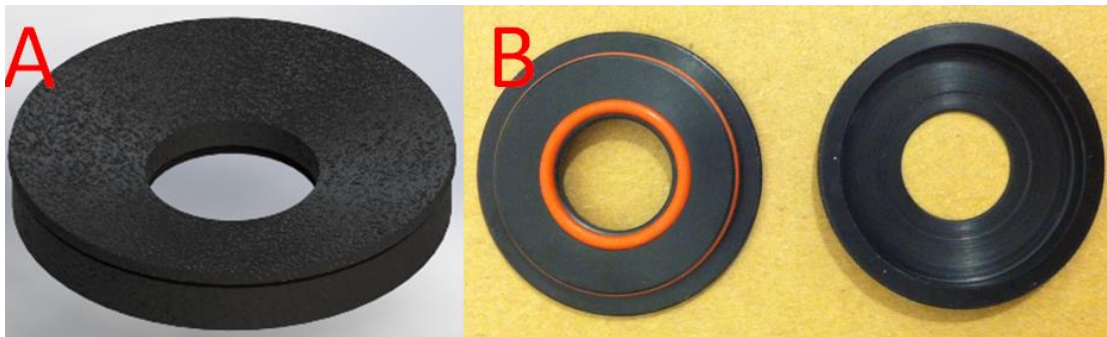


Figure 16: The perfusion chamber, which holds a circular glass slide; (A) computer model of the chamber, (B) two pieces, with the red rubber seal that ensures a watertight press fit.

The microscope arm, as seen in Figure 17 holds the lighting and imaging apparatus for DIC imaging. The arm is capable of pivoting back to allow easier access to the base plate or slide, but must be in the fully forward position for imaging. The path between the slide and the bottom of the microscope arm must be unobstructed to allow for DIC imaging.

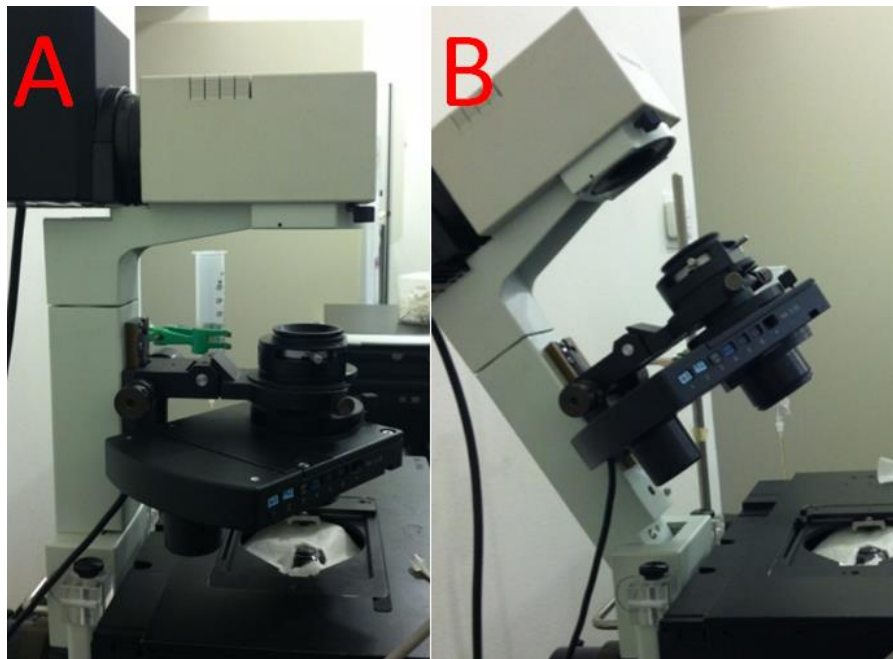


Figure 17: The microscope arm; (A) in the fully forward position, (B) in the fully back position.

Most *in vitro* calcium imaging is based on the use of a perfusion system, which streams a solution across the surface of neurons in a culture mounted to a microscope. The perfusion system at UNG, seen in Figure 18, involves a combination of parts, including the solution reservoir that holds and dispenses fresh Ringer's solution to maintain cell health during imaging, as well as magnetic connections to adjust the positions of perfusion inflow and outflow tubing.

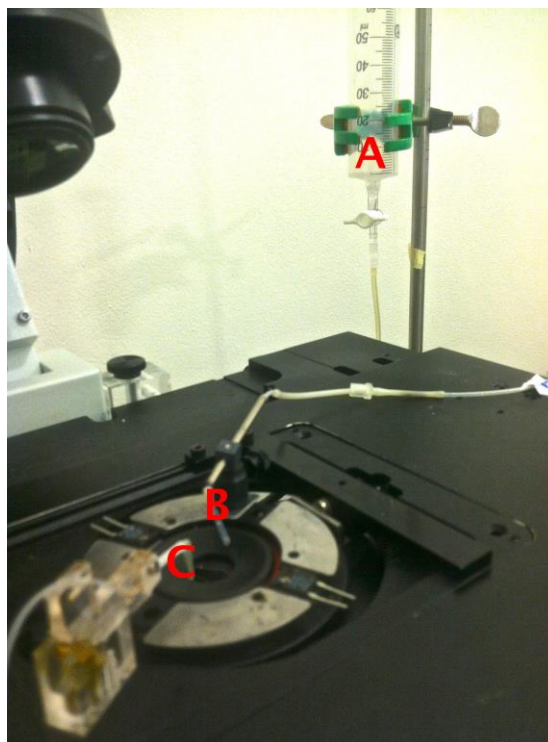


Figure 18: The perfusion system at UNG; (A) control solution reservoir at minimum height above the culture, dictating the speed of perfusion, (B) inflow tube, position affecting cell shearing, (C) the outflow tube, dictating the volume of solution in the slide chamber.

Ringer's solution is comprised of a combination of chemicals that together imitate the natural extracellular environment of the neuron. This solution can be administered by a perfusion system, which introduces fresh nutrients to the culture. Additionally, perfusion systems can administer drug treatments or nanoparticles to the culture.

Numerous companies offer perfusion setups that can be adjusted for different microscopes. For example, Warner's Instruments offers a setup that deliver stimuli to cells and are specialized to work with patch clamp technology. The current perfusion system at UNG is made from a medley of parts from different manufacturers that are not necessarily intended to fit together. However, this handmade system has the benefit of low cost.

Around the entire microscope is placed a large cardboard box. This box helps to block ambient light from entering into the system during imaging. However, it also prevents users from accessing or seeing the slide during testing. This can prevent the experimenter from becoming aware of issues related to the perfusion system, such as flooding.



Figure 19: The cardboard box light shield; it completely blocks users from seeing or accessing the sample during imaging, but also blocks a large amount of ambient light from reaching the slide.

3 Project Strategy

This chapter describes the steps taken to determine the appropriate approach to successful completion of this project.

3.1 Client Statement

The initial client statement challenged the team to design an experimental platform to investigate the interaction between Quantum Dots (QDs) and hippocampal neurons, as well as to characterize the role that QDs played in altering neuronal activity. Based on an initial proposal provided to the team by Dr. Pinato at the outset of the project¹ the following client statement was determined:

“Design a platform that allows for the determination of the relationship between quantum dots and observed voltage oscillations in hippocampal cells.”

The Centre for Biomedical Sciences and Engineering was a new campus, located in the recently renovated Palace Lanthieri in the town of Vipava, Slovenia. This relatively young laboratory offered many opportunities for improvements to the current equipment and procedures, especially for a team of four Biomedical Engineering undergraduates from Worcester Polytechnic Institute.

3.1.1 Current Methodology

The interaction between QDs and hippocampal cells was best visualized by means of detailed imaging with a research-grade microscope. Cultures of hippocampal cells were mounted on the microscope platform and immersed in a solution inside the slide chamber.

The existing microscopy system used a perfusion system to deliver the Ringer’s solution to cells. The delivery system used gravity to drive the inflow of Ringer’s solution from the solution reservoir to the slide chamber. A length of rubber tubing held on the far side of the dish used a vacuum pump to remove fluid from over the slide. The flow of liquid into the slide was termed the “Perfusion Inflow”

¹ The original document is available in Appendix A: Original Statement of Client Needs

system, while the pumping of fluid out of the slide was termed the “Perfusion Outflow” system. These systems can be seen in Figure 20.

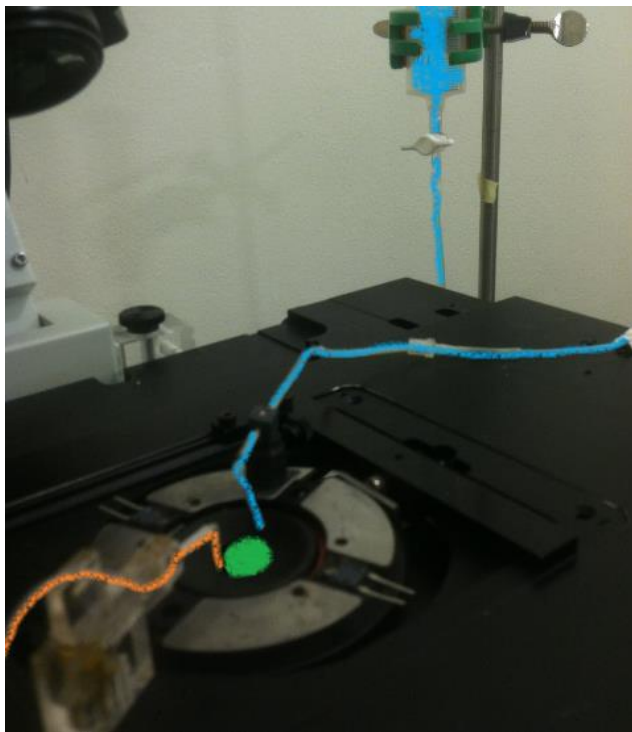


Figure 20: The path followed by the perfusion system; the “perfusion inflow” system, traced in blue, delivered fluid to the culture dish, where the “perfusion outflow,” indicated in orange, removed fluid from the top of the slide, with the volume of solution in the slide chamber indicated in green.

The solution reservoir was filled with Ringer’s solution and mounted at a certain height above the slide. A narrow tube with a valve connected the reservoir to the edge of the slide. When the valve was opened, fluid dripped into the cells’ environment at a rate proportional to the height of the solution reservoir. The height of the reservoir could be adjusted by sliding it up or down on a retort stand. To prevent fluid overflow and damage to the microscope, fluid was continuously removed by suction through the perfusion outflow system

To introduce the test solution, the experimenter first waited until the solution reservoir drained to a multiple of 10mL of volume. A preloaded micropipette containing a defined amount of the test solution was then added into the reservoir. The concentration of test solution in the micropipette was chosen to give a final desired concentration with the volume of liquid in the solution reservoir. As the

system continued to perfuse, the concentration of test solution in the slide chamber gradually increased to the desired level.

To return the system to the control condition, with no test solution in the system, the experimenter first waited until the exact moment that the solution reservoir emptied. This ensured that all of the test solution was in the tubing and that none would form a solution with anything else poured into the reservoir. The reservoir was then filled with the control solution. As the fluid perfused through the system, the concentration of test solution in the slide chamber gradually decreased. There were three primary issues with this experimental setup.

1. *The rate at which the nanoparticles and test solutions were delivered to the cells was slow and unknown.*

When the experimenter introduced the test solution or QDs into the system, the test solution took time to diffuse through the reservoir. More time was required to move the test solution through the tubing into the slide chamber. This was not ideal, as there was a period of time between the introduction of the test solution and the time that cells were exposed to the desired concentration of the test solution. Over the course of the introduction, cells experienced all concentrations between zero and maximum, and it was impossible to tell at what time full exposure occurred.

2. *The continuous perfusion required a large amount of the test solution be used.*

The entire remaining volume of liquid in the reservoir was brought to the desired concentration for each test. This volume of the reservoir was always at least 10mL, however, the actual amount of fluid in the slide chamber was assumed by UNG researchers to be approximately 0.5mL.

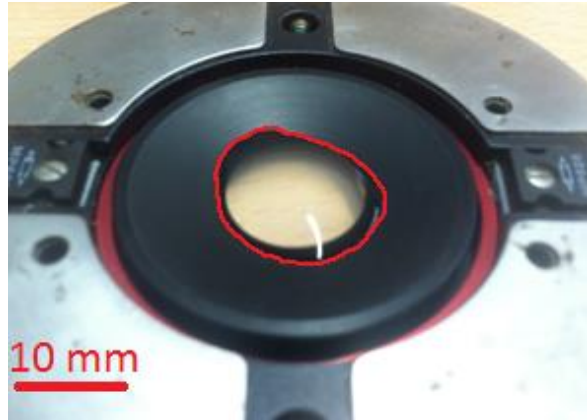


Figure 21: Volume of fluid in the slide chamber. Less than one milliliter of fluid immerses the cells in the slide chamber at any time during the test, with the liquid outlined in red for emphasis.

The large volume in the reservoir created a significant waste of test solutions. It required a much smaller volume of test solution to bring the slide chamber to the desired concentration than to bring the reservoir to desired concentration.

3. *The relative positions of the inflow and outflow tubes were highly variable.*

A small magnet was used to secure the end of the inflow tube in place. The cells likely experienced variable micro-currents, as the magnet was manually applied for each test. This may have altered the shear stresses experienced by cells and the rate of perfusion between tests. Additionally, the perfusion outflow system was secured by double-sided tape, which had to be replaced every few tests and was not reapplied in a predictable position.

3.1.2 Revised Client Statement

After using the existing experimental procedures, having conversations with researchers at UNG, performing literature reviews, and holding internal group discussions, the following revised client statement was generated:

“Design a device which allows for the rapid and controlled introduction of an experimental solution onto the slide of a microscope. This device must minimize the amount of the test solution or quantum dots used.”

The final client statement was a mutual understanding of the scope of the problem between the engineering team, researchers at UNG, and WPI advisors, as well as the problem’s solution as it prioritized the needs for waste reduction and increased efficiency of the system.

3.2 Objectives, Constraints and Functions

Objectives, constraints, and functions define the scope of the project. These are the benchmarks for either success or failure. Objectives are chosen as higher-level goals for project completion, serving as the basis for creating a design and evaluating its performance. Constraints describe the limitations of the device. Functions define the capabilities the device needs to possess. The following section defines these parameters, as chosen by the team.

3.2.1 Objectives

From the previous client statement and discussions with UNG researchers, the following five objectives were chosen as the most relevant to the success of the project. The objectives of low cost, operator friendliness, consistency, multifunctionality and streamlined condition delivery were each broken down into more detailed descriptions of the objectives.

Table 1: Top level project objectives; these objectives define the benchmark, which must be met for the project to be considered a success.

Low Cost	The total cost of all components should not exceed the budget for the project. This does not exclude use of materials which have already been purchased by UNG researchers.
Operator Friendliness	The device should be easy to set up, use, and break down.
Consistency	Multiple uses of the device should yield comparable and empirically valid results.
Multifunctionality	Device should be capable of being used with multiple types of imaging and additional microscope-based techniques.
Streamlined Condition Delivery	Device should increase the efficiency of delivery of the experimental test condition, drug, QD, or other test solution.

In order to determine the importance of these objectives, we used a Pairwise Comparison Chart² (PCC). PCCs are tools used to rank objectives in terms of their importance to the project.

Table 2: Pairwise Comparison Chart; Determines ranked objectives. The totals are a relative score of importance, with higher numbers denoting a greater importance.

	Low Cost	Operator Friendly	Consistent	Multifunctional	Streamline condition delivery	Totals
Low Cost		1	0	1	0	2
Operator Friendliness	0		0	1	0	1
Consistency	1	1		1	1	4
Multifunctionality	0	0	0		0	0
Streamlined Condition Delivery	1	1	0	1		3

The comparison revealed to the team that the device should be, from most to least important, consistent, streamlined for condition delivery, low cost, operator friendly, and multifunctional. Each of the objectives is clarified below.

1) *Consistency*

UNG was in need of a consistent, repeatable procedure. This device would continue to be a part of several experiments; therefore the need for consistency is vital to the results. The system must be reproducible in delivery, flow, and flushing methods. These components must be consistent from test to test so all of the data obtained is both comparable and valid.

2) *Streamlined Condition Delivery*

Since a variety of expensive drugs and other test solutions or nanoparticles would be sent through this system, the device needed to use a minimum amount of test solution. The device should optimize the delivery of the test solution to ensure minimal waste and rapid administration to the cells.

3) *Low Cost*

This device must be able to be manufactured using current materials and processes found in a basic laboratory setting, while requiring minimal out-of-pocket expenses. The design of this device must

² In each cell, the row objective is compared to the column objective. If the row objective is more significant, a one goes in the cell. If the column objective is more important, a zero goes in the cell. ½ is awarded for objectives of equal importance. The sums of the rows provide a relative measure of importance (Dym & Little, 2009).

also allow for more efficient use of material, particularly cell media and test solutions, to reduce the waste and need to frequently replenish supplies.

4) *Operator Friendliness*

This device must be as simple to use as possible, minimizing human error, therefore reducing the possibility of compromising data.

5) *Multifunctionality*

Being multifunctional is valuable, but not imperative, to the client. The primary concern of the client is to examine the functionality of QDs, with other experiments secondary.

3.2.2 Constraints

Constraints are the limiting factors of a design. The success of the design is heavily weighted on the constraints. Failure to understand and properly manage these, typically results in a failed design. Below is the original list of constraints for the device developed after the revised client statement.

- *Mechanical Interference* - The height and volume of the system do not interfere in any way with the imaging process.
- *Self-Supporting* - The device must be sturdy and capable of holding itself up with no other support systems or special precautions.
- *Minimal Dexterity* - The device must not require any particular skill to operate. Any operator with the requisite microscopy skills should be able to operate the device and the introduction of the test solution and microscopy must not be mutually exclusive events.
- *Manageable Set-up/Breakdown* - The device must not take more than 10 minutes to either setup or breakdown.
- *No Cell Shearing* - The device must not create a flow that produces a shearing force strong enough to cause partial or full detachment of neurons from the glass slide.

- *No Damage to the Objective Lens* - The device must not come in close contact with the delicate and expensive objective lens of the microscope.

3.2.3 Functions

Functions are the necessary tasks the device must complete in order to be a successful design. Our client statement performed four main design functions.

First, the system was able to keep the cells submerged in solution, as continuous immersion was vital to continued cell health. If the cells were at any time not immersed, their behavior would have changed, invalidating experimental results. Discussions with the UNG researchers and initial observations revealed that distressed cells, those in undesired environmental conditions, tended to exhibit baseline drift of calcium levels. This masked potential electrical activity that may have occurred; therefore it was avoided.

Secondly, the system maintained consistent placement of the inflow of fluid from the perfusion system and the outflow of fluid from the slide. A combination of magnets and tape was used to attach the perfusion inflow and outflow systems, resulting in testing inconsistencies. Varying patterns of flow over the slide caused irregular microcurrents and unpredictable cellular exposure in different regions of the slide chamber. While consistent placement of inflow and outflow tubes did not eliminate this issue, it likely helped to alleviate inconsistencies.

Another necessary function of this device was the ability to restore the initial control condition. The difference between the baseline and experimental concentrations of the test solution needed to be consistent between tests. After the introduction of the test solution or nanoparticles, the system needed to incorporate a way to lower the concentration back to control solution concentration. This involved flushing out the system to completely replace the test solution with the control solution.

Finally, the system had to be capable of blocking ambient light sources from the cell culture. Fluorescence microscopy is a delicate imaging process and any external light interference reduced the noise in images, which reduced data quality.

3.3 Project Approach

Objectives, constraints, and functions serve to guide the direction of this project. To ensure that all project requirements were met, a series of steps were followed. First, a Work-Breakdown Structure (see Appendix B: Work Breakdown Structure) was drafted. This tool orders and characterizes the various steps needed to complete the project. It was continuously updated as new tasks were identified. Additionally, a Gantt Chart (available in Appendix C: Gantt Chart) was created to allow for planning and tracking of the project status.

Following a brainstorming session, a series of design alternatives were generated. The feasibility and relative usefulness of these designs were evaluated using a number of tools, including a function-means table and a design evaluation matrix.

A series of prototypes were developed and tested. The information gained from this testing informed the design and manufacture of a final device. Protocols were developed to verify the conformity to specifications of this design, validate the design, and generate useful data for evaluation by UNG researchers.

4 Design Alternatives and Evaluations

A vital step in the design process is the generation of design alternatives. Creating multiple options to work with allows for the best possible design to be chosen and minimizes the odds of a failed project. To generate and assess designs during this process, tools such as a functions means tree and a design evaluation matrix were used. Each necessary component of the new device was evaluated to determine which of the objectives would be satisfied, and whether or not they fell within the bounds of the constraints. Through these methods, the feasibility of each combination of potential systems was considered.

Table 3: Morphological Chart of the functions and means of the device

Functions	Means			
Keep cells submerged	open-to-air perfusion	open-to-air reservoir	removable closed perfusion	
Input challenge	gravity based system	syringe into pump	cyclic pumping	micropipette
Remove challenge	vacuum and air pump	peristaltic pump	closed gravity system	
Mount inputs/outputs	polyurethane platform	carbon fiber platform	plastic ring with O-ring	
Secure mount	Magnets	adhesive polymers	tape	
Clean Equipment	UV light bulbs	Isopropyl alcohol	Ethanol	

Four alternatives that utilized a variety of the means in Table 3 were considered. With further evaluation, the team considered various designs that fulfilled the objectives. By brainstorming a diverse list of alternatives, the team highlighted design criteria and specifications that might otherwise have been overlooked.

4.1 Design Specifications

Design specifications are critical in the design process, as they provide explicit information about the requirements of the system or device. The specifications below were decided upon based on the need for adherence to the objectives, functions, and constraints. Validation criteria for each of the specifications are described in Section 5.1.8.

Table 4: Specifications of the Design; the leftmost column describes the motivating rationale for the decision, while the central column describes the exact wording. The rightmost column explains why that wording was chosen.

Needs	Specification	Rationale for Specification
Cells must be kept submerged in solution	At no point during the process of cell installation or testing shall the cell-carrying surface of the slide be exposed to air	Cells will become distressed or die if exposed to air for any significant period of time
	Device must alert the user before running out of the control solution	The perfusion in system must be a continuous flow
Cells must be able to be exposed to precise concentrations of the experimental condition	The control concentration of test solution must be +/- 1 mM the expected value initially	The ±1 mM level was agreed upon by the team and Dr. Pinato
	The experimental concentration of test solution must be +/- 1 mM the expected value	The ±1 mM level was agreed upon by the team and Dr. Pinato
	The final concentration of test solution must be +/- 1 mM the expected value	The ±1 mM level was agreed upon by the team and Dr. Pinato
Size and shape cannot provide any limitations	No part of the device must mechanically interfere with any part of the operation of the microscope	The microscope has multiple moving parts, including the stage and the arm. An incorrectly shaped device would inhibit microscope functionality by reducing its range of motion
No manual dexterity	No part of device setup, operation, or breakdown must depend on an unusual degree of manual dexterity	Injection of the test solution is a challenging task in the current microscopy setup, requiring delicate and skilled movements to inject small volumes without shearing cells.
No interference with fluorescent imaging	No device component shall intrude upon the space between the slide and the objective lens	Certain paths between the slide and lenses of the microscope must be kept clear of obstruction. In particular, no part of the design should intrude into the area either directly above or directly below the slide

Self-supporting device	The device shall be stable enough such that falling over and detachment are not concerns of experimenters	It may become necessary to directly attach a bulky micropipette or other equipment to the device. Nothing unstable will be acceptable
Quick setup and removal	The device shall take an experimenter less than ten minutes to fully set up	There is approximately thirty minutes between dye loading and calcium imaging. In this time, the experimenter must also follow the procedure outlined in <i>Appendix D: Standard Operating Procedure for Staining Cells Prior to Imaging</i> to setup the microscope. If setup took more than 10 minutes, the overall process would require more than 30 minutes.
	The device shall take an experimenter less than ten minutes to fully break down	It was agreed that the breakdown should take no longer than the setup.
Microscopy and introduction of test solution are not mutually exclusive	The introduction of the test solution and microscopy must not be mutually exclusive events	The time period immediately after the introduction of the test solution contains valuable data, as it will show the immediate cellular response to the new environment. If imaging was interrupted, this data would be lost
No cell shearing	The speed and type of flow caused by the device must not damage or disturb the network of hippocampal neurons	It will be impossible to collect data from neurons if they are not adhered to the slide surface
Constant inflow and outflow positions	Any inflows and outflows to the cell culture must remain at constant positions relative to one another and to the slide from test to test	Consistent placement of the inflow and outflow ensures a consistent volume of fluid in the slide chamber, which is ensures accurate final concentrations of test solutions
Temperature control	The temperature of the cells must be kept within 1 degree Celsius of any desired temperature between room temperature and 40 degrees Celsius	Two thermal control plug-ins exist on either side of the thermal control ring. Access to them must be unimpeded.

4.2 Design Alternatives

The team developed four possible designs which they felt were capable of fulfilling all of the above specifications.

4.2.1 Design 1: Open System with Selectable Perfusion

The initial design is based on a reasonably simple modification of the current design. Rather than a continuous perfusion, the solution inflow may be turned on by electronic or manual control. The perfusion outflow pump may also be turned on or off in the same manner. When both inflow and outflow are turned on, a known volume of solution will be left coating the sample.

When the test solution is ready to be introduced, both perfusion inflow and perfusion outflow could be switched off. The volume of the static solution remaining in the slide chamber would remain consistent, because the placement of the perfusion outflow would remain at a constant height relative to the slide. As this volume of solution is constant for every test, the precise final concentration of test solution or nanoparticles to be added could be calculated with reproducible accuracy. To return the cells to the initial control condition, perfusion outflow and inflow may both be turned back on, clearing test solution from the sample.

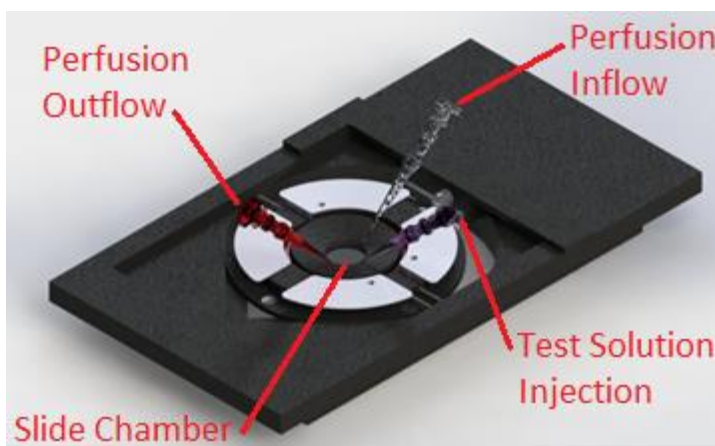


Figure 22: Computer model of the open perfusion system; the clear micropipette tip would administer control solution into the slide chamber. At the desired time, this control solution could be supplemented with the test solution by the purple micropipette tip. Waste would be removed through the red micropipette tip.

As with all design alternatives, there were several factors to consider when weighing the benefits and concerns of each idea. For this design, DIC imaging, which relies on an unobstructed view of the top of the sample, as well as the bottom, would still be able to occur. As described in Section 2.4.2, bright field illumination is necessary for DIC microscopy. Since this design would be similar to the existing setup, some components could be kept, such as the perfusion outflow pump and the gravity-fed perfusion inflow system, in order to simplify installation and reduce cost. There was also the potential for variability in the volume of liquid in the slide chamber, which might have caused variation in the concentration of the test solution. This variability might be due to issues related to suction, placement of the perfusion outflow tube, and evaporation of solution.

4.2.2 Design 2: Closed System with Selectable Perfusion

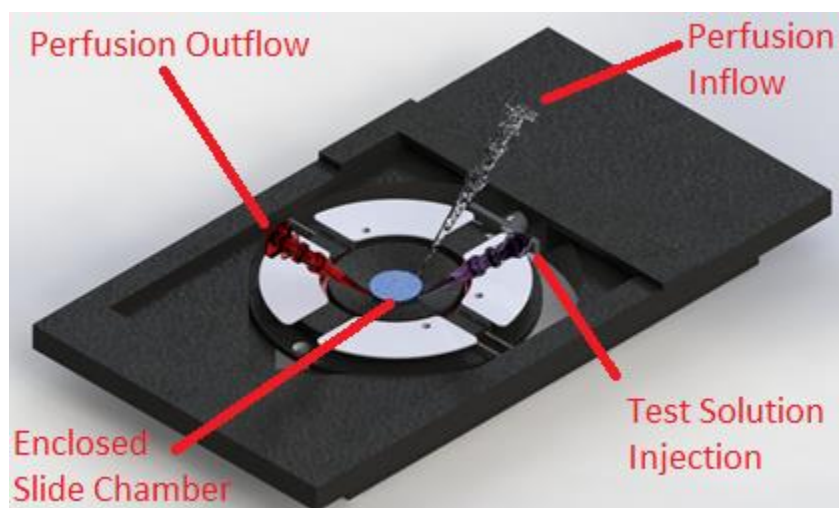


Figure 23: Computer model of the closed perfusion system; the clear micropipette tip would input control solution into the central, completely enclosed blue slide area. At the desired time, this control solution could be supplemented with the test solution by the purple micropipette tip. Waste would be removed through the red micropipette.

During setup of this closed system, a watertight seal would be made between the bottom of a small enclosure and the slide chamber. The only openings in this small chamber would be the perfusion inflow to deliver the control solution, the micropipette tip to deliver the test solution or QDs, and a small opening for perfusion outflow.

As opposed to a continuous perfusion system, the fluid inflow system could be turned on by electronic or manual control, as in the open system. The perfusion outflow system would be entirely

passive. During perfusion, the control solution would actively pump through the perfusion inflow system. This inflow would fill the enclosed slide chamber to completely cover the cells, forcing excess solution through the outflow. To introduce the test solution, the inflow pump would be switched off, to leave static solution in the slide chamber. A test solution would then be pumped into the chamber by a secondary micropipette, forcing out the control solution and flooding the enclosed area. To remove the test solution, the inflow perfusion system could be turned on to flood the system with control solution and force all test solution into the waste beaker.

This would be a fairly simple design, in that the perfusion outflow would be passive rather than requiring some type of suction or peristaltic pump. Another benefit to this design would be that the volume of liquid to which the cells are exposed is known, as it would be equal to the volume inside the enclosed slide chamber. The difficulty with this system could come with forming a consistent seal between the enclosure and slide chamber. Without an accurate seal on the device the volume, as well as the positioning of the perfusion in and perfusion out pipettes would be affected, and most likely inconsistent.

4.2.3 Design 3: Closed Loop Perfusion System

In this closed loop design, there would be no waste container. Instead, all material could be circulated through the system in a loop, with a beaker serving as a fluid reservoir. Only a small volume of liquid would be maintained in the slide chamber itself at any given time.

Initially, only the control solution would be contained throughout the system. The level of fluid in the large beaker would be kept low. When desired, a secondary syringe or micropipette could inject an appropriate amount of high concentration test solution into the beaker, which would be distributed by means of diffusion and convection.

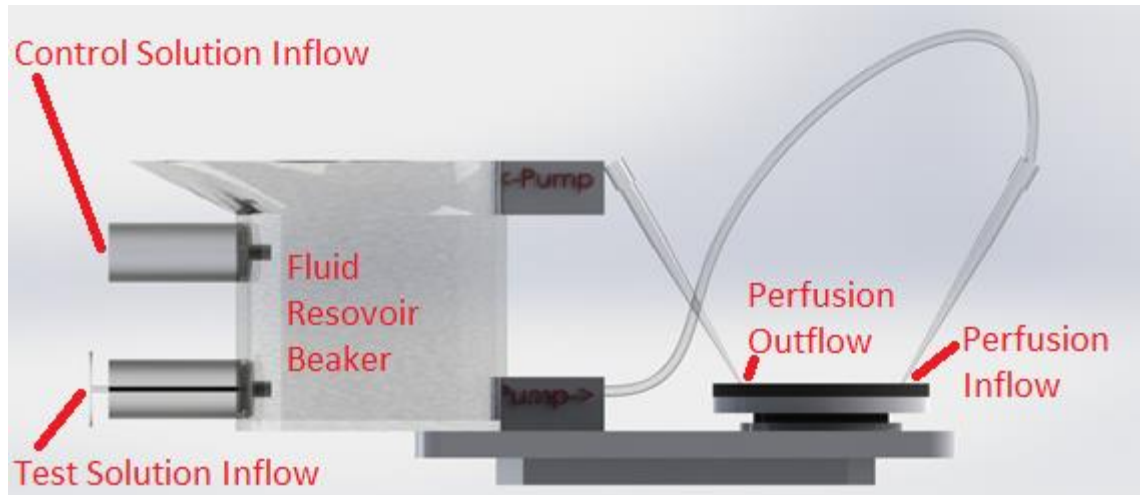


Figure 24: Computer model of the closed loop system; a cyclical, pump-based perfusion design would continuously deliver liquid to the slide chamber by pump and recycle back to a beaker with secondary syringes allowing for modification of concentration.

To return the system to a negligible level of the test solution, a large amount of the control solution, likely half a liter or more, would need to be injected into the system by a large syringe or other pump. This should not entirely remove the test solution from the system, but dilute the test solution to an arbitrarily low concentration.

One of the design objectives is to reduce the amount of test solution or QDs used in a test. This design would not only create little to no waste of the test solution or QDs, but it also would significantly reduce the amount of the control solution used, as all fluids repeatedly circulate through the system. As a closed loop system, this design would require a more complex setup and breakdown process. Two pumps would be needed, increasing the complexity and chances of failure of the device. Due to the fact that the syringes would inject solution into the reservoir rather than onto the slide itself, there would be a delayed delivery of the appropriate concentration of test solution to the cells, and it would become more difficult to return the system to the initial concentration of test solution. Depending on the desired concentrations and volumes required throughout the tests, it might be impossible to dilute the test solution to negligible levels. In addition, cell byproducts might potentially alter the effect on the solutions over the course of experimentation.

4.2.4 Design 4: Static Beaker System

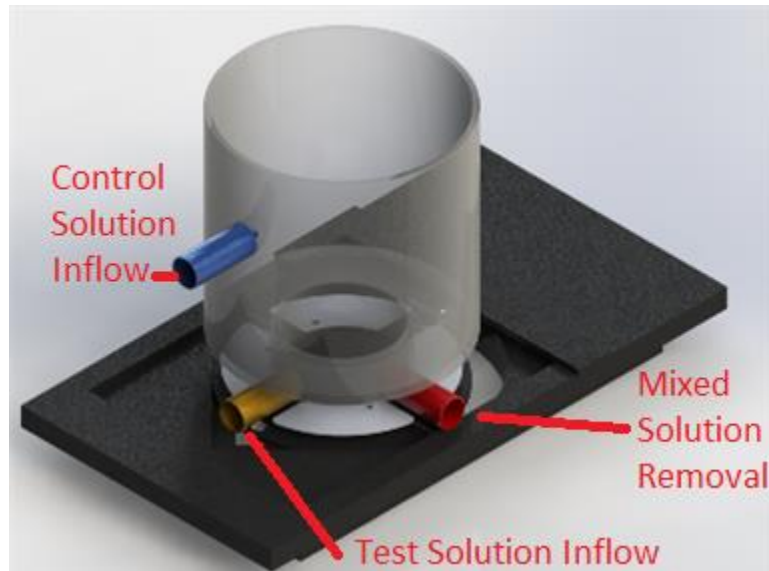


Figure 25: Computer model of the static beaker system; rather than using flow, a small amount of control solution would be above the slide, after which control or test solutions could be introduced, while mixed solutions could be removed.

The fourth and final design is a static system with no perfusion at all. Initially, the cells would be bathed in a small amount of the control solution. During an experiment, an appropriate amount of highly concentrated test solution could be injected into the slide by the yellow syringe (seen in Figure 25). Through diffusion, the small amount of control solution already in the beaker would mix with the newly injected test solution, to produce the desired concentration. To return the concentration of the test solution to a negligible level, large amounts of control solution would be injected through the blue syringe, while outflow is allowed through the red syringe. This would eventually lower the concentration of the test solution to whatever arbitrarily low level is desired by the user.

While this design idea could appear to be the simplest to implement, as it likely requires little tubing or hydraulics, there could be several downsides to the design. Maintaining the desired concentrations of solution may prove difficult, given that there would be no outflow. The increased water pressure above the cells could modify their physiological response in unexpected ways. Most importantly, a leak or other mechanical failure would douse the system with a large volume of salt solution, a catastrophic result. Such an incident could damage electronics and leave particulate coatings on optical components, reducing the utility of the microscope for future experiments.

4.3 Design Evaluation Matrix

Based on the team's chosen objectives, the following Design Evaluation Matrix³ was constructed, which compares the four possible alternative designs. Each of the five objectives was given a weight between one and ten, proportional to its importance to the success of the design.

1. *Consistency (1.0)* – The Pairwise Comparison Chart in Section 3.2.1 revealed consistency to be the most important of the five objectives. It was therefore given the maximum allowable value of one.
2. *Streamline Condition Delivery (0.8)* – Discussion with the client, along with the high cost of QDs, made delivering efficient quantities of test solutions or nanoparticles highly desirable.
3. *Low Cost (0.5)* – Any design that was too expensive for the team to construct was useless to researchers at UNG. However, only one such device would ever need to be made. The design of the device would be specific to this microscope and laboratory. Unless the laboratory either obtained a second Olympus microscope or broke the device, there would be no need for construction of a second.
4. *Operator Friendly (0.3)* – While it would be helpful and convenient for the design to be easy-to-use, functionality trumps other considerations. A device that works well and allows for the collection of good data would be more valuable than one that is easier to use. A score as high as 0.3 was awarded based on the knowledge that complicated instructions for use could increase the chance of human error, and make the device less useful.
5. *Multifunctional (0.2)* – While it would be convenient for the laboratory to have a general device, usable in other experiments, the task given to the team was to investigate the relationship between QDs and neurons. It would be acceptable for the design to only be applicable to that particular case.

It is important to note that this order of importance matches the order of importance given by the Pairwise Comparison Chart in Section 3.2.1. Given below is rationale for the scores awarded to each of the designs.

³ A Design Evaluation Matrix is a method to compare the feasibility of a variety of designs. Each of the alternative designs is given a relative weight, between zero and one, which is proportional to its importance to the success of the design. For each of these categories, the design alternative is given a score between one and ten, proportional to how well it would fulfill the objective. The products of these scores and weights are added together, generating a total score for each of the design alternatives. These scores represent a measure of relative ability for the design to fulfill the objectives of the project (Dym & Little, 2009).

4.3.1 Open Perfusion System

1. *Low Cost* (8.5) – The open perfusion system required no additional pumps and would likely be able to reuse many components of the existing perfusion system.
2. *Operator-Friendly* (6.5) – It would be easy to use this design beyond the current requirements of the existing perfusion system. However, that system would not be optimal, as it proves to potentially have leaks or run out of control solution.
3. *Consistency* (6.0) – The main source of inconsistency in the open perfusion system would be the potentially variable volume. As the volume of fluid over the slide would be defined only by the height of the outflow pump instead of by an enclosed chamber, a chance for inconsistency existed.
4. *Multifunctional* (10) – The open perfusion system required the fewest materials and left the maximum possible amount of open space above and below the slide. This would make it likely to work with a variety of imaging techniques.
5. *Streamlined Condition Delivery* (9.0) – A completely exposed droplet of liquid over the slide chamber would have made it easy to inject test solution into the system with a micropipette, requiring no additional techniques or equipment.

4.3.2 Closed Perfusion System

1. *Low Cost* (7.0) – The closed perfusion system would have required some an enclosed microfluidic chamber to be effective. As the Centre for Biomedical Sciences and Engineering had no equipment capable of producing such a chamber, it would likely have been required that construction be completed out-of-house at some cost. However, most components of the existing system would have been salvageable.
2. *Operator-Friendly* (6.0) – The chief problem of the open perfusion system would have been eliminated by the closed design, as the system volume would be strictly defined.
3. *Consistency* (8.0) – The chief problem of the open perfusion system would have been eliminated by the closed design, as the system volume would be strictly defined.
4. *Multifunctional* (2.5) – The enclosed chamber would have blocked the light path up to the microscope arm, and have made many types of imaging, including DIC, impossible.
5. *Streamlined Condition Delivery* (8.5) – A very small and precise amount of test solution or QDs would have been required for each test, minimizing waste. However, the volume used would

have needed to be greater than the volume of the chamber to ensure that the control solution would have been completely flushed out of the system.

4.3.3 Closed Loop Perfusion System

1. *Low Cost (4.0)* – The closed loop would have required at least two flux pumps, neither of which was owned by the Centre for Biological Research and Engineering. A vacuum pump was used in their previous setup. This represented a significant cost increase.

2. *Operator-Friendly (4.5)* – Management of two pumps and tracking of the total volume of a dynamic system would have been complicated tasks, which would have required significant skill and attention to manage.

3. *Consistency (5.5)* – The unclear time delay between the injection of the test solution and the time of delivery to cells would have introduced variance into the system.

4. *Multifunctional (10)* – No unnecessary components would have been placed near the slide chamber; only inflow and outflow tubes would have been needed at that location. This would have maximized the possibility for use of other imaging modalities or microscopy techniques.

5. *Streamlined Condition Delivery (2.5)* – The unknown delay might have led to inconsistency, and might also have led to an unclear relationship between the test solution and neural response.

4.3.4 Static Beaker System

1. *Low Cost (8.0)* – The static beaker system would have required no tubing or pumps, making it potentially the least expensive of the four design alternatives.

2. *Operator-Friendly (4.5)* – Balancing a large reservoir on top of a slide would have been a challenging task, and the production and use of such large quantities of solutions would have been inconvenient.

3. *Consistency (6.0)* – The design would have been dependent on potentially slow diffusion of solutions throughout the reservoir, causing an unclear relationship between the administration of the test solution and neural response.

4. *Multifunctional* (3.0) – The large reservoir would have interfered with components of the microscope needed for other types of imaging, limiting the use of the design to solely fluorescence microscopy.

5. *Streamlined Condition Delivery* (4.0) – The delivery of test solution to cells would have been entirely dependent upon slow diffusion through a large volume of fluid.

4.3.5 Finalized Matrix

Table 5 shows the finalized Design Evaluation Matrix, comparing the relative utility of the four alternatives.

Table 5: Design Evaluation Matrix of the four design alternatives; the totals on the far right are relative scores of the suitability of the design to our needs. An open perfusion system appears to be the most suitable design alternative

Objective	Low Cost	Operator Friendly	Consistent	Multifunctional	Streamline Delivery	Total
Weight	0.5	0.3	1	0.2	0.8	
Open Perfusion	8	6.5	6	10	9	21.15
Closed Perfusion	7	6.5	8	2.5	8.5	20.75
Closed Loop	4	4.5	5.5	10	2.5	12.85
Static Beaker	8	4.5	6	3	4	15.15

Based on these results, it was decided that the open perfusion system held the greatest potential for delivering successful experimental results.

4.4 Prototypes

The early phases of design and construction used readily available materials to test features of the open perfusion system and ensure that unexpected and overlooked characteristics of the design would not lead to engineering failure.

4.4.1 Prototype One: Results & Modifications

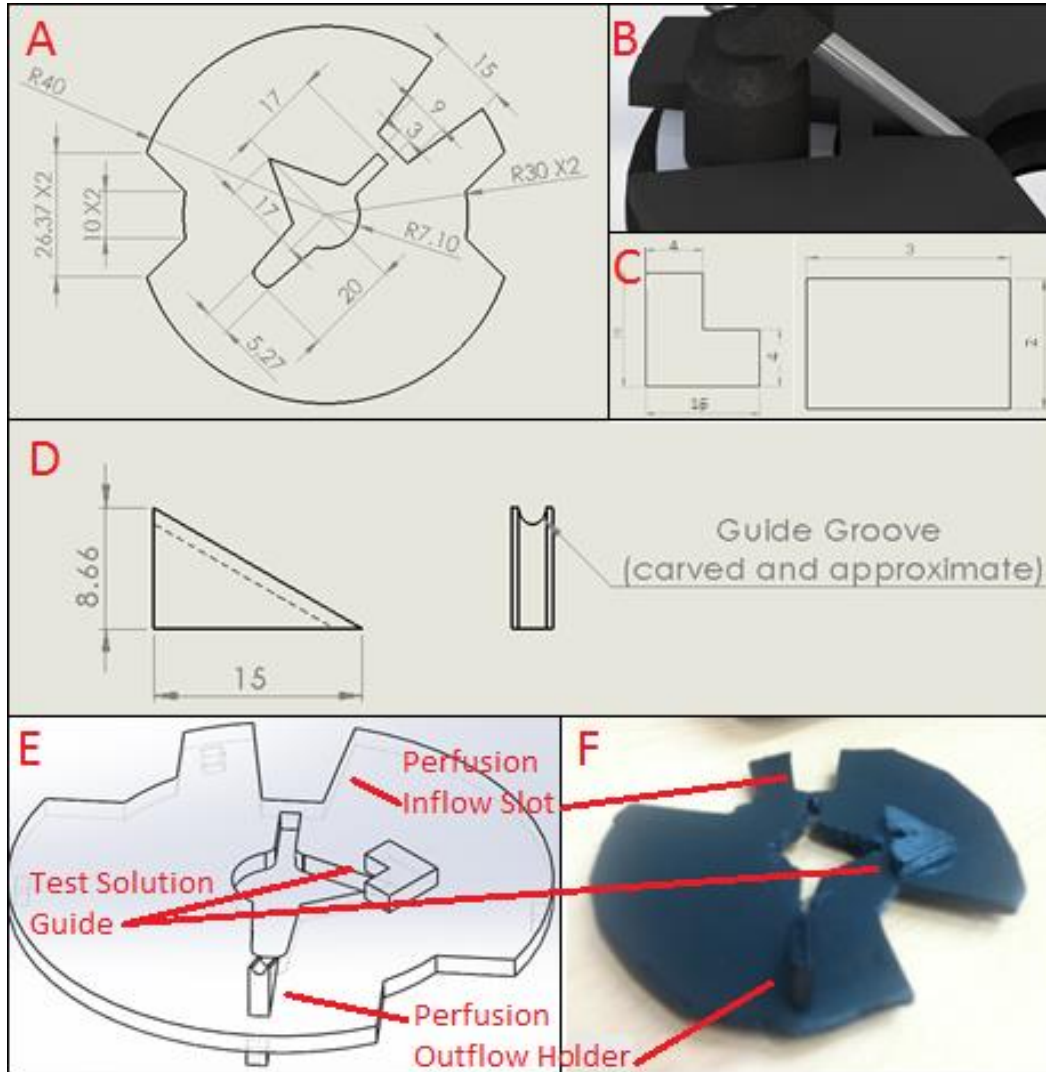


Figure 26: Components of the first prototype design; (A) dimensioned drawing of the disc which formed the basis of the first prototype design, with cutouts on the left and right to allow for access to the thermal control plug-ins, a teardrop-shaped groove at the 10:00 position that helps to stabilize the micropipette used to inject the test solution into the slide chamber, and two cuts at 90 degree angles from the orientation of the teardrop shape to allow access to the slide for the perfusion inflow and outflow systems, respectively, (B) computer model of the magnetic perfusion inflow holder in contact with two notched edges of the disk, (C) additional components to be glued to the main disk, (D) a guide component for holding the test solution micropipette, (E) a computer model of prototype one, showing the slot for the perfusion inflow system, the holder for the perfusion outflow pipette, and the test solution in guide system, and (F) the assembled disk of prototype one

The focus of the first prototype was the standardization of the locations of the perfusion inflow and outflow components of the design. To do this, a layer of 3mm black polyurethane (trade name hobbycolor⁴) was cut to the measurements specified in Figure 26A, using a combination of hacksaw, wire cutter, sandpaper, and drill techniques.

This part of the design was intended to be placed on top of the thermal control ring. Cutouts on the left and right sides of the device allowed access to the thermal control plug-ins and therefore, would allow temperature-controlled experiments. As the intent of this design was to test the placement of perfusion inflow, perfusion outflow, and test solution injection components, the decision was made to use the existing magnetic perfusion inflow system, but to replace the perfusion outflow system with a micropipette tip, connected by rubber tubing to the outflow pump. A groove was cut into the lower left of the disk, to allow the perfusion outflow tube access to the edge of the slide. On the top right of the disk, an angled wedge was cut out. This enabled the round, magnetic perfusion inflow holder to be slid from the outside to the inside of the thermal control ring until it made contact with both sides of the wedge, therefore maintaining a relatively consistent position from test to test. The magnetic holder and wedge-shaped cut can be seen in Figure 26B.

Additionally, several other pieces of the same material were cut out using the same hand tools as the primary disk. The left-hand component seen in Figure 26C, glued to the top of the disk as seen in Figure 26E, was intended as a guide for injection by micropipette into the slide. Contacting the micropipette to both this groove and the adjacent notch (the test solution guide of Figure 26E and F) would ensure that test solution is injected from the same angle on each test. Four copies of the right-hand component seen in Figure 26C, glued to the bottom of the disk, are designed to hold the device in place by hooking over the edges of the metal plates on the thermal control ring.

Additionally, a triangular component seen in Figure 26D was cut out. This was designed to hold the outflow micropipette tip at an appropriate angle, such that the tip would barely make contact with the edge of the slide. Such an arrangement would keep the cells bathed in solution while minimizing the actual volume of solution in the slide chamber.

A computer model and assembled version of prototype one can be seen in Figure 26E and F, respectively. The physical device only significantly differed from the computer model in the precision of the cuts.

⁴ Gutta Glass hobbycolor Art.-Nr. 2512121

However, initial testing quickly determined several issues with this design. First, the metal holder used to keep the thermal control ring in place caused an interference with the edge of the assembly, preventing the assembly from being flush against the top surface.



Figure 27: The interference of prototype one with the metal holder; prototype sits just on top of the holder, preventing a flush and consistent placement.

Consistent placement of the device is important to maintain the volume in the slide chamber and eventually to delivering precise concentrations of test solutions.

Second, the hobbycolor material proved to be too malleable even for the purposes of short-term, prototype use. The material acts more like a piece of semi-rigid foam than a piece of hard plastic, and was deformed during early use.

4.4.2 Prototype Two: Results & Modifications

To alleviate the issues of prototype one, two major changes were made. First, the material for the disk was changed to a 5mm sheet of plexiglass. The team's hope was that the stronger, more rigid surface would improve the accuracy of the cuts and produce a more durable component that could be extensively tested.

Second, a large cut was made in the side of the base, to avoid interference with the metal holder (Figure 28). Due to significantly easier manufacturing, all components other than the main plate were still comprised of hobbycolor.

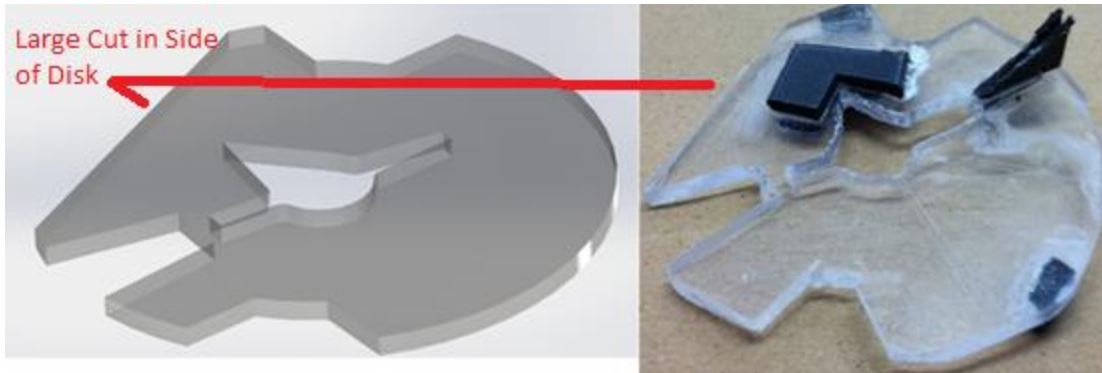


Figure 28: Computer model and real model of the revised prototype; note the flat surface on the left side of these images, intended to avoid interference with microscope components

The other major improvement in prototype two was the addition of a light shield, as seen in Figure 29. This component is designed to block all ambient light from reaching the sample. This part was designed as two hollow cylinders comprised of a UV resistant material, connected by a ring of the same material. The lower cylinder would have a diameter equal to the outer diameter of the entire prototype, and the upper cylinder would have a diameter exactly equal to the diameter of the microscope arm above. Slits in the side of this component would allow for the perfusion inflow and outflow systems, as well as allow for the introduction of the micropipette, when needed.



Figure 29: The light shield of prototype two; (A) computer model of the prototype two light shield, with various holes are cut into the sides to allow for the perfusion systems and the injection of the test solution, (B) the disk of prototype two and light shield, and (C) the assembled prototype two

The light shield component seen in Figure 29B and C was manufactured from metal repurposed from aluminum cans. This material was chosen for its ease of processing, UV blocking capabilities, and availability. Connections between the pieces of aluminum were made with electrical tape.

Two major issues were revealed by this test. These can be seen in Figure 30. First, the tight fit between the top of the light shield and the microscope arm caused mechanical interference when trying to image any part of the slide besides the exact center. This is an undesirable outcome, as it severely limits the regions of the cell culture that can be imaged.

Second, the angle of the intended injection from the micropipette interfered with another microscope component, the camera.

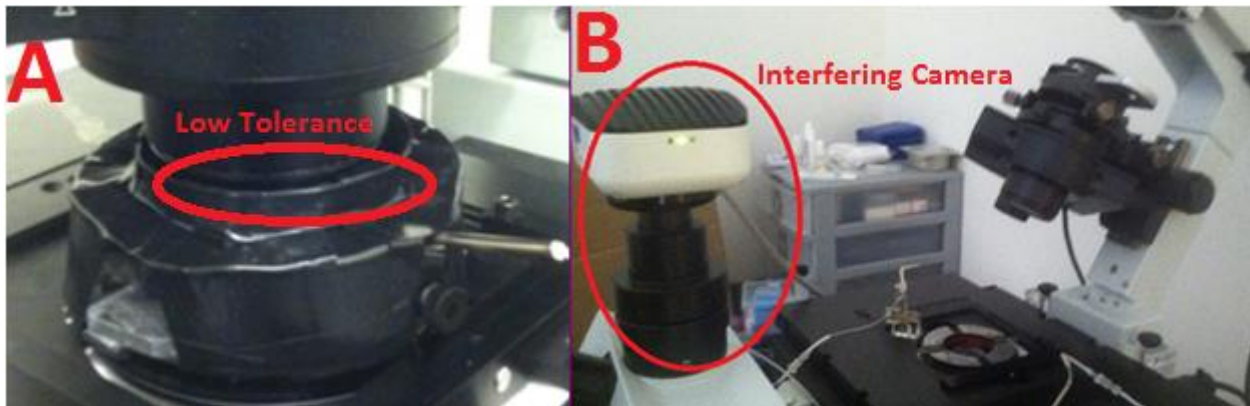


Figure 30: Issues with prototype two; (A) there is not enough space between the microscope arm above and the light shield below for the microscope to image every section of the slide without mechanically interfering with the light shield, (B) the microscope camera exists at the same angle relative to the slide as the opening for test solution injection, making injection by micropipette difficult.

While overall successful, there were clear changes to be made for future iterations of the design to ensure that there would be no further mechanical interferences.

4.4.3 Prototype Three

The third design iteration, seen in Figure 31, addressed the changes deemed necessary from prototype two. The micropipette guide was moved by 45 degrees to allow user access from an angle without mechanical interference with the camera.

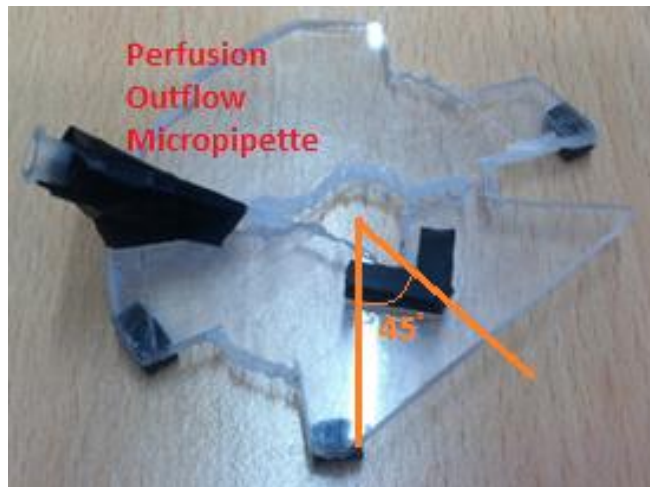


Figure 31: Prototype three, featuring a 45 degree shift in pipette access point; note the taped on micropipette, which serves as the perfusion out system

More significantly, the top section of the light shield was modified from that of prototype two, as seen in Figure 32. The diameter of the top section was increased to avoid any possible interference with the microscope arm. To minimize the entrance of light through this new opening, the height of the light shield was maximized, as to not interfere with the hinged movement of the microscope arm.

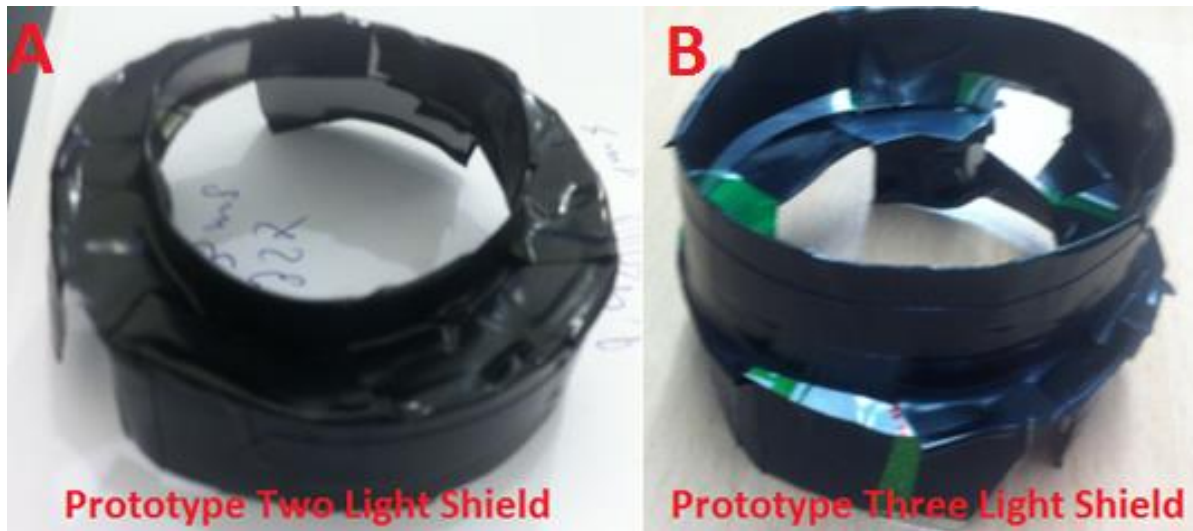


Figure 32: A comparison of the prototype two and three light shields; (A) the shorter light shield of prototype two, and (B) the taller light shield of prototype three

This prototype appeared to work well for the purposes of blocking light from entering the sample. The increased height meant that the microscope arm extended below the top edge of the shield, leaving few direct paths by which light from the outside environment could reach the slide.

Second, the repositioned opening for injection of the test solution significantly increased the ease of use for the experimenter, reducing the required degree of manual dexterity.

4.4.4 The Low Fluid Alarm

To satisfy the need for the cells to be constantly bathed in solution outlined in Section 0, it must be possible for some part of the device to alert the user before the control solution in the reservoir runs out. To accomplish this, a system known as the Low Fluid Alarm was created.

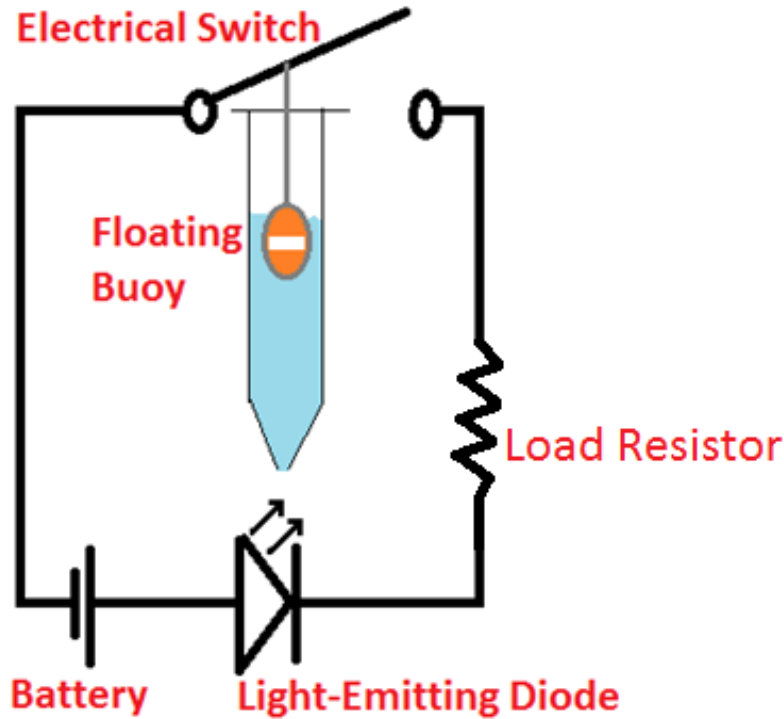


Figure 33: A simplified diagram of the Low Fluid Alarm system; a floating buoy inside the reservoir moves with the level of solution. As the level decreases a circuit is completed that turns on a light-emitting diode.

The Low Fluid Alarm is based around a floating buoy, which will rise and fall with the level of solution left in the syringe. This buoy must have three properties; (1) have a density lower than that of water (1 g/cm^3), (2) have enough mass to pull down on an electrical switch (a mass dependent on the exact construction of the switch), (3) fit into the fluid filled syringe with a minimum of friction against the walls. The tube has an inner diameter of 28mm, meaning that any object serving as the buoy must be no larger than this. Combined, these properties ensure that the buoy will move up and down smoothly with the level of the control solution in the reservoir.

To accomplish this, a microcentrifuge tube was chosen, seen in Figure 34A. These are small, sealable plastic containers, typically used for the storage of a few microliters of solution during centrifuging. They are highly nonreactive, easily cleaned, have dependable properties over a wide range of conditions, and are naturally buoyant when closed.

Small stones were added one by one to the inside of the tube, with the buoyancy of the tube tested in warm water after the addition of each stone. An equilibrium point was determined, at which

the tube held exactly as many stones as possible while still remaining buoyant, satisfying properties one and two. The filled tube can be seen in Figure 34B.

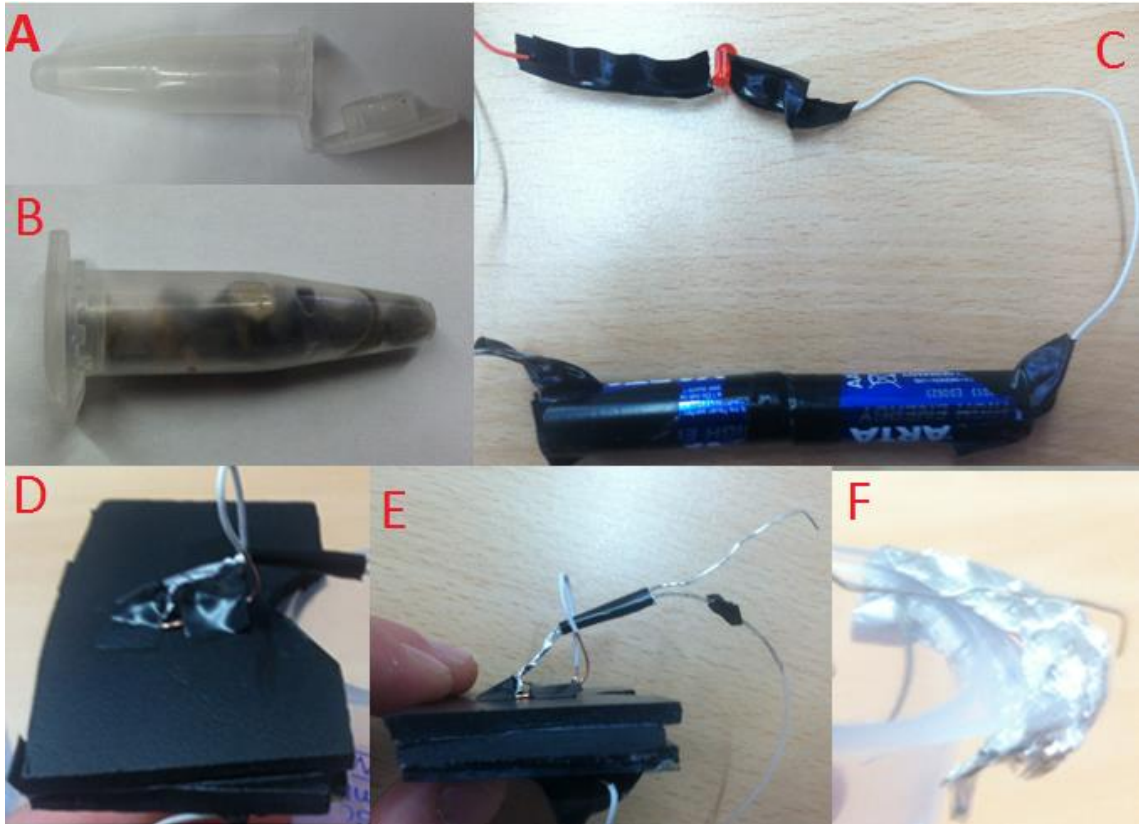


Figure 34: Major components of the Low Fluid Alarm; (A) An empty microcentrifuge tube, (B) the microcentrifuge tube after the addition of stones to increase mass, (C) electrical components of the visual indicator system, (D) a detachable component which fits over a flange of the solution reservoir, to allow for the installation and removal of the alarm, (E) the electrical switch of the device, in which can be seen the plastic fiber that either pushes up on or pulls down on the length of rigid wire, depending of fluid level in the reservoir, and (F) the contact of the electrical switch, comprised of a rigid wire and aluminum foil.

The next design decision was the determination of an indicator. Both auditory and visual alarms were considered. A visual indicator was determined to be the preferable choice. First, the necessary components were already available to the team. Second, a bright visual indicator would always be immediately noticeable in the darkened microscopy room, while the noise of an alarm might be lost in the nearby sounds of a centrifuge, multiple biological hoods with loud fans, and a noisy heating unit.

To create this visual indicator, it was first necessary to determine of the voltage requirements of an available, but undocumented, red light-emitting diode. Brief experimentation demonstrated that two AA batteries, in series, were sufficient to meet the power requirements and cause immediate noticeable luminosity, particularly in the darkened room where imaging occurs. This corresponded to a voltage of about 3V. A series of variously valued resistors were also added in series to the circuit. It was empirically determined that a 300Ω resistor was the component with the greatest resistance that still allowed a bright response from the visual indicator. This resistor was included because in the absence of a load resistor, diodes quickly burn out.

The electrical components were connected in series and in the proper relative orientations by twisted lengths of copper wire and electrical tape. This can be seen in Figure 34C. While solder would have been a preferable method of connection, material constraints forced the use of less sophisticated methods.

The key section of the design, however, was the large electrical switch, located at the top of the solution reservoir. The mechanical components of this switch were based around a thin piece of semi-rigid plastic fiber. One end of the fiber was tied to the tube, while the other was connected to a platform consisting of pieces of black polyurethane (the hobbycolor material described in the Section 4.4.1). The black section could freely slide onto and off of an overhang on the top of the syringe. Taped to this tubing was a piece of wire. This wire was electrically connected to the positive terminal of the batteries by a thin and flexible aluminum wire. On the opposite flange of the syringe was wrapped a piece of aluminum foil. This was connected to the negative terminal of the light-emitting diode. A small loop of wire was used to help the rising and falling piece of rigid wire stay aligned. Testing of this design was detailed in Section 5.1.2. The assembly can be seen in Figure 34D, E, and F.

4.4.5 Beta Design

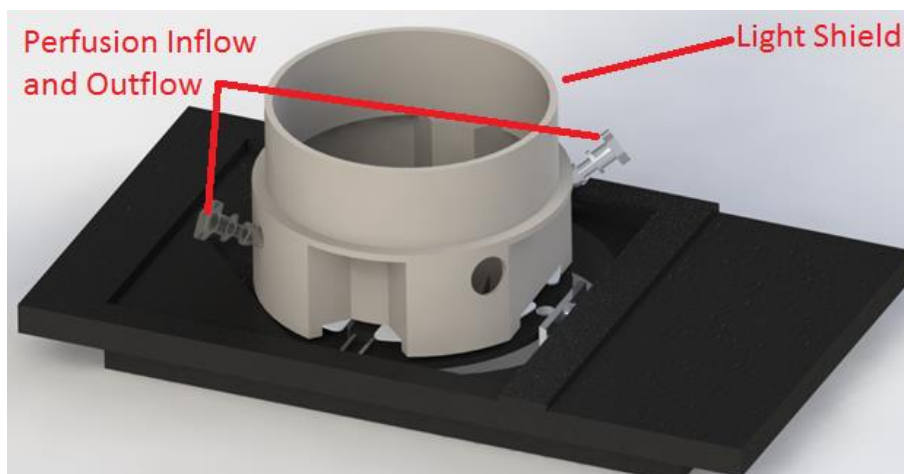


Figure 35: Computer model of the beta design; two plastic components fit over the top of the thermal control ring, holding the perfusion inflow and outflow micropipettes in steady positions relative to the slide chamber with the light shield placed over the component.

The beta design utilized the best features of each of the previous prototypes. First, it featured the most complete light shield of any of the designs, utilizing the appropriate diameter found in prototype three. The use of 3D printing allowed us to have holes exactly as large as needed to accept the micropipette tips, but no larger, minimizing light which entered into the system. This degree of precision was not achievable with any previous manufacturing technique.

Second, both the perfusions inflow and outflow of the system were based on micropipettes, rather than based on inconsistent flexible tubing. The micropipettes used as inflow and outflow were fixed in place by superglue to ensure consistent patterns of flow and volume of liquid.

One potential concern was that the low diameter of the end of the inflow might cause a jet of high velocity water to enter into the system, which could potentially have caused cell shearing. However, the exact position of the inflow micropipette was chosen so as to make this impossible. Since the outflow pipette tip contacted the top surface of the water to ensure a consistent volume in the slide chamber, the inflow was placed approximately 2mm from the slide. This ensured that drops of fluid still gently rolled down the side of the slide chamber, as in the original perfusion system.

A guide, located at a slight angle away from the inflow, allowed for the injection of any test solution without the need for any particular degree of manual dexterity. While attempts were made for

this input to be more accessible to left-handed users, no angle existed which did not cause either a mechanical interference or require a user's arm to be held at an awkward angle.

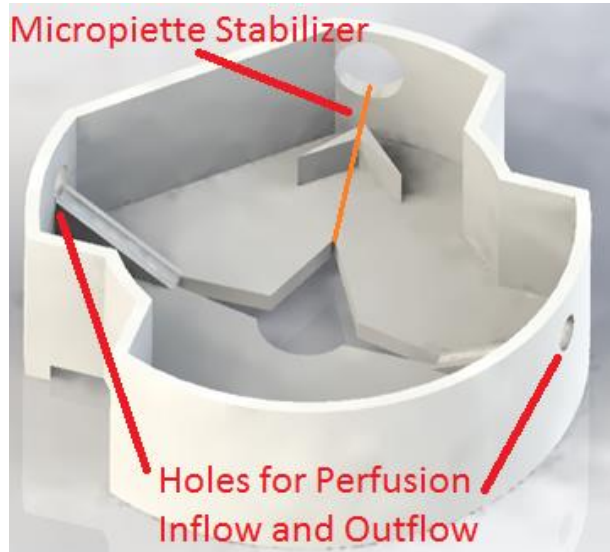


Figure 36: Interior View of bottom section of the Beta Design; on left and right, holes and guided channels allow for the introduction of perfusion inflow and outflow components into the slide chamber, as well as stabilize that allowed for direct injection of test solutions via micropipette.

The printing of the device as two components was for manufacturability purposes. 3D printers generally print plastic components using two materials. There is both the material used for the structural components of the part itself, and a “matrix” material, which fills the vertical space below solid parts of the components. Printing in two parts used a minimum of matrix material, as the only locations in which it would be needed are the holes which allow for micropipette entry. This lowered production time and costs to the printing facility, which were both beneficial outcomes. At the time of final assembly, these two sections would permanently glued together into the configuration seen in Figure 35.

4.4.6 Modifications to Beta Design

The CAD model was converted into a stereolithography file and printed in 3D by a MakerBot® type 3D printer, available for free student use at the International Centre for Theoretical Physics in Trieste, Italy. Printing of the beta design was successful, resulting in components virtually indistinguishable from the CAD models.

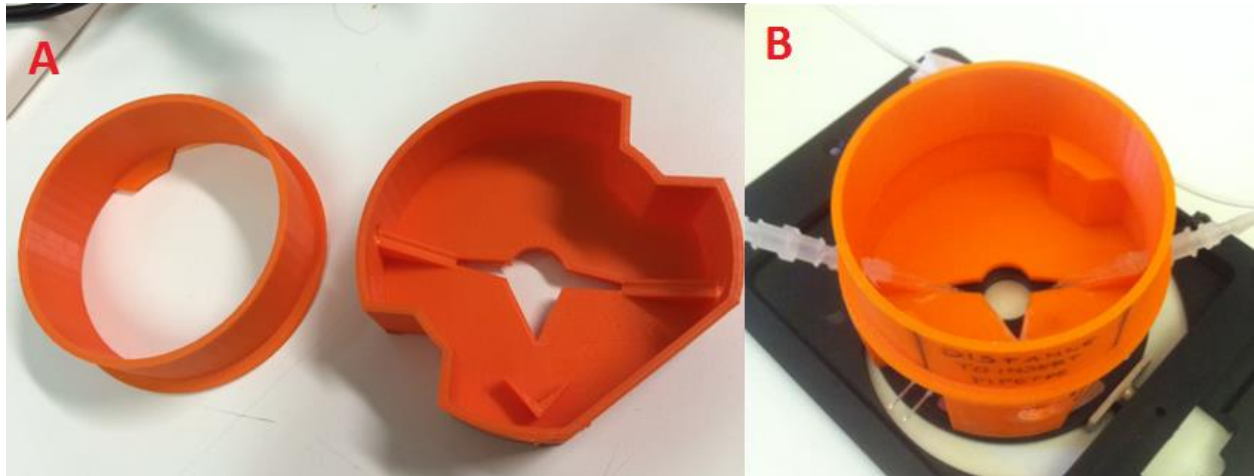


Figure 37: The printed beta design; (A) the two parts of the device after removal from the 3D printer, and (B) the superglued and assembled beta design, mounted on top of the thermal control ring

Although largely successful, a few problems were uncovered with the design, mostly related to the addition of the micropipette tips for the perfusion inflow and outflow systems. The existing holes in the side of the device did not allow micropipette tips to be placed at the appropriate locations relative to the slide. Both holes had to be drilled out to a wider diameter, to allow for clearance at the proper angle. This process was advantageous in terms of the stability of the design, as it allowed the micropipette tips to be secured by superglue to both the top and bottom edges of the holes.

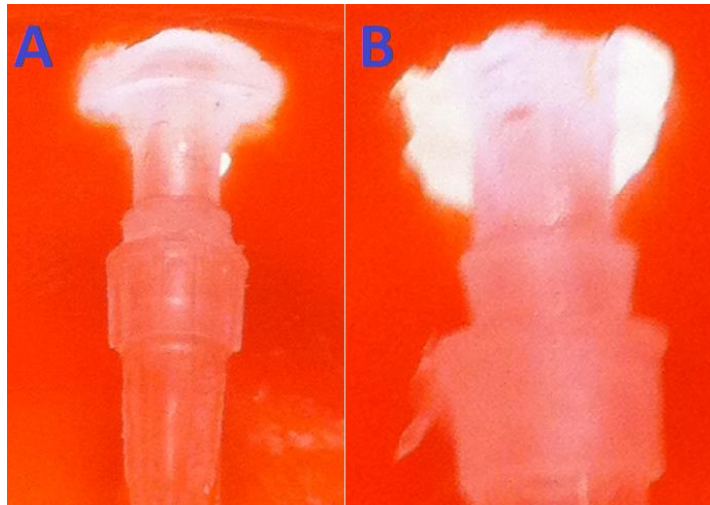


Figure 38: Expanded holes in the side of the printed components, allowing for insertion of the micropipette tips in the proper locations; (A) the drilled out hole for the perfusion inflow, and (B) the drilled out hole for the perfusion outflow

Second, the micropipette tips extend below the bottom plane of the device. This causes no issues while the device is inserted into the microscope, as the tips rest inside the slide chamber. However, on flat surfaces, the micropipette tips are the first components to contact, making them susceptible to damage. This can be prevented so long as the device is stored upside-down when not in use. Markings to this effect were added to the outside of the structure. Additional markings included explicitly declaring the in and out perfusion systems and giving a measurement line to help with the injection of the test solution.

5 Design Verification

Each of the four designs discussed in Section 4.2 were considered as a solution to the engineering challenge. The chosen design was created and tested in the laboratories at the University of Nova Gorica. After generating these design alternatives and considering the results of the Design Evaluation Matrix (Table 5), the open perfusion system was decided upon as the most viable of the four alternatives. In order to verify whether the beta design addressed the objectives, functions, and constraints established in Chapter Three, the team used a variety of experimental tests and procedures. The testing process, materials and methods are discussed in this chapter.

5.1 Verification Experiments

Compliance to the specifications was established through a series of seven design verification test experiments. Each of these experiments tested one or more related specifications.

5.1.1 Mechanical Interference

The purpose of the first experiment was to ensure the device could be set up, secured, used, and taken down without mechanically interfering with the microscope or damaging cells (Appendix E). The device was placed atop the thermal control ring and secured, where it independently remained in place. Tubing was connected to the perfusion inputs and outputs, and the microscope arm lowered without mechanical interference. All of these actions were completed within 10 minutes. An initial DIC image was captured, and time-lapse calcium imaging began prior to injection of TTX into the culture. The injection of TTX required a surprisingly high degree of dexterity, as it was difficult to guide the pipette directly into the culture through the small hole in the side of the device. Imaging was stopped and the time-lapse data evaluated. No interference with image quality was detected during the time of test solution injection. A DIC image was taken after perfusion was turned off. When compared to the original image, no cell damage was detected. Device disassembly required less than 10 minutes time.

5.1.2 Low Fluid Alarm

This experiment tested the effectiveness of the Low Fluid Alarm (Appendix F). The Low Fluid Alarm (detailed in Section 5.1.2) was tested by pouring a large amount of water into the reservoir, then switching the valve to the 'open' position and allowing the system to drain. The light-emitting diode

remained off until the solution reached a critically low level. The light-emitting diode indicated that experimenters needed to refill the reservoir, ensuring that data would not be lost due to cellular exposure to air.

5.1.3 Perfusion Effectiveness

This experiment tested the device's ability to track changes in concentration as a function of time (Appendix G). In order to do this, the team decided to utilize a spectrophotometer. A 9x 2:1 serial dilution of 2X Bromophenol Blue ink was prepared in a series of nine cuvettes, whose optical densities were recorded at a wavelength of 590 nm⁵ to create a standard curve. Next, the cell culture dish was filled with 100% dye and the perfusion system turned on. At 4 second time points, 15µL samples were taken and inserted into new cuvettes. The optical densities of these cuvettes were measured by spectrophotometer. The equation calculated to infer the concentration of dye as a function of time was determined to be $\text{Concentration (M)} = 167.7 \exp(-0.285 * t_{\text{Elapsed}})$. The equation implies an exponential decay of dye concentration. Based on this equation, after five minutes, the concentration would be reduced to a small enough level to conclude that the perfusion system effectively flushes out test solutions from the culture.

5.1.4 Consistent Inflow and Outflow Positions

This experiment determined whether or not the relative positions of micropipette tips of the perfusion inflow and outflow system were stable (Appendix H). In order to check that these positions remained constant, the distance between micropipette tips was measured with calipers as 15.85mm. The device was then shaken vigorously and measured again with calipers, this time measuring 15.64mm. Since the difference between the two values was 210 microns and this is likely within the range of measurement error, this provided strong evidence that the positions of the micropipette tips were constant, relative to one another.

⁵ This frequency was chosen as it is near the peak of the absorption spectrum of Bromophenol Blue

5.1.5 Thermal Control Compatibility

This experiment tested whether it is possible for the thermal regulation equipment to be used in conjunction with the device (Appendix I). The thermal control ring of the microscope has two plug-ins, to which a separate system must be connected to ensure temperature control over the course of a test. The device did not restrict access to these plug-ins.

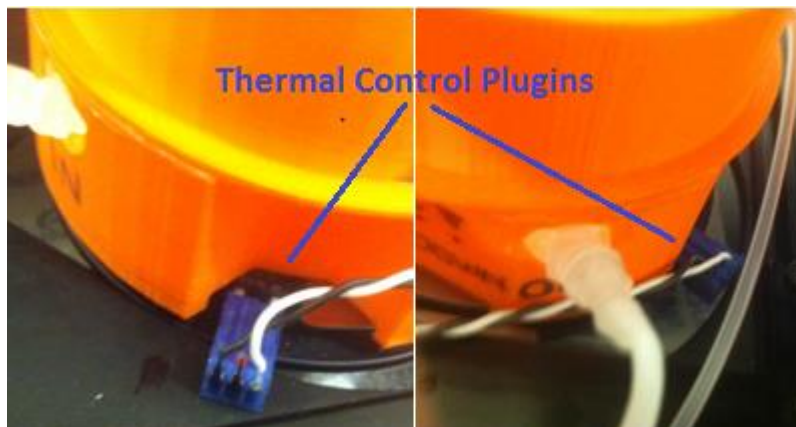


Figure 39: Plug-ins of the thermal control ring; note that the device does not prevent the connection of the thermal control ring to the external thermal control system

5.1.6 Constant Volume

This experiment tested whether the volume of liquid left in the slide remained constant between tests (Appendix J). Fluid volume variation was determined by covering the slide with 1mL of water, turning on the perfusion outflow pump, and waiting until the volume was constant with respect to time. When a stable volume was reached, the pump was turned off and a micropipette was used to remove incremental volumes of water until the slide chamber was empty. This test was repeated nine times, and yielded an average volume of 200 μ L with a standard deviation of 24.13 μ L. The results of this experiment surprised UNG researchers, who previously understood the chamber volume to be 500 μ L. This implied that they had been exposing cells to higher concentrations of drug treatments than intended, as the positions of the perfusion outflow tubes are similar in both the old setup and in the device.

5.1.7 Light Blocking Capability

This experiment tested whether the device would interfere optically with the quality of fluorescence imaging by allowing significantly more ambient light into the system than the previous setup. The protocol for this experiment can be found in Appendix K. With only distilled water over the slide, the background light which eventually reached the camera was tested under three conditions: with nothing blocking the light, with the previous setup (described in Section 2.4.2) blocking the light, and with the device blocking the light. The data from the three conditions was analyzed and compared. It was observed that while both light blocking techniques performed significantly better than an exposed system, neither showed a significantly greater capability to shield light than the other.

5.1.8 Individual Specification Verification

Below are listed all of the individual specifications of the design, as well as the deterministic questions which allowed the team to decide whether or not the specification was satisfied.

Table 6: An overview of the state of completion of the various specifications

ID	Specification	Deterministic Questions	Validated?
001	At no point during the process of cell installation or testing shall the cell-carrying surface of the slide be exposed to air	At any point in the completion of Protocol A, were the cells exposed to the open air? <input type="checkbox"/> Yes <input checked="" type="checkbox"/> No If no, then the specification is validated	<input checked="" type="checkbox"/> Specification Met <input type="checkbox"/> Specification Not Met
002	Device must alert the user before running out of the control solution	In Protocol B, is the answer to step 2 “No,” indicating the Low Fluid Alarm does not report a false positive result for low fluid level in the reservoir? <input checked="" type="checkbox"/> Yes <input type="checkbox"/> No Is the answer to step 6 “Yes,” indicating that Low Fluid Alarm correctly reports	<input checked="" type="checkbox"/> Specification Met <input type="checkbox"/> Specification Not Met

		critically low levels of fluid in the reservoir? <input checked="" type="checkbox"/> Yes <input type="checkbox"/> No If both answers are yes, then the specification is validated	
003	The control concentration of test solution must be +/- 1 mM the expected value initially	Self-Evident. The initial concentration of the test solution is defined by the composition of the control solution. It will always be zero.	<input checked="" type="checkbox"/> Specification Met <input type="checkbox"/> Specification Not Met
004	The experimental concentration of test solution must be +/- 1 mM the expected value	Are any of the values found in Protocol F, step six greater than 0.20mL away from the mean average of the ten values, indicating that concentration variance of greater than 1mM could be due to volume fluctuation? <input checked="" type="checkbox"/> Yes <input type="checkbox"/> No If no, than the specification is validated.	<input type="checkbox"/> Specification Met <input checked="" type="checkbox"/> Specification Not Met
005	The final concentration of test solution must be +/- 1 mM the expected value	Refer to the equation in step 18 of protocol C. This equation defines the relationship between concentration and time in the perfusion system. Based on this equation, how long would the system require to drop below the 1mM level? <i>Extrapolating from the collected data, the time required to reduce the concentration from 1 M to 1mM is 24.28 seconds.</i> Is this time less than five minutes, indicating that the test solution may be flushed from the slide within a reasonable time frame?	<input checked="" type="checkbox"/> Specification Met <input type="checkbox"/> Specification Not Met

		<p><input checked="" type="checkbox"/> Yes <input type="checkbox"/> No</p> <p>If yes, than the specification is satisfied.</p>	
006	<p>No part of the device must mechanically interfere with any part of the operation of the microscope</p>	<p>In protocol A, are the answers to steps six and seven both “No,” indicating that the microscope arm does not interfere with the light shield?</p> <p><input checked="" type="checkbox"/> Yes <input type="checkbox"/> No</p> <p>In protocol E, is the answer to step three “No,” indicating that the device does not interfere with the plug-ins of the thermal control ring?</p> <p><input checked="" type="checkbox"/> Yes <input type="checkbox"/> No</p> <p>If both answers are yes, than the specification is validated</p>	<p><input checked="" type="checkbox"/> Specification Met</p> <p><input type="checkbox"/> Specification Not Met</p>
007	<p>No part of device setup, operation, or breakdown must depend on an unusual degree of manual dexterity</p>	<p>Are any issues with manual dexterity observed in Protocol A steps 5, 13, or 18?</p> <p><input checked="" type="checkbox"/> Yes <input type="checkbox"/> No</p> <p>If no, then the specification is validated</p>	<p><input type="checkbox"/> Specification Met</p> <p><input checked="" type="checkbox"/> Specification Not Met</p>
008	<p>No device component shall intrude upon the space between the slide and the objective lens</p>	<p>In protocol A, step five, was there any interference with the space between the slide and the objective lens?</p> <p><input type="checkbox"/> Yes <input checked="" type="checkbox"/> No</p> <p>If no, then the specification is validated</p>	<p><input checked="" type="checkbox"/> Specification Met</p> <p><input type="checkbox"/> Specification Not Met</p>

009	The device shall be stable enough such that falling over and detachment are not concerns of experimenters	<p>At any point in the completion of protocol A was either knocking over or detachment of the device an issue?</p> <p><input type="checkbox"/> Yes <input checked="" type="checkbox"/> No</p> <p>If no, then the specification is validated</p>	<p><input checked="" type="checkbox"/> Specification Met</p> <p><input type="checkbox"/> Specification Not Met</p>
010	The device shall take an experimenter less than ten minutes to fully set up	<p>Is the noted time in protocol A, step five less than ten minutes, indicating that the device was set up in less than this amount of time?</p> <p><input checked="" type="checkbox"/> Yes <input type="checkbox"/> No</p> <p>If yes, then the specification is validated</p>	<p><input checked="" type="checkbox"/> Specification Met</p> <p><input type="checkbox"/> Specification Not Met</p>
011	The device shall take an experimenter less than ten minutes to fully break down	<p>Is the noted time in protocol A, step eighteen less than ten minutes, indicating that the device was fully broken down in less than this amount of time?</p> <p><input checked="" type="checkbox"/> Yes <input type="checkbox"/> No</p> <p>If yes, then the specification is validated</p>	<p><input checked="" type="checkbox"/> Specification Met</p> <p><input type="checkbox"/> Specification Not Met</p>
012	The introduction of the test solution and microscopy must not be mutually exclusive events	<p>Was it possible to inject the TTX in protocol A, step 13, indicating that injection of test solution can be simultaneous with fluorescent imaging?</p> <p><input checked="" type="checkbox"/> Yes <input type="checkbox"/> No</p> <p>If yes, then the specification is validated</p>	<p><input checked="" type="checkbox"/> Specification Met</p> <p><input type="checkbox"/> Specification Not Met</p>

013	<p>The speed and type of flow caused by the device must not damage or disturb the network of hippocampal neurons</p>	<p>Compare the images taken at the five XY coordinates noted in protocol A, step eight between step eight and step sixteen.</p> <p>Are all neuron noted in step eight still present at the time of step sixteen?</p> <p><input type="checkbox"/> Yes <input checked="" type="checkbox"/> No</p> <p>If yes, then the specification is validated</p>	<p><input type="checkbox"/> Specification Met</p> <p><input checked="" type="checkbox"/> Specification Not Met</p>
014	<p>Any inflows and outflows to the cell culture must remain at constant positions relative to one another and to the slide from test to test</p>	<p>Are comparable distances noted in Protocol D, steps one and three, indicating that the micropipette tips do not move?</p> <p><input checked="" type="checkbox"/> Yes <input type="checkbox"/> No</p> <p>If yes, then the specification is validated</p>	<p><input checked="" type="checkbox"/> Specification Met</p> <p><input type="checkbox"/> Specification Not Met</p>
015	<p>The temperature of the cells must be kept within 1 degree Celsius of any desired temperature between room temperature and 40 degrees Celsius</p>	<p>Was the answer to protocol E, step three “yes,” indicating that it is possible to connect the thermal control system?</p> <p><input checked="" type="checkbox"/> Yes <input type="checkbox"/> No</p> <p>If yes, then the specification is validated</p>	<p><input checked="" type="checkbox"/> Specification Met</p> <p><input type="checkbox"/> Specification Not Met</p>

6 Discussion and Results

UNG's Centre of Biomedical Sciences and Engineering at Vipava studied the mechanism of interaction between QDs and hippocampal neurons in order to explore the possibility to use them to evoke action potentials in single neurons.

6.1 Device Implementation

The beta design of the device was used in calcium imaging experiments to validate its effectiveness and viability to gather data and further research interests at the Centre. Initially, the device was used in experiments with well-understood test solutions containing Tetrodotoxin (TTX) and Gabazine.

TTX, a neurotoxin derived from puffer fish, is a drug known to block sodium ion channels. Since sodium ions initiate the depolarization of action potentials, blockage of the sodium ion channels significantly decreases neuronal electrical activity. Two-dimensional time-lapse calcium images of neurons injected with 5 μ L of TTX were taken with both the original and new perfusion setups. In each case, the activity of cells decreased, as seen in Figure 40.

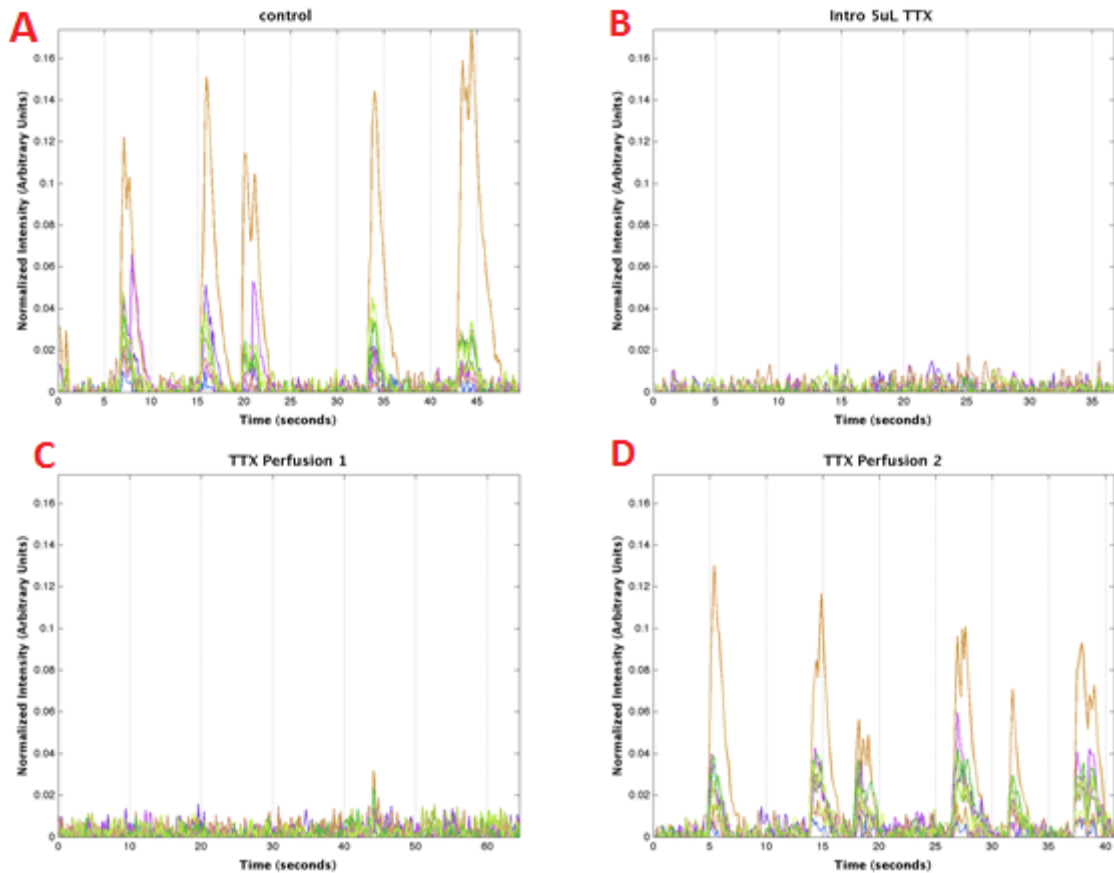


Figure 40: Calcium imaging of multiple neurons, each a different color, with TTX and perfusion system; (A) control series shows the basic activity of the network, (B) immediately after the addition of TTX, when activity stops, (C) perfusion system is opened, the first calcium event is witnessed after 47 seconds (D) 150 seconds after the perfusion is opened, the culture is actively firing again at almost the same magnitude as the control, indicating little photobleaching.

When perfusion was turned on and TTX flushed away, activity returned after 5 minutes(Figure 40D). Additionally, the similarity between the magnitude of signal in these tests suggests that the effect of photobleaching on OGB is negligible even with repeated long-term exposures. Both the new perfusion system, as well as the old, successfully diluted the culture solution enough for cells to regain activity in five minutes.

Gabazine, an excitatory neurotransmitter discussed in Section 2.2.2, is known to elicit synchronous action potentials by inhibiting chlorine ion flux across the cell membrane. Since chlorine ions lower the membrane potential, the inhibition of chlorine results in only excitatory stimulus. 2D

time-lapse calcium imaging confirmed this outcome, as 5 μ L of 10 μ M Gabazine elicited increases in synchronicity and magnitude when injected into the culture (Figure 41).

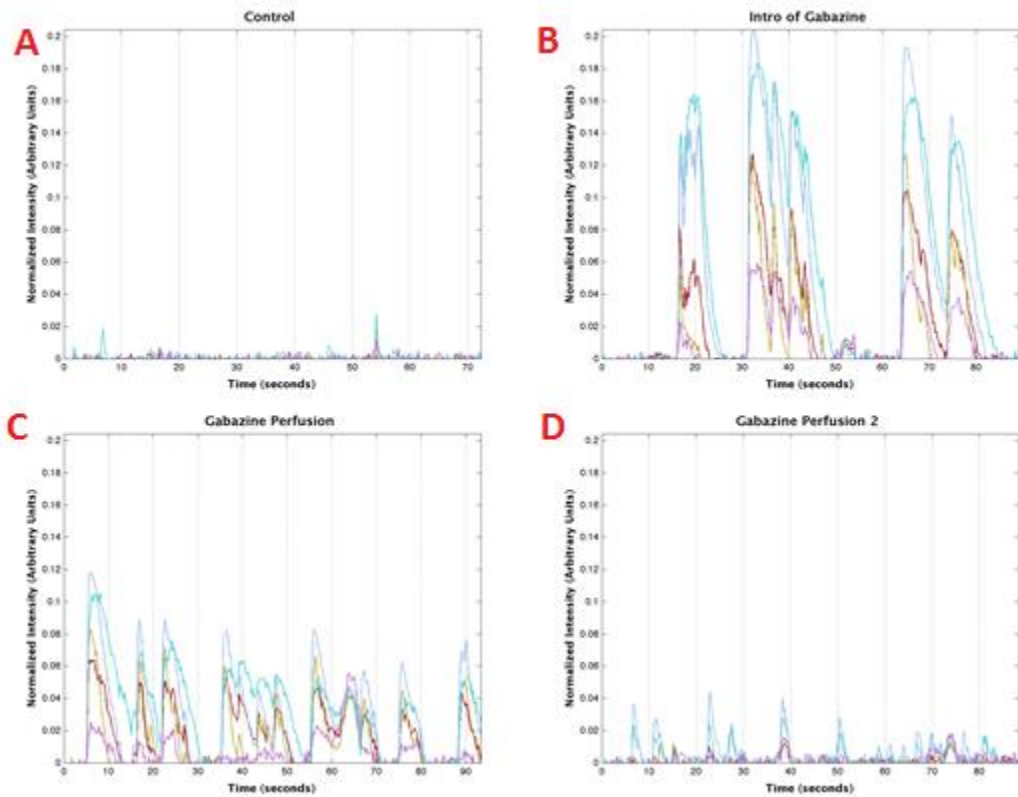


Figure 41: Calcium imaging of multiple neurons, each a different color, with Gabazine and perfusion system; (A) control series shows the basic activity of the network, (B) activity immediately after the addition of Gabazine, with large increases in the magnitude and synchronicity of activity, (C) activity just after the perfusion system is opened, with immediate decrease in activity (D) 150 seconds after the perfusion is opened, the activity of the culture significantly reduced, although still somewhat synchronous.

Similarly to TTX, turning on the new perfusion system caused the effects of Gabazine to diminish overtime as it was washed away. Specifically, the results show decreasing synchronicity and overall occurrences of action potentials (Figure 41C). However, in this experiment, the photobleaching effect cannot be ruled out as error as in the TTX perfusion experiment, because the final test has such low and inconclusive signal.

6.2 Quantum Dot Experimentation

After the device's effectiveness in experiments was validated using TTX and Gabazine, experiments using Quantum Dots (QDs) were run to begin gathering new data. In Vipava, researchers used the Qdot-655 by Invitrogen, a division of Life Technologies. Previous research had shown, as discussed in Section 2.3, that when QDs were excited by radiation, they exhibited an electric dipole moment, or local change in voltage, which induced action potentials in neurons. The Qdot-655 was a CdSe-core, ZnS-shelled quantum dot with a polyethylene-glycol (PEG) surface coating (Figure 7). These QDs had a peak emission wavelength at 655nm, which was in the red spectrum of light and a broad excitation spectrum between 400nm and 750nm (Figure 9). Some Qdot-655 had additional biomolecules attached to their PEG surface coating to allow for specific biomolecule binding. UNG researchers conducted tests using Qdot-655 conjugated with both streptavidin and carboxyl (COOH-) functional groups.

Streptavidin Qdot-655 have been used to conjugate to biotin proteins, allowing further conjugation to antibodies for targeted delivery in living systems. However, researchers at UNG did not conjugate Qdot-655 with any other biomolecule for experiments. When Qdot-655 was imaged using multi-plane 3D reconstruction imaging, the QDs showed slight adherence to the membranes of neurons, although most remained suspended in solution. A control calcium recording was taken which demonstrated spontaneous fluctuations, as shown Figure 42A. Upon injection of Streptavidin Qdot-655, the synchronicity of the culture increased dramatically, meaning each neuron was firing in phase, while the magnitude of electrical activity from individual neurons slightly decreased.

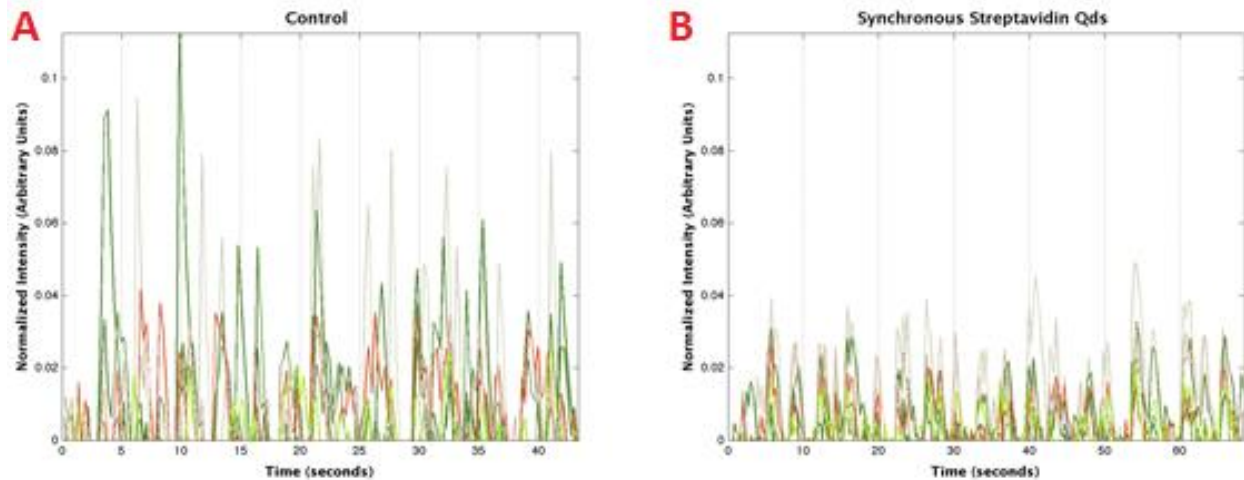


Figure 42: Calcium imaging of multiple neurons, each a different color, with 0.8nm of Streptavidin QD-655, (A) a control recording, showing spontaneous activity with different magnitudes in different neurons, and (B) recording after introduction of QDs, with increased synchronicity and decreased magnitude of activity.

Together, the streptavidin protein and the PEG surface coating was a relatively large complex conjugated to the Qdot-655 in comparison to the size of the nanoparticle, as seen in Section 2.3. This large barrier could have shielded the electric dipole moment of the QD and prevented its efficient interaction with ion channels on the cell membrane.

Carboxyl-coated (COOH-) Qdot-655s are reactive, organic biomolecules that served as a foundation for conjugation to more complex molecules, such as Streptavidin. A 2D time-lapse calcium image of these QDs in neuron culture revealed that the QDs strongly adhered to the cell membrane of neurons. A 3D reconstruction was created in order to confirm this hypothesis, as seen in Figure 43.

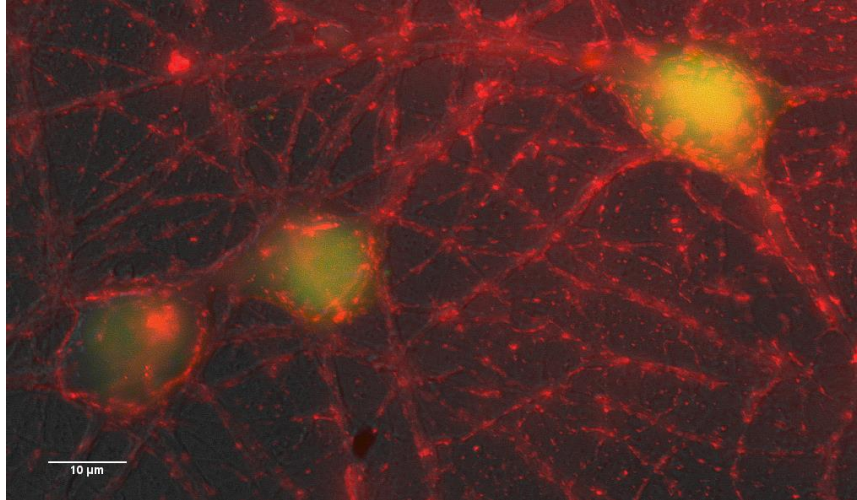


Figure 43: A 3D reconstruction of carboxyl-coated Quantum Dots (red) attached on the cell membrane of hippocampal neurons treated with Oregon Green BAPTA (green) to show intracellular calcium.

The inside of the neuron was loaded with OGB dye, which fluoresced around 488nm, illustrating the most calcium rich areas of the cell. Carboxyl-coated Qdot-655 fluoresced around 655nm and attached to the soma, dendrites and axons of the neurons.

2D calcium imaging time-lapses were recorded of Carboxyl-coated Qdot-655 interacting with neurons. In the control recording, the calcium activity of the neuron was spontaneous. When Carboxyl-coated Qdot-655 were injected into the culture, the calcium events became more synchronous, with the calcium events in some neurons much stronger. Additionally, the intensity of calcium activity in each neuron became more equivalent.

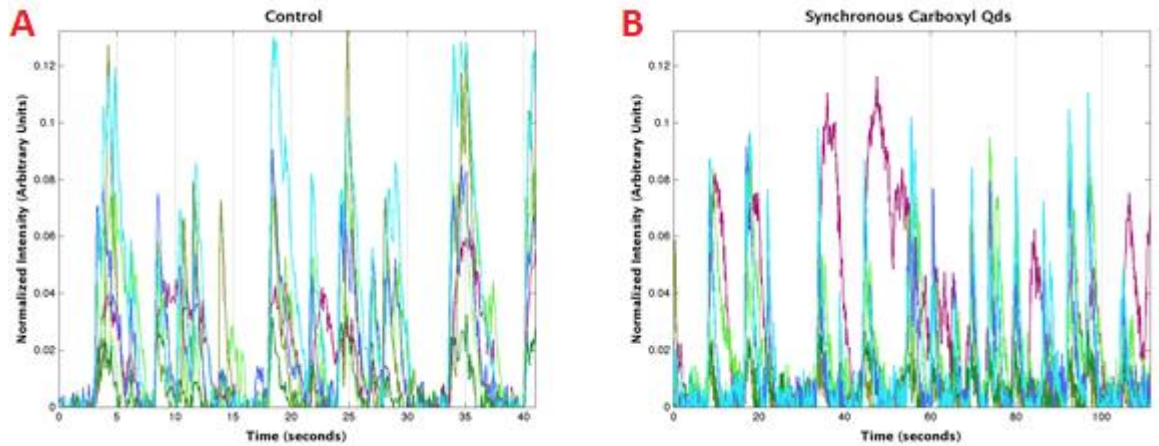


Figure 44: Calcium imaging of multiple neurons, each a different color, with 0.8nm of carboxyl-coated QD-655, (A) a control recording, showing spontaneous activity with different magnitudes in different neurons, and (B) recording after introduction of QDs, with increased synchronicity and equivalent magnitudes of activity.

In order to understand the mechanism of interaction of between Qdot-655 and neurons using calcium imaging, additional experiments were conducted to compare to QD experiments using drugs with known and well-characterized effects on neuronal electrical activity. A time-lapse calcium recording was performed with Gabazine to compare with the QD interaction, as seen in Figure 45. In the control recording (Figure 45A), calcium activity was low.

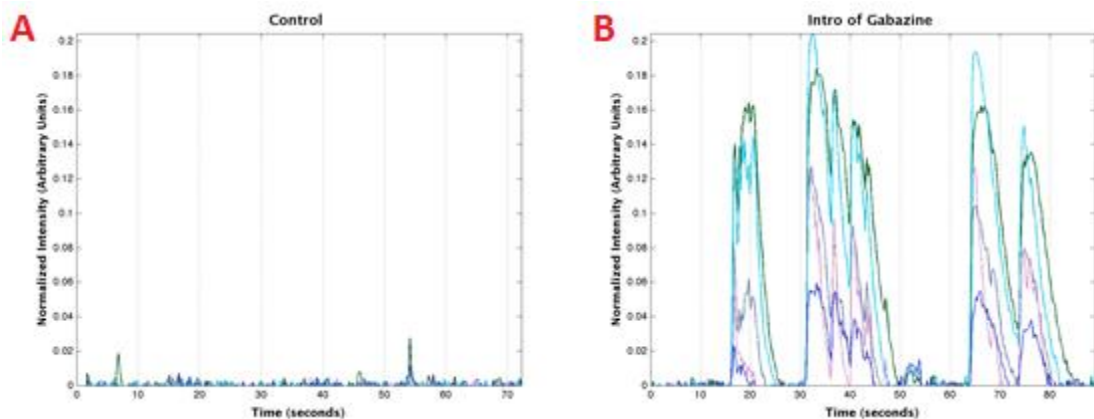


Figure 45: The effect of Gabazine on neuron cultures, (A) a control recording shows weak, spontaneous activity, and (B) after the introduction of Gabazine, recording shows increased magnitude and synchronicity of activity.

Notice that when Gabazine was introduced into the culture, calcium activity increased in both synchronicity and magnitude. These results show that carboxyl-coated QDs interacted with neurons to cause similar synchronous activity to Gabazine.

Finally, a validation experiment was conducted with a combination of Qd-655 and TTX. TTX can be used to rule out secondary calcium signals as the source for activity in calcium imaging, as seen in Figure 46.

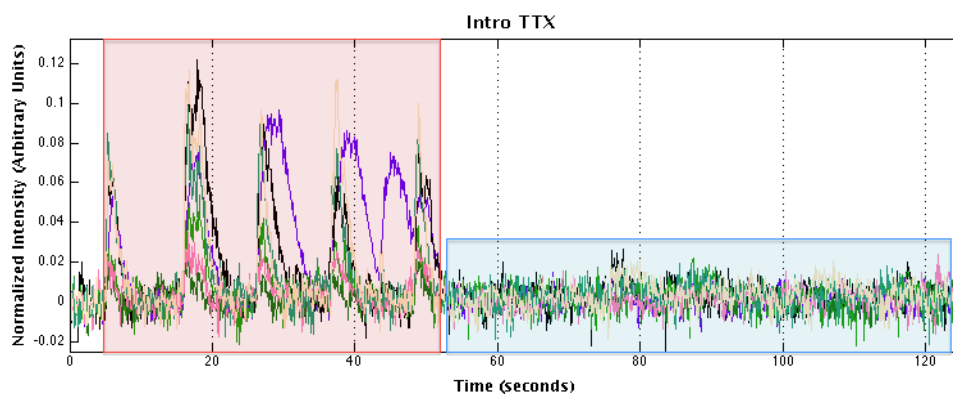


Figure 46: The effect of TTX on calcium activity of hippocampal neurons stimulated by carboxyl-coated QD; with calcium signals affected by QDs seen highlighted in red and, the lack of calcium activity as a result of TTX seen in blue.

Carboxyl-coated Qdot-655 was introduced into a network of neurons and caused synchronous activity. Then, TTX was introduced midway through the recording and most calcium activity stopped. This implies that the majority of the calcium signals recorded resulted from the electrical activity of neurons.

6.3 Design Considerations

As with any design, there is a pressing need to discuss its social impact. Whether it is a global consideration or a local concern, the following section analyzes the impact of this project on the surrounding world.

6.3.1 Economic Impact

If this drug delivery platform is successful, the University of Nova Gorica will economically benefit. The device will inject drug treatments directly into cell culture, rather than into the solution reservoir, maximizing the efficiency of the drug delivery process, as treatments are not lost in the perfusion tubing. This increased effectiveness will therefore decrease the amount of money UNG spends on various drug treatments and nanoparticles.

6.3.2 Environmental Impact

The 3D printing process wastes material, as it has a filler polymer that must be cut out before the final design can be printed. Additionally, UNG uses Cadmium core QDs, which contain heavy metals that are known to be toxic to living systems and dangerous to the environment if not disposed of properly.

6.3.3 Societal Influence

The research at UNG deals with neuroplasticity, important in memory formation. QDs have been shown to alter the plasticity of neurons, which can be used to stimulate neurons and study neuroplasticity *in vivo*. By increasing the efficiency of experiments, our device will help to further knowledge in a groundbreaking field of neuroscience. Understanding the external effects of materials and chemicals on hippocampal neuron cultures will better elucidate the working of the human brain.

6.3.4 Political Ramifications

Students from the United States of America created a design to be used by Italian researchers at a Slovenian laboratory. This multicultural environment requires the cooperation of Slovenian, Italian, and American governments.

6.3.5 Ethical Concerns

The ethical concerns of our design are limited to the usage of non-sustainable plastic materials, as well as waste of 3D printer polymer filler. Additionally, the use of Cadmium core QDs may be of concern, as Cadmium is a toxic heavy metal that may be harmful to the environment.

6.3.6 Health and Safety Concerns

The fluorescence feature of the Olympus microscope used at UNG emits ultraviolet radiation that may significantly damage vision after prolonged exposure. Our device includes a light shield that blocks the microscope operator's eyes from harmful UV light. The test solutions used in experiments are potentially harmful, as Gabazine has been known to cause epilepsy and Tetrodotoxin is known to have powerful neurotoxic properties.

6.3.7 Manufacturability

Our device is detailed in SolidWorks and may be easily manufactured using 3D printing. This allows for future modifications and reproduction of the device. Additionally, all other components can be procured for low costs in bulk, making larger scale production feasible.

6.3.8 Sustainability

The perfusion system itself requires no energy to operate, although the Low Fluid Alarm is powered by two AA batteries. Additionally, the microscope and perfusion outflow pump both require electricity to function. The final product is minimalistic and uses materials already existent in the laboratory.

7 Final Design and Validation

Research at the University of Nova Gorica requires coordination between a variety of different systems and procedures. First is the Olympus microscope, capable of capturing fluorescence and DIC images with sub-micrometer resolution. Images of cells are processed and crucial data is derived from these results. In between the microscope and the data is the perfusion system, which provides necessary nutrients to maintain cell health and introduces various treatments into the culture. The original perfusion system at UNG was both unwieldy and inefficient, so the team set out to improve upon the treatment delivery and the convenience of the system.

7.1 Design Workflow

A Gantt chart (Appendix C: Gantt Chart) and a work breakdown structure (Appendix B: Work Breakdown Structure) were created to describe all tests to run and data to acquire over the course of the team's time at UNG. In order to ensure the device would not mechanically interfere with the microscope, dimensions were measured and used to produce computer aided design (CAD) drawings of design alternatives. Upon completion of CAD drawings, the group visited a local hardware store to purchase necessary materials, and created the first prototype from polyurethane. The first prototype had dimensions which interfered with the microscope components and prevented imaging when placed onto the thermal control ring. A second prototype was constructed primarily using Plexiglass, rather than polyurethane, as the primary material, and aluminum cans were used to manufacture a rudimentary light shield. This prototype was functional; however, the diameter of the light shield mechanically interfered with the arm of the microscope and inhibited the movement of the microscope stage, preventing imaging of all areas of the slide. To alleviate this issue, a final prototype design was manufactured out of the same materials as the second, which was demonstrated to have no mechanical interference with the microscope components.

The final CAD drawing was sent to be 3D printed at another facility. The printed device was comprised of two separate components and made of ABS, a thermoplastic polymer with a glass-transition temperature of 105⁰C, much higher than the maximum experimental temperature of 37⁰C experienced on the microscope. After gluing the two components together, micropipette tips and tubing were set with glue, and the device was used in experiments. A final addition to our device was a Low Fluid Alarm for the perfusion system. This alarm activated a small light-emitting diode next to the computer screen to inform the experimenter of the need to refill the reservoir with solution.

7.2 Design Assembly

Using SolidWorks 2012 x64 Edition computer modeling software, two 3D models were created. The first of these models incorporated mounts for the later addition of perfusion system components and a guidance system to increase the ease of injection of test solutions into the sample. The bottom of this part was shaped to fit over the thermal control ring of an Olympus IX81 inverted microscope without mechanically interfering with any microscope component. A hole in the bottom of this component allowed for clear light paths to both the microscope arm above the sample and to the objective lens below.

The second of these models was shaped to fit on top of the first and extend as far as possible upwards without resulting in mechanical interference. This component prevented large amounts of ambient light from reaching the slide.

These components were converted to .STL files and sent to the 3D Printing Laboratory at the International Centre for Theoretical Physics (ICTP) for printing. They were successfully printed out of orange ABS plastic. The matrix polymer was removed from both components. The second of the components was superglued on top of the first to combine them into a single device.

Micropipette tips were connected to thin rubber tubing and inserted into the mounts on either side of the device. The tips of these micropipettes were positioned such that, when the device was placed in the microscope, the outflow tip was in contact with the edge of the slide in the chamber and the inflow tip recessed approximately 2 mm back from the edge on the opposite side. This positioning required drilling out two holes in the side of the device to a greater area. Once positioned, the micropipette tips were superglued into place.

Separately from the above, an indicator system was created to alert the user of a critically low level of control solution in the perfusion inflow system. Three pieces of 3mm black polyurethane were cut to size and glued together, such that they fit over a flange of a Henke Sass Wolf Norm-Ject 60mL syringe. A microcentrifuge tube was filled with enough stones so that it had just enough buoyancy to remain floating in 37°C water, while still having the greatest possible mass. This tube was connected to the black polyurethane piece by a length of plastic fiber, such that when the polyurethane was fitted over the flange, the centrifuge tube hung down inside the syringe to a height of between ½ and 1 inch from the bottom.

The opposite flange of this syringe was covered with a layer of aluminum foil, attached on the inside by superglue. Thin wiring was connected to the plastic tubing and the polyurethane piece to form a simple electrical switch across the top of the syringe. This switch remains naturally open when the syringe is filled with fluid, but closes when it is not. This switch was placed in series by long lengths of copper wire with a 300 Ω resistor, a red light-emitting diode of unknown origin, and two AA batteries.

7.3 Financial Considerations

While the team was able to manufacture the existing design using entirely free or available materials, production of future versions would likely not be equally inexpensive. The primary cost of the design is due to the 3D printing process.

There is no realistic alternative to 3D printing for production of these parts, particularly considering the limited manufacturing facilities available to the Centre for Biomedical Sciences and Engineering. While the team was able to print at no charge, thanks to the support of Carlo Fonda at ICTP, it is presumptuous to assume that ICTP would continue to offer its free services in the future. However, various companies exist which can print in 3D for little more than the price of materials. The price of 3D printing was estimated using the website 3Dprintingpricecheck.com. The light shield component could be printed by several companies for approximately €7.26 (\$10), while the perfusion component could be printed for approximately €10.89 (\$15), totaling approximately €18 (\$25) to 3D print the design using ABS plastic.

Micropipette tips, which serve as the perfusion inflows and outflows, are readily available in excess in the laboratory. In most cases, after a single use for other applications, they would be discarded. As the pipettes for this design do not necessarily need to be biologically sterile, they may be repurposed from tips that would otherwise be thrown out and cost UNG nothing. The same can be said of the micropipette tube and aluminum foil required for the Low Fluid Alarm.

Superglue is readily available at a convenience store approximately 50 meters from Centre for Biomedical Sciences and Engineering, where it costs €3.30 (\$4.55).

The thin plastic fiber used for the Low Fluid Alarm was purchased in bulk for €1.00 (\$1.38).

Tubing and tubing connectors are readily available due to proximity to the Slovenian Wine Research Institute, and added no additional cost to the design. Future tubing and connectors may be

purchased from Warner Instruments for less than €16.69 (\$23.00) and €20.32 (\$28.00), respectively (specialized tools for Electrophysiology and Cell Biology Research).

A spool of insulated copper wire for the Low Fluid Alarm was purchased by the team for €6.50 (\$4.72) at a local hardware store. The length of wire purchased is sufficient for dozens of additional designs, if desired or needed.

Simple red light-emitting diodes can be purchased for less than € 0.36 (\$0.50) each.

Electrical tape can be purchased for less than €2.90 (\$4.00).

Even in low quantities, AA batteries may be purchased for no more than € 0.73 (\$1.00) each. These prices reduce significantly when the batteries are purchased in bulk.

A summary of the manufacturing costs is presented below:

Table 7: Costs of all materials needed to manufacture the beta device

Component	Cost (Euro)	Cost (USD)
3D Printed Light Shield	Free	Free
3D Printed Design Bottom	Free	Free
Micropipette Tips	Readily available	Readily available
Microcentrifuge Tube	Readily available	Readily available
Plastic Fiber	€1.00	\$1.38
Superglue	€3.30	\$4.55
Tubing and Accessories	Readily available	Readily available
Copper Wire	€6.50	\$8.95
AA Batteries (2)	€1.45	\$2.00
Electrical Tape	€2.90	\$4.00
Hobbycolor Polyurethane	€3.39	\$4.67
Red light-emitting diode	€0.36	\$0.50
Total Cost⁶	€18.85	\$25.97

⁶ Calculated according to the US Dollar/Euro conversion rate of 16Dec2013

Table 8: Costs of all materials needed to manufacture any future devices. Copper wire and plastic tubing were purchased in large enough quantities that there exists enough excess for many future devices. Microcentrifuge tubes and micropipette tips can be easily procured from lab waste.

Component	Cost (Euro)	Cost (USD)
3D Printed Light Shield	€7.26	\$10.00
3D Printed Design Bottom	€10.89	\$15.00
Micropipette Tips	Readily available from laboratory waste	Readily available from laboratory waste
Microcentrifuge Tube	Readily available from laboratory waste	Readily available from laboratory waste
Plastic Fiber	Readily available after bulk purchase	Readily available after bulk purchase
Superglue	€3.30	\$4.55
Micropipette Tubing	€16.69	\$23.00
Micropipette Connectors	€20.32	\$28.00
Copper Wire	Readily available after bulk purchase	Readily available after bulk purchase
AA Batteries (2)	€1.45	\$2.00
Electrical Tape	€2.90	\$4.00
Hobbycolor Polyurethane	€3.39	\$4.67
Red light-emitting diode	€0.36	\$0.50
Total Cost⁷	€66.56	\$91.72

These costs are considered acceptably low by both the team and the University of Nova Gorica.

⁷ Calculated according to the US Dollar/Euro conversion rate of 16Dec2013

7.4 Device Verification Testing

Calipers were used to measure the distance between the micropipette tips of the device. The device was shaken vigorously in an attempt to alter micropipette position and calipers were used to re-measure the distance between tips.

The device was placed on top of the thermal control ring, and thermal plug-ins were connected and disconnected from the ring. Perfusion tubing was secured to the micropipette tips and the microscope arm was lowered over the device. The pump was turned on and a DIC image was captured prior to turning the perfusion system on. The perfusion system was turned on and a time-lapse image was recorded. A second DIC image was taken after the perfusion system was turned off.

The perfusion effectiveness was tested using spectrophotometry. The slide chamber was filled with 2X Bromophenol Blue ink. The perfusion system was turned on, and a 15 μ L sample was taken from the slide chamber at time points of four seconds. These samples were deposited into a series of nine cuvettes whose optical densities were recorded by spectrophotometer. The concentrations were plotted as a function of time using a standard curve of optical density as a function of concentration determined by a 9x 2:1 serial dilution of the Bromophenol Blue ink.

The consistency of slide chamber volume was tested. The slide chamber was again filled and the outflow pump turned on to suction out excess fluid. When the volume in the slide chamber stabilized, the pump was turned off. A micropipette was used to remove the remaining liquid by 20 μ L increments. This test was repeated nine times.

To determine the amount of ambient light entering the system, a slide of only distilled water was mounted in the slide chamber and fitted onto the thermal control ring. Two 15-second fluorescent images were taken for each of three light-blocking parameters: the installed device, a cardboard box surrounding the microscope, and no light shield. The average intensities of light in each of these three conditions were recorded and statistically compared.

The Low Fluid Alarm was mounted on top the solution reservoir. Its effectiveness was tested by pouring 50mL of fluid into the reservoir while the perfusion inflow valve was closed. The perfusion inflow valve was then opened and the fluid was allowed to flow from the reservoir. The light-emitting diode was monitored for activity.

7.5 Experimental Validation Testing

The effects of TTX, Gabazine, and QDs were studied using an identical test procedure. A neuron culture was viewed under a microscope and one glass slide was inserted into a petri dish containing 1.5mL Ringer's solution and 0.7 μ L OGB dye. The petri was covered with aluminum foil and left for 40 minutes. Tweezers were used to remove the slide from the petri dish and place it into the slide chamber (Appendix L). The slide was submerged in Ringer's solution and the slide chamber was fitted into the thermal control ring and placed onto the microscope setup. The device was secured onto the thermal control ring and the microscope arm was lowered. Perfusion tubing was attached to the micropipette tips protruding from the device. The perfusion outflow pump was turned on and the reservoir inflow valve was opened.

The xenon lamp was powered up by first turning on the lamp, waiting for ten seconds, then turning on the main power supply. The microscope camera was turned on, and then Slidebook5 software calibrated for use with the xenon lamp was opened. A new slide file was saved as the day's date.

A control DIC image was taken to identify the location of neurons. ROIs were drawn around each of the identified neurons in the field of view. Time-lapse fluorescent images were recorded to assess initial culture conditions. The perfusion reservoir valve was closed and a selected dose of test solution was injected into the culture via micropipette through the micropipette guidance hole. A fluorescent time-lapse recording was begun immediately following treatment. Cell activity was visualized using a graph of the average intensity of each ROI as a function of time. The culture in test solution was imaged once or twice more, depending on experimental need. Once sufficient data was acquired, the reservoir valve was opened and a one-minute fluorescent time-lapse image of drug perfusion out was taken every two minutes.

At this point, the experiments varied depending on the test solution in use. If the cells were still alive and showed only minor photobleaching, then the reservoir valve was again closed; a second test solution was introduced into the culture, and the experimental process was repeated. If the cells exhibited a significant amount of photobleaching, then the reservoir valve was closed and the pump turned off. The breakdown instructions Appendix M: Standard Operating Procedure for Breakdown of the Olympus Microscope were followed. Data analysis was performed using the MATLAB script of Appendix N: MATLAB Script used for Data Analysis and Presentation.

8 Conclusions and Recommendations

The Centre for Biomedical Sciences and Engineering in Vipava is a new facility that could benefit from the presence of innovative engineering students, able to solve problems and implement improvements to laboratory experimental procedures and setups. Additionally, these refinements are intended to produce meaningful experimental data that is able to advance research in neuroscience and nanotechnology.

As engineering students tasked with studying the mechanism of interaction between Quantum Dots (QDs) and hippocampal neurons, this project took on both a design and a research component. As such, the Conclusions and Recommendations will have both engineering and experimental facets.

8.1 Engineering Design Conclusions

1. *Blocks ambient light during florescent imaging*

The Centre is a new facility and all available space has not yet been renovated. As a result, the current laboratory space can be congested at times. The microscope used for calcium imaging, a light sensitive procedure, is set up in this busy area. To improve this setup, the team designed a compact device to shield ambient light from the microscope. The device was easier to assemble and maneuver, as it did not require the experimenter to remove the existing cardboard light shield each time. Additionally, the device was less likely to contaminate the culture, as sometimes the cardboard deposited debris into the slide chamber. The device shielded the slide from light as well as the previous light shield, had a smaller profile, and was easier to handle than the previous technique.

2. *Maintains more consistent volume of solution in slide chamber*

The previous setup included movable perfusion inflow and outflow mounts that changed position between each experiment, making it difficult to maintain precise volumes of solution in the slide chamber. The new device had consistent inflow and outflow placement that improved the precision of volume in the slide chamber, but still had some variability.

3. *Removes 99% of test solution in under 30 seconds with perfusion*

Validation testing with TTX demonstrated that the device could restore control conditions and return calcium activity in cultures. The perfusion outflow appeared to reduce the concentration of test solution in the slide chamber to less than 1% in thirty seconds.

4. *Signals to user when control solution is low*

The Low Fluid Alarm was used during QD experiments effectively alerted the experimenter when control solution levels were low. The light-emitting diode was bright enough to be seen in the darkened laboratory, and its use prevented culture damage due to exposure to air.

8.2 Experimental Conclusions

1. *Quantum Dots work as an anti-IPSP agent*

As discussed in Section 2.2.2 and seen in Section 6.1, Gabazine produces synchronous activity in neurons because it blocks anion channels in the synapse that normally inhibit action potentials. In effect, Gabazine only permits excitatory potentials, meaning that when one neuron generates an EPSP above the action potential threshold, all connected neurons generate action potentials synchronously. As shown in section 6.2, the addition of QDs also elicited synchronous activity; when one neuron activated, the other neurons activated. Additionally, it has been shown that Quantum Dot only induce dipole moments very close (<20nm) to ion channels, as discussed in Section 2.3.2. Therefore, QDs work as anti-IPSP molecules in the synapse, using a mechanism similar to that of Gabazine.

2. *Quantum Dots in solution may also work as anti-EPSP agents*

In addition to synchronous activity, cultures showed uniform amplitudes of calcium activity among all neurons after the addition of QDs. This effect is interesting and unexpected. As discussed in Section 2.4.1, different neurons in culture will typically show different levels of calcium activity with non-ratiometric dyes, due to different cell volumes and different intracellular accumulation of dye. This is considered to be one of the downfalls to using traditional non-ratiometric dyes, and prevents quantitative comparison between experiments. However, as seen in Section 6.2, when QDs are introduced into cultures, all neurons exhibit uniform and generally decreased activity. Thus, uniform application of QDs in a culture, such as when applied in solution, acts similarly to an anti-EPSP drug that uniformly reduces the amount of activity in culture.

3. *Few QDs are needed to change activity in neurons*

Although Streptavidin-coated and carboxyl-coated QDs had the same final concentration (0.8nM) in culture, streptavidin-coated QDs did not adhere to the cell membrane as much as carboxyl-coated QDs, as shown in Section 6.2. Not only were QDs present at the nanomolar concentration, but

also few Streptavidin QDs adhered to neurons. Therefore, an low number of QDs need to physically interact with neurons to elicit electrical activity.

8.3 Engineering Device Recommendations

1. *The device should be black rather than orange*

If the team was not operating under a small budget in a new facility, more money could have been spent on materials. Orange ABS plastic was the cheapest for the ICTP to 3D print, but this color does not provide optimal light absorption. In the future, light shields should be made with non-glossy, black materials to minimize reflected ambient light from reaching the culture.

2. *Use microfluidic devices in perfusion system*

A more detailed investigation could be made into the fluid dynamics of the perfusion system on the microscope. Microfluidic devices can be manufactured at the Elettra Sincrotrone in Trieste, Italy that would enable closed-system alternatives to be explored, as seen in Section 4.2.2. As discussed, closed systems have the benefit of only one source of pressure, highly tunable flow rates, and constant volumes, but are generally harder to manufacture. Additionally, microfluidic devices would allow accurate drug delivery with minimal waste of materials. With access to a manufacturing laboratory, closed-loop microfluidic systems could be developed cheaply and efficiently.

3. *Modify the opening for micropipette injection*

The device currently has a small opening that allows the insertion of a micropipette to inject drugs directly into the culture, as described in Section 5.1.1. While in theory, this component is a good method to deliver drugs, in practice the opening is hard to use with small volumes (0.2-2 μ L) of test solutions. The surface of the culture has to come into contact with the micropipette in order to release the test solution into the culture, requiring care and dexterity. In the next iteration of the design, a door should be made that would provide more visibility to the operator when injecting test solutions. This door should be accessible from both sides to accommodate right and left-handed individuals.

4. *Create a bright field illumination cap for the condenser on the microscope arm*

With the current device, there is only one remaining way for ambient light to enter the culture. On the microscope arm, there is a condenser that focuses brightfield white light during DIC imaging

before it shines on the culture, as seen in Figure 17B. In the future, an inexpensive, removable cover should be made for use during fluorescence imaging.

5. *Focus on standardization to better accommodate future international students*

Future research at UNG should be based on the idea of standardization of all test protocols. The Centre is less than a year old, but already is forging relationships with other universities and collaborating with students from overseas. In their early years, the Centre will confront issues of equipment setup, protocol refinement, material acquisition, and pressure for results. Care should be taken to document every step of processes, making the learning curve of new students much smaller. Overall, Standard Operating Procedures should be available for all typical lab activity, for the purposes of documentation, repeatability, and consistency. To this end, the has provided Standard Operating Procedures for many of the techniques needed to study QD-neuron interactions with calcium imaging. These procedures are documented in Appendices D, L, M, O, P, and Q.

8.4 Experimental Recommendations

1. *Study the effects of fluorescence on QD-neuron interactions*

The existing setup at the Centre is limited to the study of QD-neuron interaction with calcium imaging. A more robust way to characterize the activity of neurons would be to correlate calcium activity in the network with electrophysiological recordings from individual neurons. With electrophysiological recordings, any wavelength and intensity of light can be used to excite the QDs, while preserving the ability to record their activity independently.

Furthermore, the wavelength of light used to excite the calcium dyes also excited the QDs. In the case of OGB, the excitation wavelength was 488nm. This was not the peak excitation wavelength of Qdot-655 and may have impacted the strength of the induced dipole in the QD, which induces electrical activity in neurons. With a larger dipole moment, the QDs could elicit stronger neural signals.

2. *Refine protocols for ratiometric calcium dyes such as FURA-2*

Ratiometric dyes, such as FURA-2, respond to changing calcium levels in a cell by changing their peak fluorescence excitation wavelength. This allows a ratio of bound-to-unbound dye to be calculated during experiments, circumventing problems inherent in calcium imaging, including photobleaching and

uneven distributions of dye. Ratiometric dyes provide quantitative data that may be compared more confidently among experiments.

Additionally, both FURA-2 and QD-655 are excited best in the UV range. This allows the most efficient excitation of QDs during calcium imaging, with the best chance of producing a strong dipole moment and eliciting electrical activity in neurons.

3. *Determine dose-response curves for different surface coatings of Qdot-655*

Dose response curves may be used to identify the most ideal concentration of Qdot-655 to stimulate neurons. Different surface coatings are expected to induce different levels of activity in the cells, but with varying levels of toxicity.

4. *Use optical tweezers*

A nearby laboratory in Trieste, Italy, used optical tweezers to localize large vesicles (1-10 μ m) to certain parts of neurons and release very precise concentrations of molecules. This can be used to study the interaction of one or more QDs with particular parts of the neuron, including the synapse, while limiting cell toxicity. Additionally, QDs can be visualized as they interact with neurons.

5. *Characterize effect of polymer/biomolecule coatings on dipole moments*

While the presence of PEG coatings and other biomolecules limited toxicity and provided functionality to the QDs, these coatings also serve as physical barriers to electric dipoles. To maximize the potential for QDs to stimulate neurons, the optimal balance of excitation wavelength and intensity can be paired with different surface to coatings in order to identify a nontoxic QD that has a strong dipole moment. This method might not require studying the QD-neuron interaction, but rather the Qdot-655 itself.

Works Cited

- Long-Wavelength Calcium Indicators*. (2005, September 15). Retrieved from life technologies: <http://tools.lifetechnologies.com/content/sfs/manuals/mp03010.pdf>
- Alberts, J. L. (2008). *Molecular Biology of the Cell*. Garland Science.
- Alivisatos, A. (1996). Semiconductor Clusters, Nanocrystals, and Quantum Dots. *Science*, 271(5251), 933-937.
- Andlin-Sobocki, P. J. (2005). Cost of disorders of the brain in Europe. *European Journal of Neurology*, 21(10), 12(s1), 1-27.
- Azevedo, F., Carvalho, L., Farfel, J., Ferretti, R., Leite, R., Jacob Filho, W., . . . Herculano-Houzel, S. (2009). Equal numbers of neuronal and nonneuronal cells make the human brain an isometrically scaled-up primate brain. *Journal of Comparative Neurology*, 513(5), 532-541.
- Ballabh, P., Braun, A., & Nedergaard, M. (2004). The blood–brain barrier: an overview: Structure, regulation, and clinical implications. *Neurobiology of Disease*, 16(1), 1-13.
- Bear, M., Connors, B., & Paradiso, M. (2007). *Neuroscience: Exploring the Brain*. Lippincott Williams & Wilkins.
- Bootman, M., Reitdorf, K., Walker, S., & Sanderson, M. (2013). Ca²⁺-Sensistive Flupresent Dyes and Introcellular Ca²⁺ Imaging. *Cold Spring Harbor Protocols*, 2013(2), 83-99.
- Cheng, Z., Levi, J., Xiong, Z., Gheysens, O., Keren, S., Chen, X., & Gambhir, S. S. (2006). Near-Infrared Fluorescent Deoxyglucose Analogue for Tumor Optical Imaging in Cell Culture and Living Mice. *Bioconjugate Chemistry*, 17(3), 662-669.
- Cooper, G., & Hausman, R. (2013). *The Cell: A Molecular Approach*. Boston: Boston University.
- Cossart, R., Ikegaya, Y., & Yuste, R. (2005). Calcium imaging of cortical networks dynamics. *Cell Calcium*, 37, 451-457.
- Dym, C., & Little, P. (2009). *Engineering Design: A Project Based Introduction*. United States of America: John Wiley & Sons.
- Fields, R. D., & Stephen-Graham, B. (2002). New Insights into Neuron-Glia Communication. *Neuroscience*, 298(5593), 556-562.
- Hamill, O. P., Marty, A., E, N., B, S., & J, &. S. (1981). Improved Patch-Clamp Techniques for High-Resolution Current Recording from Cells and Cell-free Membrane Patches. *Pflugers Archly*, 391(2), 85-100.
- Hardman, R. (2006). A Toxicologic Review of Quantum Dots: Toxicity Depends on Physicochemical and Environmental Factors. *Environmental Health Perspectives*, 114(2), 165.
- Haydon, P. (2001). Glia: listening and talking to the synapse. *Nature Reviews Neuroscience*, 2(3), 185-193.

- Howarth, M., Takao, K., Hayashi, Y., & Ting, A. (2005). Targeting Quantum Dots to Surface Proteins in Living Cells with Biotin Ligase. *Proceedings of the National Academy of Sciences of the United States of America*, *102*, pp. 7583-7588.
- Ingram, J. M., & Zhang, C. X. (2013). FRET Excited Ratiometric Oxygen Sensing in Living Tissue. *Journal of Neuroscience Methods*, *214*(1), 45-51.
- Innocenti, B., Parpura, V., & Haydon, P. (2000). Imaging Extracellular Waves of Glutamate during Calcium Signaling in Cultured Astrocytes. *The Journal of Neuroscience*, *20*(5), 1800-1808.
- Jingxia, Z., Lanju, X., Tao, Z., Guogang, R., & Zhuo, Y. (2008). Influences of nanoparticle zinc oxide on acutely isolated rat hippocampal CA3 pyramidal neurons. *NeuroToxicology*, *30*(2), 220-230.
- Johnston, M. (2004). Clinical disorders of brain plasticity. *Brain and Development*, *26*(2), 73-80.
- Logothetis, N. K., Pauls, J., Augath, M., & Trinath, T. &. (2001). Neurophysiological Investigation of the Basis of the fMRI Signal. *Nature*, *412*(6843), 150-157.
- Lugo, K., Miao, X., Rieke, F., & Lin, L. (2012). Remote switching of cellular activity and cell signaling using light in conjunction with quantum dots. *Biomedical Optics Express*, *3*(3), 448-454.
- Lüscher, B., & Keller, C. (2004). Regulation of GABAA receptor trafficking, channel activity, and functional plasticity of inhibitory synapses. *Pharmacology & Therapeutics*, *102*(3), 195-221.
- McEwen, B. (1999). Stress and Hippocampal Plasticity. *Annual Review of Neuroscience*, *22*, 105-122.
- Michalet, X., Pinaud, F., Bentolila, L., Tsay, J., Doose, S., Li, J., . . . Weiss, S. (2005). Quantum Dots for Live Cells, in Vivo Imaging, and Diagnostics. *Science*, *307*(5709), 538-544.
- Murphy, D. (2013). *Fundamentals of Light Microscopy and Electronic Imaging*. Wiley-Blackwell.
- Qdot Nanocrystals—Section 6.6*. (n.d.). Retrieved from life technologies:
<http://www.lifetechnologies.com/us/en/home/references/molecular-probes-the-handbook/ultrasensitive-detection-technology/qdot-nanocrystal-technology.html#head1>
- specialized tools for Electrophysiology and Cell Biology Research*. (n.d.). Retrieved from Warner Instruments:
<https://www.warneronline.com/Documents/uploader/2011%20Warner%20catalog%20-%20Perfusion%20section.pdf>
- Stosiek, C., Garaschuk, O., & Holthoff, K. &. (2003). In vivo Two-photon Calcium Imaging of Neuronal Networks. *Proceedings of the National Academy of Sciences*, *100*(12), 7319-7324.
- Wiocur, G., Wojtowicz, M., Sekeres, M., Snyder, J., & Wang, S. (2006). Inhibition of Neurogenesis Interferes With Hippocampus-Dependent Memory Function. *Hippocampus*, *16*(3), 296-304.
- Zhao, J., Xu, L., Zhang, T., Ren, G., & Yang, Z. (2009). Influences of nanoparticle zinc oxide on acutely isolated rat hippocampal CA3 pyramidal neurons. *NeuroToxicology*, *30*(2), 220-230.

Appendices

Appendix A: Original Statement of Client Needs

Below is listed the original declaration of UNG's initial research for this project, provided to the team on 20 June 2013.

Modulation of neuronal electrical activity by nanoparticles

Modulation of electrical activity by metal/semiconductor nanoparticles, or conductive nanostructured materials is of great interest in biomedical engineering applications. For example, it has been recently shown that Quantum Dots (QDs) affect cell's electrical status and can be exploited as photostimulators¹; culturing neurons on carbon nanotubes affects electrical connectivity and synaptic strength²; ZnO₂ nanoparticles affect voltage-dependent Na⁺ and K⁺ currents and evoked action potentials in acutely isolated rat hippocampal CA3 pyramidal neurons³. The electrical interaction of neurons with nanomaterials is an important issue to be addressed not only for toxicological issues⁴, but also for potential further developments in the field of tissue engineering and neuroprosthetics.

QDs are semiconductor nanocrystals with peculiar optoelectronic properties widely exploited for cell fluorescence imaging. Indeed, QDs are very bright light emitters, do not bleach, and they are therefore considered promising candidates for new generation fluorescence microscopy⁵. Excited QDs experience electron-hole separation. As a consequence, the corresponding electrical dipole moment can perturb the cell membrane potential by the generation of an electric field.

Some of our preliminary experiments have shown that acute treatment of cultured hippocampal neurons with ZnS shelled CdSe QDs (Qdot 655 ITK) produce immediate synchronous Ca²⁺ oscillations of the entire culture. Although reminiscent of Bicuculline-induced epileptic bursts⁶, the nature and origin of such oscillations has not been further explored.

The project will explore the effects of the interaction between semiconductor nanoparticles (QDs) and neuronal cells, with electrophysiological and Ca²⁺ imaging techniques. Cultured hippocampal neurons (>7 DIV) will be whole-cell-patch-clamped and the cell membrane voltage monitored during application of QDs. QDs induced electrical effects on neurons will be pharmacologically characterized, by applying distinct and specific ion channel blockers (TTX, TEA, 4AP, APV, CNQX etc.). Dynamic Ca²⁺ imaging technique will be used in addition to patch clamp electrophysiology for multiple cell monitoring of network activity⁷.

¹ Katherine Lugo et al., "Remote Switching of Cellular Activity and Cell Signaling Using Light in Conjunction with Quantum Dots," *Biomedical Optics Express* 3, no. 3 (February 8, 2012): 447.

² Giada Cellot et al., "Carbon Nanotube Scaffolds Tune Synaptic Strength in Cultured Neural Circuits: Novel Frontiers in Nanomaterial-tissue Interactions," *The Journal of Neuroscience: The Official Journal of the Society for Neuroscience* 31, no. 36 (September 7, 2011): 12945–12953.

³ Jingxia Zhao et al., "Influences of Nanoparticle Zinc Oxide on Acutely Isolated Rat Hippocampal CA3 Pyramidal Neurons," *NeuroToxicology* 30, no. 2 (March 2009): 220–230.

⁴ Z. Yang et al., "A Review of Nanoparticle Functionality and Toxicity on the Central Nervous System," *Journal of The Royal Society Interface* 7, no. Suppl. 4 (June 2, 2010): S411–S422.

⁵ Fabien Pinaud et al., "Probing Cellular Events, One Quantum Dot at a Time," *Nature Methods* 7, no. 4 (March 30, 2010): 275–285.

⁶ R D Traub and R K Wong, "Cellular Mechanism of Neuronal Synchronization in Epilepsy," *Science (New York, N.Y.)* 216, no. 4547 (May 14, 1982): 745–747.

⁷ Rosa Cossart, Yuji Ikegaya, and Rafael Yuste, "Calcium Imaging of Cortical Networks Dynamics," *Cell Calcium* 37, no. 5 (May 2005): 451–457.

Appendix B: Work Breakdown Structure

At the outset of the project, the team determined a list of tasks which would need to be accomplished during the limited time at UNG.

1. Design Process

1.1.1. Initial client statement discussion

- 1.1.1.1.1. Initial client/sponsor contact
- 1.1.1.1.2. Generate questions on working environment
- 1.1.1.1.3. Discuss need for design
- 1.1.1.1.4. Generate questions for client/sponsor interview
- 1.1.1.1.5. Propose equipment revisions
- 1.1.1.1.6. Research neurobiology and microscopy

1.1.2. Preliminary testing with current equipment

- 1.1.2.1.1. Familiarize with equipment on site
- 1.1.2.1.2. Develop current testing protocols
- 1.1.2.1.3. Document sources of error and labor
- 1.1.2.1.4. Perform laboratory testing with current design
- 1.1.2.1.5. Propose new perfusion design

1.1.3. Develop design alternatives

- 1.1.3.1.1. Write Background
- 1.1.3.1.2. Develop objectives tree
- 1.1.3.1.3. Develop a function-means tree
- 1.1.3.1.4. Current state of the field
- 1.1.3.1.5. Previous research and perfusion options
- 1.1.3.1.6. Brainstorm design alternatives

1.1.4. Prototyping

- 1.1.4.1.1. List materials, methods, budget for improving design
- 1.1.4.1.2. Buy materials
- 1.1.4.1.3. Build initial prototype
- 1.1.4.1.4. Test prototype

2. Documentations

2.1.1. Contact

- 2.1.1.1.1. Initial client introduction letter
- 2.1.1.1.2. Agendas for meetings with sponsor
- 2.1.1.1.3. Project Design Presentations
- 2.1.1.1.4. Project Design Proposal

2.1.2. Final presentation

2.1.3. Research

- 2.1.3.1.1. Annotated bibliography
- 2.1.3.1.2. Detailed background
- 2.1.3.1.3. Laboratory experimental notebook with data
- 2.1.3.1.4. Experimental SOPs

2.1.4. Design

- 2.1.4.1.1. Design Notebook with CAD and code
- 2.1.4.1.2. Experimental results and validation
- 2.1.4.1.3. Final prototype and SOP

3. Project management

3.1.1. Files and Data

- 3.1.1.1.1. Organize and maintain electronic files
 - Manage team communications
 - 3.1.1.1.2. Create and modify agendas
 - 3.1.2. Personnel
 - 3.1.2.1.1. Develop and maintain Gantt chart
 - 3.1.2.1.2. Schedule deadlines
 - 3.1.2.1.3. Schedule laboratory time
 - 3.1.2.1.4. Create and modify to-do lists
- 4. Laboratory testing
 - 4.1.1. Inventory and stock materials
 - 4.1.2. Prepare cell culture medium
 - 4.1.3. Hippocampal cell passaging and maintenance
 - 4.1.4. Testing with current equipment
 - 4.1.5. Optimize ratiometric-imaging protocol
 - 4.1.6. Drug perfusion with ion blockers
 - 4.1.7. Treatment with Quantum Dots
 - 4.1.8. Testing with final design
 - 4.1.9. Data analysis

Appendix C: Gantt Chart

Below is a Gantt Chart, detailing the expected general timeline for completion of the various steps of the project. While the true timeline for tasks varied in several areas, it served as a roadmap

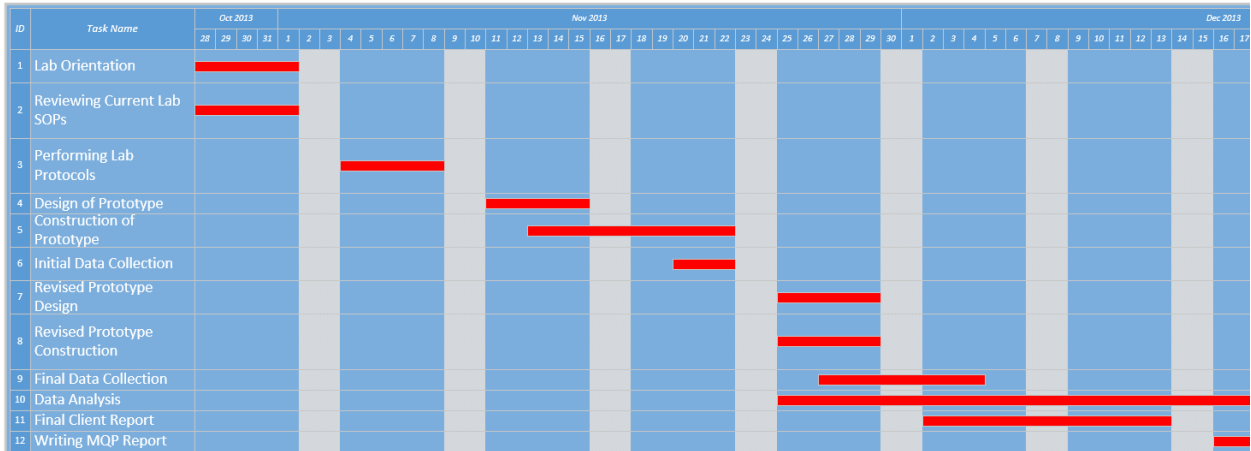


Figure 47: A visual representation of work to be completed, as understood by the team at the outset of the project

Appendix D: Standard Operating Procedure for Staining Cells Prior to Imaging

This standard operating procedure describes the process by which cells are loaded with OGB dye prior to calcium imaging.

Materials:

1. Small (35 x 10 mm) Petri Dish
2. Large (100 x 15 mm) Petri with Plated Cells
3. Dye (Fura-2 or Oregon Green)
4. Tweezers
5. Ringer's Solution

Procedure:

1. Pipette 1.5mL of Ringer's Solution into small Petri dish
Note: This should be just enough liquid to cover the bottom of the dish
2. Add desired dye. This will be either
 - a. 1.5uL Fura-2
 - b. 0.7uL Oregon Green
3. Remove tweezers from ethanol filled Falcon tube and allow to air dry
4. Using tweezers, remove one glass slide from larger 4-slide Petri and place into the smaller dye-Ringer's Petri
5. Cover small Petri with aluminum foil to avoid photo bleaching from the UV in the room
6. Place larger Petri back to incubator
7. Leave the small petri dish at room temperature for ~30 minutes for cells to absorb dye

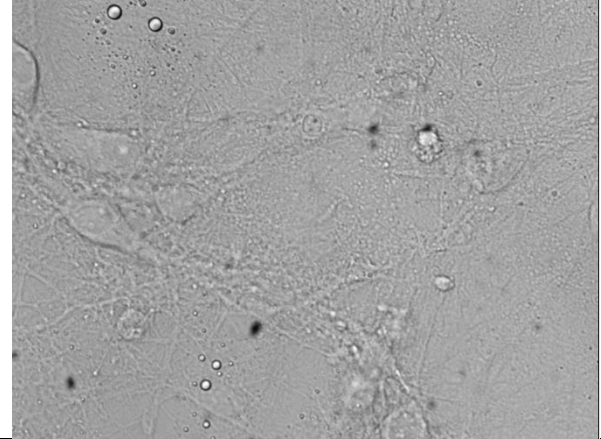
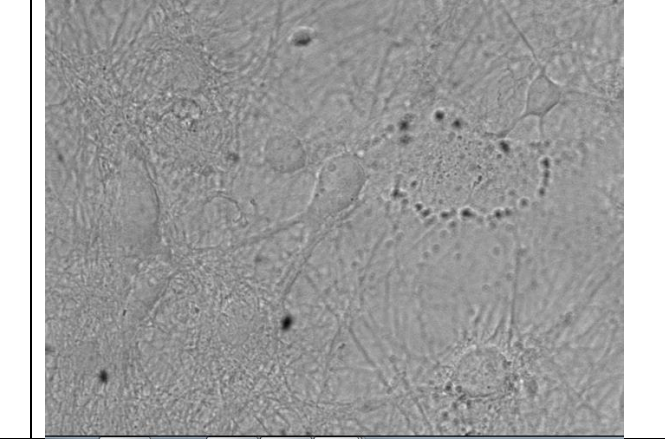
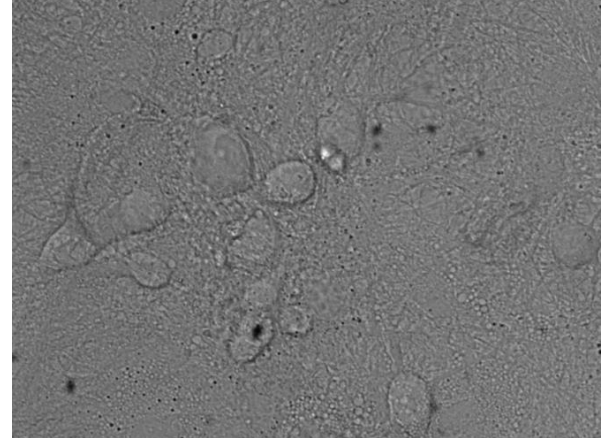

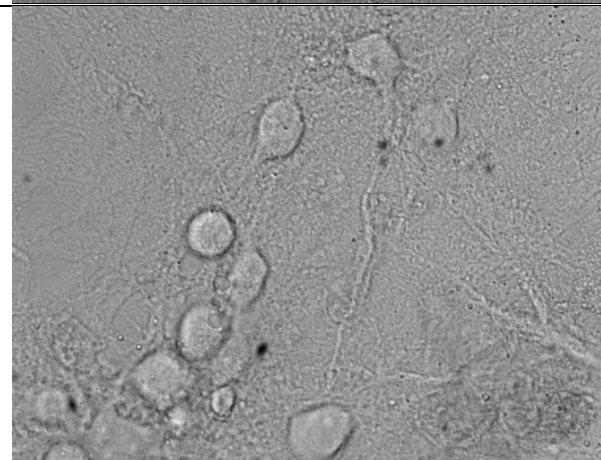
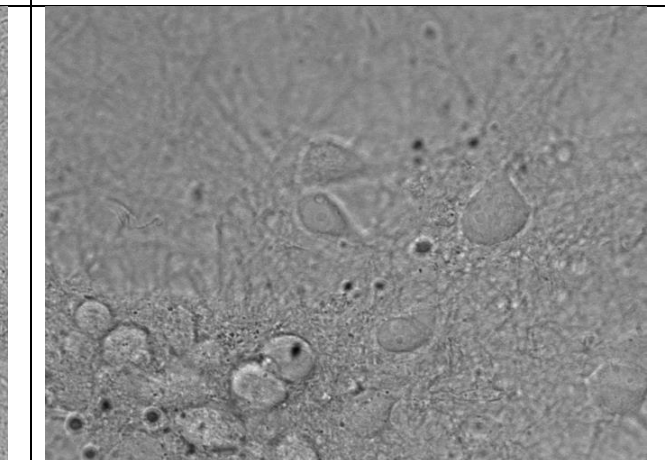
Appendix E: Verification Protocol Testing for Mechanical Interference, Cell Shearing, and Issues of Manual Dexterity

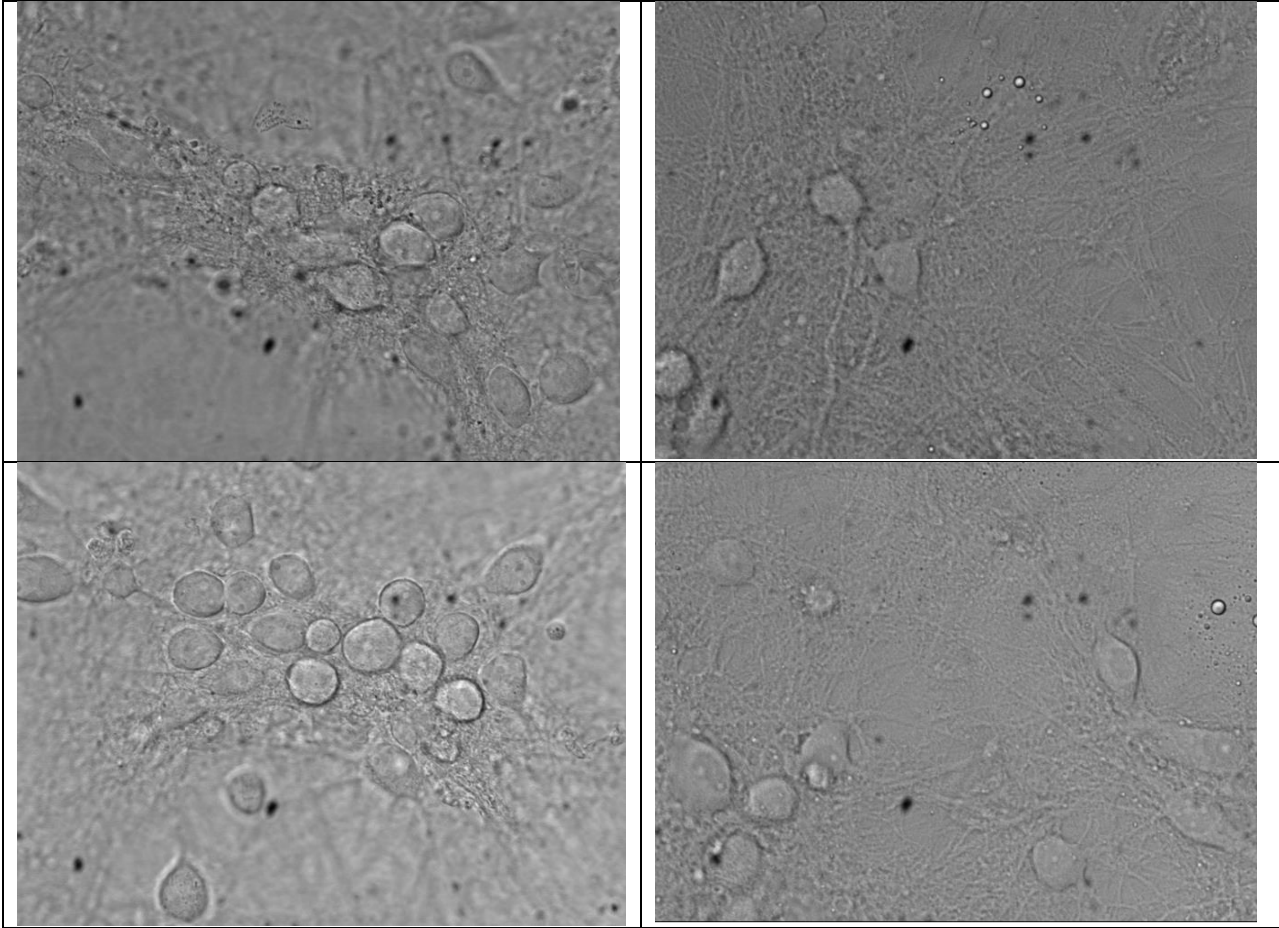
This verification protocol was followed and completed to test compliance with specifications 001, 006, 007, 008, 009, 010, 011, 012, and 013.

Step	User Instruction	Documentation of Result
1	Load a slide of networked cells (at least five DIV) with Oregon Green Dye, according to Appendix D: Standard Operating Procedure for Staining Cells Prior to Imaging	N/A
2	Image the cells under a visible light microscope	Do the cells appear to be alive, viable and have formed a neural network? <input checked="" type="checkbox"/> Yes <input type="checkbox"/> No
3	Transfer the cells to the primary microscope.	N/A
4	Obtain a stopwatch or other timekeeping device	N/A
5	Using the stopwatch, determine the required amount of time for a user to set up the device.	Total setup time: <u>0</u> min <u>44</u> sec Did the user have any dexterity-related issues with device setup? <input type="checkbox"/> Yes <input checked="" type="checkbox"/> No Does the device mechanically interfere with or intrude upon the space between the slide and the objective lens? <input type="checkbox"/> Yes <input checked="" type="checkbox"/> No
6	Lower the microscope arm down to the imaging position	Does the microscope arm mechanically interfere with the device? <input type="checkbox"/> Yes <input checked="" type="checkbox"/> No
7	Using the manual lever, move the imaged location of the slide to the top, bottom, left, and right extents of the slide.	Does the microscope arm mechanically interfere with the device while imaging any location on the slide?

		<input type="checkbox"/> Yes <input checked="" type="checkbox"/> No
8	Identify five distinct clusters of cell on the slide, all of which appear to be alive and networked. Note the XY coordinates of these five locations, and take a DIC image of each of them.	Locations with Viable Cells: X ₁ : 56.080 Y ₁ : 46.514 X ₂ : 56.304 Y ₂ : 46.514 X ₃ : 56.231 Y ₃ : 46.185 X ₄ : 56.828 Y ₄ : 46.439 X ₅ : 57.110 Y ₅ : 46.078
9	Begin perfusion of ringer's solution over the cells	N/A
10	Identify a region of cells on the slide. This location may be one of the viable cell locations from step 8	Chosen location: X: 57.193 Y: 46.078
11	Begin an indefinitely long fluorescent time-lapse capture of this location	N/A
12	Stop the perfusion system	N/A
13	While continuing to image the region of cells, introduce TTX into the cell culture	Were there difficulties related to the introduction of TTX to the cell culture? <input checked="" type="checkbox"/> Yes <input type="checkbox"/> No
14	Restart the perfusion system	N/A
15	End the timelapse capture	N/A
16	Revisit the same XY coordinates from step N. Image each of these locations	N/A
17	Shut off the perfusion system	N/A
18	With the stopwatch, time how long is required to disconnect the device from the microscope	Total breakdown time: <u> 5 </u> min <u> 12 </u> sec Did the user have any dexterity-related issues with device breakdown? <input type="checkbox"/> Yes <input checked="" type="checkbox"/> No

Each of the rows below represents an XY coordinate of the microscope before and after the process of testing. They show completely different fields of view in each image, implying that the same section of the slide was not imaged, despite the microscope being commanded to image an identical XY coordinate.

Before Testing	After Testing
	
	
	



Appendix F: Verification Protocol Testing Used to Test the Low Fluid Alarm

This verification protocol was followed and completed to test compliance with specification 002.

Step	User Instruction	Documentation of Result
1	With the perfusion in system off (valve in the perpendicular position), fill the control solution syringe with distilled water	N/A
2	Attach the low ringer alarm apparatus to the perfusion in syringe, with the float inserted directly into the chamber of the syringe	Is the LED indicator on while the water level in the syringe is full? <input type="checkbox"/> Yes <input checked="" type="checkbox"/> No
3	Turn off the lights	N/A
4	Begin video recording of the syringe and LED	N/A
5	While recording, move the valve to the open position to allow fluid to flow out of the syringe	N/A
6	Continue recording as the water level lowers until either the LED turns on or all fluid has exited the syringe	Does the LED indicator turn on some amount of time before the fluid in the perfusion in system is drained? <input checked="" type="checkbox"/> Yes <input type="checkbox"/> No
7	Stop the recording	N/A
8	Allow the perfusion system to fully drain	N/A
9	Remove the low ringer alarm apparatus	N/A

Appendix G: Verification Testing Protocol Used to Determine Concentration of a Substance in the Slide Chamber as a Function of Perfusion Time

This verification protocol was followed and completed to test compliance with specification 005.

Step	User Instruction	Documentation of Result																					
1	<p>Prepare a serial dilution of 2X Bromophenol Blue ink in a series of nine cuvettes. These should contain the following percent concentrations of ink:</p> <p>17.50 % 8.750 % 4.375 % 2.187 % 1.093 % 0.546 % 0.273 % 0.136 % 0.068 %</p>	N/A																					
2	Analyze these cuvettes by use of spectrophotometer, using a wavelength of 590 nm. Record the reported optical densities	<table border="1"> <thead> <tr> <th>Percent Concentration Ink</th> <th>Optical Density</th> </tr> </thead> <tbody> <tr> <td>17.5</td> <td>2.844</td> </tr> <tr> <td>38.75</td> <td>2.83</td> </tr> <tr> <td>4.375</td> <td>2.32</td> </tr> <tr> <td>2.1875</td> <td>1.202</td> </tr> <tr> <td>1.09375</td> <td>0.689</td> </tr> <tr> <td>0.546875</td> <td>0.363</td> </tr> <tr> <td>0.2734375</td> <td>0.201</td> </tr> <tr> <td>0.1367188</td> <td>0.139</td> </tr> <tr> <td>0.0683594</td> <td>0.1</td> </tr> </tbody> </table>	Percent Concentration Ink	Optical Density	17.5	2.844	38.75	2.83	4.375	2.32	2.1875	1.202	1.09375	0.689	0.546875	0.363	0.2734375	0.201	0.1367188	0.139	0.0683594	0.1	
Percent Concentration Ink	Optical Density																						
17.5	2.844																						
38.75	2.83																						
4.375	2.32																						
2.1875	1.202																						
1.09375	0.689																						
0.546875	0.363																						
0.2734375	0.201																						
0.1367188	0.139																						
0.0683594	0.1																						
3	Fill the perfusion in syringe with distilled water	N/A																					
4	Set up the device with a blank, clean slide	N/A																					
5	Add 250 mL of 2X Bromophenol Blue ink into the culture dish	N/A																					
6	Turn on the perfusion out system to lower the level of blue ink down to a stable level	N/A																					
7	Obtain a stopwatch	N/A																					
8	Simultaneously begin the stopwatch and turn on the perfusion in system	N/A																					

9	After four seconds, sample 15 mL ⁸ of solution from the slide with a micropipette	N/A			
10	Add this to a cuvette along with 985 μL distilled water	N/A			
11	Repeat steps 5-10 two more times	N/A			
12	Repeat steps 5-10, using a time of eight seconds instead of four seconds	N/A			
13	Repeat steps 5-10, using a time of twelve seconds instead of four seconds	N/A			
14	Repeat steps 5-10, using a time of sixteen seconds instead of four seconds	N/A			
15	Repeat steps 5-10, using a time of zero seconds instead of four seconds	N/A			
16	Analyze the obtained samples into a spectrophotometer, using a wavelength of 590 nm. Record the reported optical densities	Time (sec)	Trial 1	Trial 2	Trial 3
		0	0.751	0.728	0.659
		2	0.372	0.459	0.579
		4	0.422	0.429	0.633
		8	0.344	0.263	0.273
		12	0.102	0.143	0.120
16	0.050	0.077	0.064		
17	Clean and replace all materials	N/A			
18	Use the data to determine the average concentration in the slide as a function of time. Report the equation and R ² value which best describes the trend to the right.	Equation: $y = 167.7e^{-0.285x}$ R ² Value: 0.951			

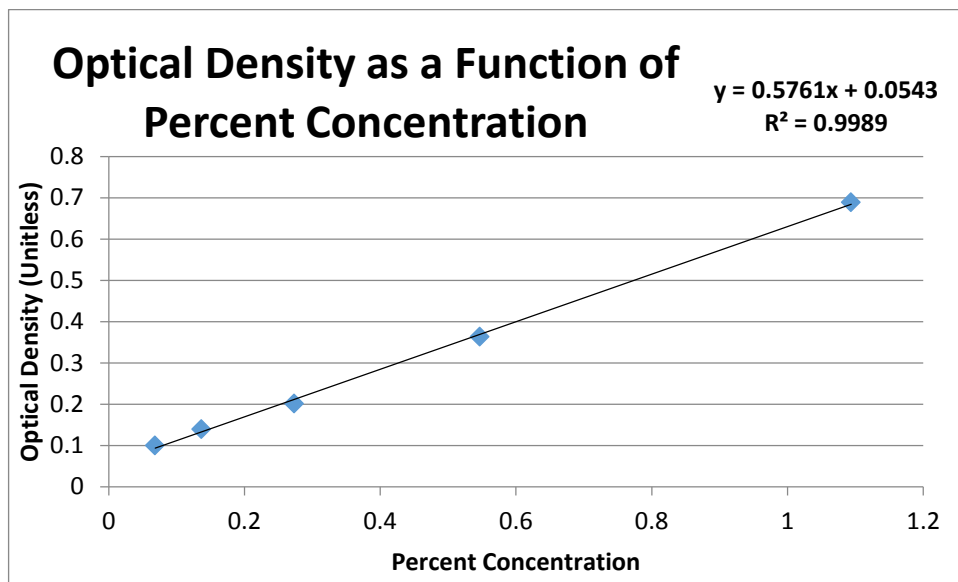
Determination of the Relationship Between Concentration and Time

Below is listed the raw data of the standard curve, collected in step 2.

Percent Concentration	Ink Volume	Water Volume	Optical Density
17.5	175.0	825.0	2.844
8.75	87.5	912.5	2.83
4.375	43.8	956.3	2.32
2.1875	21.9	978.1	1.202
1.09375	10.9	989.1	0.689
0.546875	5.5	994.5	0.363
0.2734375	2.7	997.3	0.201
0.13671875	1.4	998.6	0.139
0.068359375	0.7	999.3	0.1

⁸ This value was determined to keep all optical densities below one, and was based on the results of step 2. UNG experimenters noted that the performance of the available spectrophotometer dropped significantly at values greater than one.

Only values with optical densities below 1.0 are used, due to concerns from UNG staff about the validity of the spectrophotometer above this level.



A linear relationship between optical density and percent concentration of ink is revealed. This relationship may be described by:

$$\text{Optical Density} = (0.5761) * (\text{Percent Concentration}) + (0.0543)$$

or, alternatively

$$\text{Percent Concentration} = \frac{\text{Optical Density} - 0.0543}{0.5761}$$

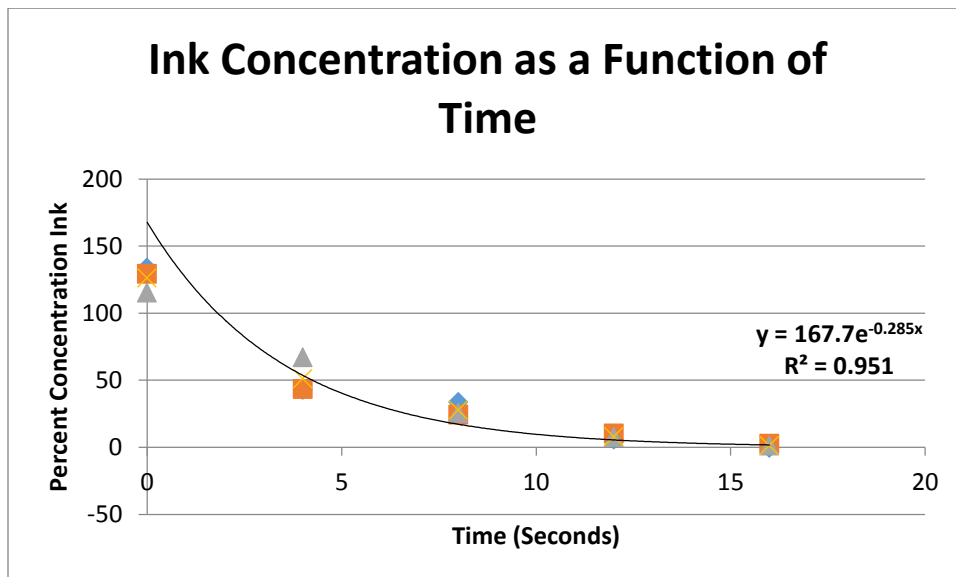
When applied to the collected time dependence data from the slide, we find the following

Time	Optical Density			Average
	Trial 1	Trial 2	Trial 3	
0	1.21	1.17	1.05	1.143333333
4	0.422	0.429	0.633	0.494666667
8	0.344	0.263	0.273	0.293333333
12	0.102	0.143	0.12	0.121666667
16	0.05	0.077	0.064	0.063666667

	Percent Concentration			
Time	Trial 1	Trial 2	Trial 3	Average
0	2.006075334	1.936642944	1.728345773	1.890354684
4	0.638257247	0.650407915	1.004513105	0.764392756
8	0.502864086	0.362263496	0.379621593	0.414916392
12	0.082798125	0.153966325	0.114042701	0.116935717
16	-0.007463982	0.039402881	0.016837355	0.016258751

However, these are the concentrations after 15 microliters extracted from the slide had been diluted in 985 additional microliters of fluid. Therefore, the true concentrations extracted from the slide may be found by multiplying these by the final volume of liquid (1mL) by the original volume of liquid, 15 microliters.

	Original Percent Concentration			
Time	Trial 1	Trial 2	Trial 3	Average
0	133.7383556	129.1095296	115.2230516	126.0236456
4	42.55048313	43.36052769	66.96754036	50.95951706
8	33.52427241	24.15089973	25.30810623	27.66109279
12	5.519875022	10.26442169	7.602846728	7.795714479
16	-0.497598797	2.626858763	1.122490308	1.083916758



Appendix H: Verification Protocol Testing the Consistency of Positions of the Inflow and Outflow

This verification protocol was followed and completed to test compliance with specification 014.

Step	User Instruction	Documentation of Result
1	Using calipers, measure the distance between the tips of the micropipettes used in the perfusion in and out systems	Distance: _____15.85_____mm
2	Vigorously shake the device	N/A
3	Using calipers, measure the distance between the tips of the micropipettes used in the perfusion in and out systems	Distance: _____15.64_____mm

Appendix I: Verification Protocol Testing for Compatibility with the Thermal Control Setup

This verification protocol was followed and completed to test compliance with specification 015.

Step	User Instruction	Documentation of Result
1	Connect the two thermal control plug-ins to the sides of the thermal control ring	N/A
2	Insert the thermal control ring into the microscope	N/A
3	Place the device flush on top of the thermal control ring, as in typical imaging	Are there any mechanical interferences which would cause a reduction in imaging capability? <input type="checkbox"/> Yes <input checked="" type="checkbox"/> No
4	Record this position by camera	N/A

Appendix J: Verification Protocol Testing the Consistency of Fluid Volume in the Slide Chamber

This verification protocol was followed and completed to test compliance with specification 004.

Step	User Instruction	Documentation of Result
1	Set up the device, with the perfusion in systems and perfusion off systems both disabled	N/A
2	Using a micropipette, fill the slide area with at least 1 mL of distilled water	N/A
3	Turn on the perfusion out pump. Wait for the level of fluid in over the slide to stabilize	N/A
4	Turn off the perfusion out pump	N/A
5	Using a micropipette, remove all remaining liquid from the slide. Note how much fluid was removed.	Removed Volume ₁ : 240 µL
6	Repeat steps 2-5 an additional nine times	Removed Volume ₂ : 230 µL Removed Volume ₃ : 240 µL Removed Volume ₄ : 250 µL Removed Volume ₅ : 230 µL Removed Volume ₆ : 240 µL Removed Volume ₇ : 240 µL Removed Volume ₈ : 190 µL Removed Volume ₉ : 190 µL Removed Volume ₁₀ : 190 µL

Appendix K: Verification Testing the Effectiveness of the Light Shield

This verification protocol was followed and completed to test compliance with specification 008.

Step	User Instruction	Documentation of Result
1	Set up the microscope for fluorescent imaging	N/A
2	Place a slide containing only distilled water into the slide holder and insert it into the microscope	N/A
3	Turn off the room lights	N/A
4	With neither the box nor the device blocking light from the slide, collect two 15 second trials of fluorescence imaging data.	Two stacks of images should be saved
5	With the box from the prior UNG setup blocking light from the slide, collect two 15 second trials of fluorescence imaging data	Two stacks of images should be saved
6	With the device from the prior UNG setup blocking light from the slide, collect two 15 second trials of fluorescence imaging data	Two stacks of images should be saved
7	For each of the six collected stacks of images, use the microscope Region of Interest tool to calculate the average intensities as a function of time of the entire field of view	Six text files containing the record of intensity as a function of time should be saved
8	Offload these data files from the microscope computer	N/A
9	Remove and dispose of the slide used	N/A
10	Analyze the results	Analysis below

Each of the trials of light intensity as a function of time is plotted below.

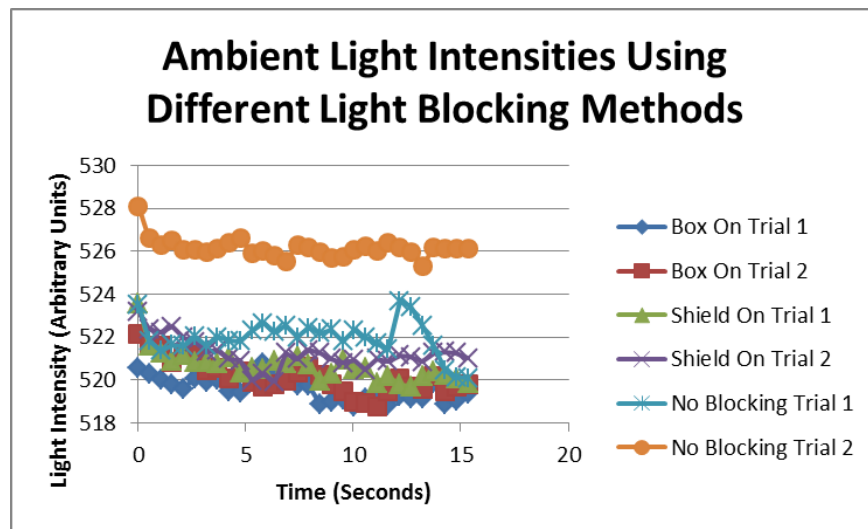


Figure 48- Verification testing of the light shield performance. Each line represents one trial tracking intensity as a function of time

It can be seen from this data that while an unblocked system clearly allows more light into the system than the light shield or the box, it is difficult to compare the efficiency of the box as compared to the efficiency of the light shield. A bar chart, which combines the two trials for each condition, underscores this difficulty.

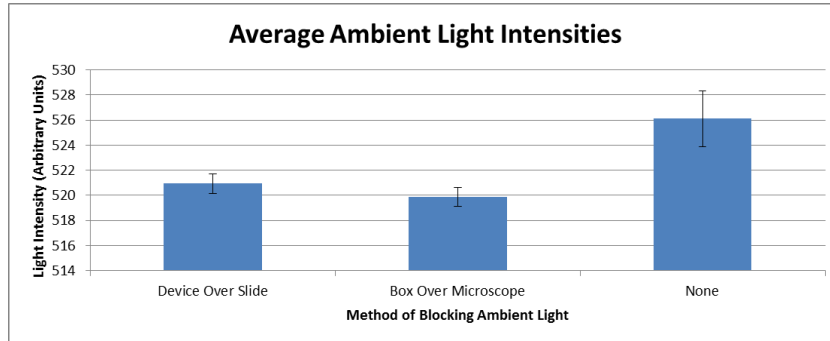


Figure 49- The light blocking performance of the device. Error bars are +/- 1 standard deviation about the mean. It can be seen that the device clearly outperforms an unshielded system, but demonstrates no significant difference in light-blocking performance as compared to the box

It is concluded that while it is unclear whether the device represents a significant improvement in light blocking over the box previously used, it at least does no worse than the box, and performs significantly better than an unshielded microscope.

Appendix L: Standard Operating Procedure for Insertion of a Slide into the Slide Chamber

This standard operating procedure describes the method by which a cell-covered slide should be inserted into the slide chamber

Materials

- Sterilized tweezers
- Ringer's Solution
- Mounting plate (bottom half of the slide chamber)

Mounting Cells

1. Carefully, using sterile tweezers, lift the slide of stained cells and place into mounting plate
2. Firmly press the top half of the slide chamber down over the top of the slide
3. Add Ringer's Solution to the edges of the slide
Note: Add Ringer's Solution slowly (drop wise), and not directly to the cells. This will prevent cells from either washing out or detaching

Appendix M: Standard Operating Procedure for Breakdown of the Olympus Microscope

This operating procedure contains all steps to follow in order to return the microscopy setup to its idle state

Procedure:

1. Run distilled water through the perfusion inflow tubing system to rinse out the system
2. Add distilled water into the slide chamber. Suck up this water with the perfusion outflow system
3. Turn off the pump
4. Disconnect the perfusion inflow and outflow tubing from the device
5. Remove the device and thermal control ring
6. Remove the slide from the slide chamber. Dispose of in a biohazard container if appropriate
7. If any part of the microscope setup is wet, remove the napkin that surrounds the objective lens and replace this napkin
8. Turn off the camera
9. Turn off Xenon lamp. Leave a note near the on/off switch indicating at what time the lamp was turned off
10. Log off of the computer

Appendix N: MATLAB Script used for Data Analysis and Presentation

Below is documented the MATLAB 2013A function which was used to process data produced by the SlideBook5 software.

```
% function calciumtraces.m
% Script to read and plot data of individual folders containing .txt files
% intensity data for non-ratiometric dyes
%
% Edit the Foldercontents variable to select more specific files
clear all; close all;

Foldercontents = dir('*.txt');    % ALTERABLE: read filenames to struc

set(0,'DefaultAxesXGrid','on');    % set some default plot parameters
set(0,'DefaultAxesYGrid','off');
axismaximum=0;                    % counters for plotting
NumFiles = length(Foldercontents); % number of files
for D=1:length(Foldercontents);    % for each file
    filename = Foldercontents(D).name; % get filename from dir struc
    fid = fopen(filename,'r');        % open text file
    firstline=fgetl(fid);            % get first Line
    titlestring(D)={firstline(13:end)}; % extract file title
    currLine=1;                      % set counter for current line
    while currLine<=5                % skip 5 lines of header
        firstline=fgetl(fid);
        currLine = currLine + 1;
    end
    numcols=sum(isspace(firstline)); % How many ROIs are there?
    if D==1                          % set color scheme for plotting
        colors=rand((numcols),3);
    end
    textformat = repmat('%s ',1,numcols);
    data = textscan(fid,textformat); % Scan in data columns
    fclose(fid);                      % close text file

% ----- Now just Raw data-----

time = data{3};                      % time, third data column
time = cell2mat(cellfun(@str2num, time, 'UniformOutput', false));
figure
for i = 4:numcols                    % for the rest columns
    templine = data{i};              % cell array data to arrays
    templine = cell2mat(cellfun(@str2num, templine, 'UniformOutput', false));
    f0=templine(1);                  % set prelim f0 value
    for j=2:length(templine)-1      % for each value in Line
        newline(j-1)=(templine(j)-f0)/f0; % normalize
        if f0 > templine(j-1)      % find global min so far
            if f0 > templine(j+1)
```

```

        f0 = templine(j);
    end
end
end
fmax=max(newline);      % set max & min for plotting
fmin=min(newline);
if fmax > axismaximum
    axismaximum=fmax;
end
time=(time(1:end-2)./1000)'; % fit time vector to plot
hPlot=plot(time,newline); % plot handle
set(hPlot,'Color',colors(i,:));
set(hPlot,'LineWidth',1)
hold on
end

hTitle=title(titlestring{D}); % Set plot settings
hXLabel=xlabel('Time (seconds)');
hYLabel=ylabel('Normalized Intensity (Arbitrary Units)');
xlim([0 max(time-1)])
set([hTitle, hXLabel, hYLabel], ...
    'FontName' , 'AvantGarde');
set([hXLabel, hYLabel] , ...
    'FontSize' , 12 , ...
    'FontWeight' , 'bold' );
set( hTitle , ...
    'FontSize' , 14 , ...
    'FontWeight' , 'bold' );
clearvars -except...
Foldercontents D NumFiles axismaximum titlestring colors
end

for k=1:NumFiles
    h_ax=gca(figure(k)); % for each plot
    ylim([0 axismaximum]); % set the axis
    print('-dtiff',[titlestring{k} '.tif'])
end

```

Appendix O: Standard Operating Procedure for the Production of Ringer's Solution

Ringer's Solution is a clear solution, which mirrors the concentrations of major ions and sugars in brain fluid. It is perfused over cells during neuron microscopy in order to keep the cells alive.

Chemicals

- NaCl
- KCl
- CaCl₂
- MgCl₂
- Glucose
- Hepes
- NaOH

Materials

- A 500mL volumetric flask
- A 500mL beaker
- Digital pH meter
- Stirrer plate and stirrer
- Micropipettes

Table 9- Ingredients for 500mL Final Volume of Ringer's Solution

Material	Final Concentration (mM)	Measurements (mL)
NaCl	145	14.5mL
KCl	3	1.5mL
CaCl ₂	1.5	0.75mL
MgCl ₂	1	0.5mL
Glucose	10	0.9g
Hepes	10	5mL

Based on desired final concentration and volume, a certain volume of each stock solution should be added to the sterile 500mL beaker. This volume may be calculated for each solution according to the following equation.

$$\text{Volume}_{\text{StockSolution}} = \frac{(\text{Final Concentration}) \times (\text{Final Volume})}{(\text{Concentration of Stock Solution})}$$

Procedure:

1. Add de-ionized water to the 500mL beaker until it is approximately filled to the final desired volume
2. Place beaker onto a stirrer plate and add in a stirrer rod. Begin mixing the solution
3. Add ingredients into de-ionized water
4. Cover solution with parafilm to transfer
5. Calibrate the pH meter
 - a. Turn on calibration device. Wait.
 - b. Remove cap from electrode and rinse gently with de-ionized water, catch waste in 100mL beaker
 - c. Press "CAL" then set Buffer 1 to pH 10.00 using the "°C" button

- d. Submerge electrode in falcon tube of 10pH buffer solution. Wait until calibration is calculated.
 - e. Remove electrode from buffer 10, rinse with de-ionized water, gently dap the electrode tip to dry
 - f. Set buffer 2 to pH 7.00
 - g. Insert electrode into 7pH buffer solution and wait until calibrated
 - h. Press "CAL"
 - i. Rinse off electrode tip with de-ionized water and place into Ringer's solution
 - j. Put on safety goggles before dealing with the 2M NaOH
6. Using a micropipette, add **drops** of NaOH until the pH meter indicates that an acidity of 7.4 has been reached
 7. Transfer the solution to a volumetric flask
 8. Seal the top of the volumetric flask with Parafilm
 9. Wash and replace all materials

Appendix P: Standard Operating Procedure for Production of Complete Neuron Medium

Complete neuron medium is a combination of simple neuron medium and fetal bovine serum (FBS). It is used for the long-term storage of hippocampal neuron cells.

Materials:

1. Syringe
2. Pore size .22 micron filter
3. 2 x Falcon Tube

Chemicals and Measurements:

1. Neuron Medium
5mL per one large (100 x 15 mm) Petri dish
2. FBS serum
10% of total volume
3. ARA-C Glial Inhibitor
1:3000 of ARA-C: Medium

Procedure:

1. Add neuron medium to Falcon tube with auto-pipette
2. Add FBS serum to same Falcon tube with auto-pipette
3. Using pore size .22 filter and syringe, filter the new medium
 - a. Attach filter to empty falcon tube
 - b. Add in small amounts of new medium
 - c. Push through filter with plunger
4. Once filtered, we add ARA-C glial inhibitor
5. Label: Date, "Complete Neuron Medium, 10% Serum"
6. Refrigerate the solution
7. Clean the biological hood

Appendix Q: Standard Operating Procedure for Changing of Cell Medium

To ensure long-term hippocampal neuron health, the medium in their petri dish needs to be changed every three days. Below is listed the procedure for this process.

Chemicals:

1. Neuron Medium
 - a. 3mL per one large Petri dish
2. FBS Serum
 - a. 5% of total volume
3. Waste beaker
4. 5mL auto-pipette

Procedure:

1. Remove medium and FBS serum for refrigerator and bring to room temperature
2. Calculate amount of medium and FBS serum needed
 - a. $(3\text{mL} * \# \text{ of Petri dishes} = \text{total volume})$
 - b. $(0.05 * \text{total volume} = \text{FBS volume})$
 - c. $(\text{total volume} - \text{FBS volume} = \text{neuron medium volume})$
3. Add neuron medium to empty falcon tube
4. Add FBS serum to falcon tube with medium
5. Remove cell plates from incubator
6. Slowly remove 2.5 mL (of half) of the medium in the cell Petri using a 5mL auto-pipette and dispose into waste beaker
 - a. Note: gently insert pipette at edge of Petri and suction slowly
7. Add 2.5mL of new medium to each plate
 - a. Note: ass SLOWLY to edge of plate without touching tip of pipette to the current medium
8. Cover Petri dishes and place back in incubator carefully as not to dislodge cells from glass plates
9. Replace original neuron medium and FBS serum to the refrigerator
10. Clean the biological hood